Physiological Events that Underlie Cell Death and Shrinkage in the Grape Berry

A thesis submitted for the degree of Doctor of Philosophy

Lishi Cai

B.S.Chem. / M. Viticulture & Oenology

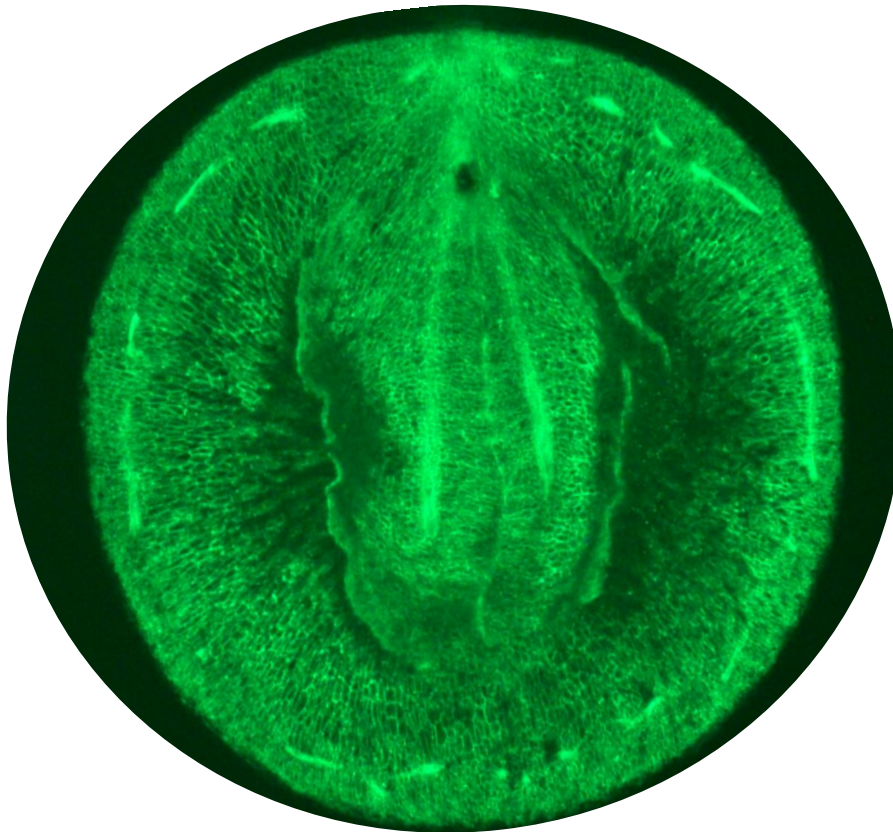School of Agriculture, Food and Wine
The University of Adelaide

THE UNIVERSITY
of ADELAIDE

Adelaide, Australia
December 2023

Shrivelled Shiraz berries (Photograph L. Cai)

Shiraz berry longitudinal section with FDA staining showing cell death (the dark area between the berry centre axis and berry skin (Photograph L. Cai)

Table of Contents

Chapter 1 Literature review

Chapter 2

2D oxygen distribution mapping and 3D Micro-CT analysis of grape berries: Exploring the hypoxia link to mesocarp cell death across varieties

Chapter 3

Towards a model explaining cell death and berry shrinkage in Shiraz: Comparing rootstocks and other varieties

Chapter 4

Effect of application of Kaolin and Pinolene on Shiraz and Grenache berry cell death, mass loss and ethanol accumulation

Chapter 5 Concluding remarks and future perspectives

Abstract

Late-ripening berry shrinkage and mesocarp cell death of some *Vitis vinifera* L. varieties have caused increasing concerns in many wine regions worldwide due to the significantly decreased yield and deterioration of quality of both grape and wine. This can result in excess sugar accumulation, lower anthocyanins, poor flavour development (e.g., lower terpenoids) in grapes, and in wines, higher ethanol and more dead/stewed fruit characters. This phenomenon is variety-dependent, very typical in Shiraz, while it rarely occurs in Grenache. The underlying reason for this phenomenon remains elusive, with factors such as heat stress and berry hypoxia being suggested as potential contributors. The main aims of my research were to determine the physiological cause of cell death and berry shrinkage and to explore models to predict their occurrences. To examine in detail the berry microstructure (porosity) and oxygen concentrations in berries for Shiraz and compared to other varieties, based on the hypothesis that hypoxia in the grape berry is a contributing factor to cell death. To explore ways to ameliorate cell death and berry shrinkage in Shiraz, the effect of rootstock, bunch exposure and antitranspirants were trialled in my research.

Chapter 1 first reviews the structure and development of grape berries, specifically addressing water regulation throughout various stages. This is examined in the context of berry water loss (backflow to the vine and transpiration from the berry) and mesocarp cell death across different varieties. Subsequently, the discussion delves into factors that may influence cell death and shrinkage, with an emphasis on high temperature and hypoxia. The role of excessive ethanol accumulation as an indicator of berry cell death is also examined. Lastly, practical applications to monitor and alleviate berry cell death and shrinkage are summarised, including the use of drought-tolerant rootstock and the application of antitranspirants.

The experiments conducted in this study took place at the vineyards on the Waite Campus of the University of Adelaide from 2018 to 2022. Firstly, in Chapter 2, berry internal oxygen concentration ($[O_2]$) (by oxygen micro-electrode) and berry porosity (by Micro-CT) were measured in berries at

different development phases of different varieties, including Shiraz, Chardonnay, Cabernet Sauvignon and Grenache. Secondly, for Chapter 3, experiments were conducted in Grenache, Cabernet Sauvignon and Chardonnay and Shiraz on own roots or different rootstocks (Ramsey, Ruggeri 140, Schwarzmann and 420A). Berry mass change and cell vitality, berry ethanol concentration, water potential, plant area index, pruning mass per vine and canopy ambient temperature during growing seasons were measured. Lastly, in Chapter 4, the effects of two film-forming antitranspirants Kaolin ($Al_4Si_4O_{10}(OH)_8$) and Pinolene (Di-1-*p*-menthene) were examined on berry cell death and mass loss in Shiraz and Grenache to test the hypothesis that these treatments may impede oxygen diffusion into the berry and/or decrease berry temperature thereby influencing cell death and berry shrinkage.

In Chapter 2, the porosity of grape berries using high resolution Micro-CT examined links between mesocarp cell death and hypoxic areas determined from the $[O_2]$ distributions in different grape varieties at different development stages. The gas exchange pathway (porous gas-filled microstructure) started from the lenticels on the pedicel, but only extended to the berry centre and the mesocarp periphery. Steep $[O_2]$ gradients and hypoxic regions towards the mesocarp interior were predicted since oxygen diffusion to these parts may be confined predominantly to the liquid phase with low conductance. The occurrence of cell death in the mesocarp may be linked to the microstructure of the berry, as it typically happens in the inner mesocarp where there are no direct porous pathways and where hypoxia is prevalent. As berry development progressed, hypoxia increased, as both the porosity in the brush area and the network of bundles decreased over time. Furthermore, Grenache berries, which exhibit minimal cell death and berry shrinkage, maintains the porous structures throughout development with less extensive hypoxic regions as compared to Shiraz berries. Porous channels were discovered that extended into the seeds, which changed during development.

Chapter 3 explores the physiological cause of berry mesocarp cell death and its consequences by exploring the correlations between temperature, ethanol accumulation, berry shrinkage and cell death in different grape varieties. The effects of temperature on cell death are clearly non-linear with larger effects as temperatures rise. A model is presented that can be used to predict cell death in Shiraz berries based on berry temperatures that can explain both the time course of increased cell death during ripening and the increase in variance. A separate model was developed to describe the accumulation of ethanol which is also non-linear with temperature but also interacted with sugar accumulation. In both models the non-linear effects of temperature indicate a clear threshold in temperature above which both ethanol and cell death increase sharply. Cabernet Sauvignon berries behaved similarly to Shiraz and the Shiraz models may also be applied to this variety. It is proposed that 35 °C may be considered a tipping point for ambient temperature in the field for susceptible varieties such as Shiraz and Cabernet Sauvignon. Varieties with lower hypoxia like Grenache or table grape varieties may have higher heat tolerance and accumulate less ethanol (EtOH) during heatwaves. Shiraz berries on drought tolerant/high vigour rootstocks and on the east side of the canopy (for north-south oriented rows) exhibited a tendency for larger berries, especially during hotter seasons, possibly due to a decreased heat stress through combination of better water uptake and more bunch shading. An allometric analysis between berry sugar content and fresh mass accumulation based on a single sampling was developed to track the progression of berry development that can indicate more accurately the initiation of berry shrinkage. The onset of berry shrinkage is not necessarily strictly dependent on the degree of cell death since shrinkage also depends on the timing of cell death with respect to when sugar inflow via the phloem likely ceases in late ripening.

In Chapter 4, the effects of two film-forming antitranspirants Kaolin ($Al_4Si_4O_{10}(OH)_8$) and Pinolene (Di-1-p-menthene), on berry cell death and mass loss on Shiraz and Grenache is reported. Neither Kaolin nor Pinolene significantly influenced bunch temperature or internal O_2 concentration, and no influence on berry cell death and [EtOH] could be detected. Pinolene reduced the degree of berry

shrinkage and total soluble solids (TSS) possibly by restricting berry transpiration but without impacts on sugar content.

In summary, the primary factors contributing to cell death in the berry mesocarp appear to be direct effects of elevated temperature and the indirect effect of higher temperature inducing hypoxia from increased O_2 demand from respiration. The ethanol accumulation under hypoxia is likely to be a contributing factor to cell death. Hypoxia in the mesocarp is likely to depend on the complex geometry of porous regions in the berry and how these change during development. The variation in the anatomy of the porous structures between different grape varieties may explain differences in heat tolerance. The effect of rootstock and bunch exposure on berry mass for Shiraz is small but may become more significant under hot conditions. The application of Pinolene on grape bunches can decrease berry shrinkage without impacts on sugar content, O_2 inflow, bunch temperature, berry cell death or ethanol levels. Understanding the physiological factors contributing to late season berry shrinkage and cell death, along with assessing the impact of strategies to monitor and alleviate these issues, will offer researchers and growers valuable information regarding enhancing berry flavour development and optimizing yield during berry ripening.

Declaration

I certify that this work contains no material which has been accepted for the award of any other degree or diploma in my name, in any university or other tertiary institution and, to the best of my knowledge and belief, contains no material previously published or written by another person, except where due reference has been made in the text. In addition, I certify that no part of this work will, in the future, be used in a submission in my name, for any other degree or diploma in any university or other tertiary institution without the prior approval of the University of Adelaide and where applicable, any partner institution responsible for the joint award of this degree.

I give permission for the digital version of my thesis to be made available on the web, via the University's digital research repository, the Library Search and also through web search engines, unless permission has been granted by the University to restrict access for a period of time.

Lishi Cai   Date: 27/11/2023

Panel of supervisors

Principal Supervisor

Emeritus Professor Stephen Tyerman

0000-0003-2455-1643

The University of Adelaide

Co-Supervisor

Dr. Vinay Pagay

0000-0003-1916-2758

The University of Adelaide

Independent Advisor

Dr. Zeyu Xiao

0000-0002-1044-3126

Charles Sturt University (previous affiliation during supervision)

Acknowledgements

Studying my PhD at the University of Adelaide has been an extraordinary journey, and I would like to thank the University of Adelaide and Wine Australia for scholarships and funding to conduct my PhD.

Among the many people I would like to acknowledge, I must start by expressing my deepest gratitude to my principal supervisor, Emeritus Professor Steve Tyerman. I am thankful for his invaluable lessons on how to conduct research, especially for letting me know that research can be so much fun. Thanks to you for all your support throughout this enjoyable journey, for being so inspiring, always encouraging and such a wonderful role model. You are always there for me. Thank you, Steve, you are the reason everything is possible.

I would also like to thank my co-supervisors, Dr. Vinay Pagay for your support and guidance and my independent advisor, Dr. Zeyu Xiao, I truly value and appreciate the feedback you have given, with special mention for your support during the oxygen sensor training.

Thanks for Assoc. Prof David Jeffery for your support as my Postgraduate Coordinator. I would like to thank Dr. Agatha Labrinidis from Adelaide Microscopy for the expert technical assistance. I thank Benjamin Pike for your support at the Waite vineyards. I thank Dr. Apriadi Situmorang for your support and help. Special thanks to Wendy Sullivan, for your expert technical advice and all your support throughout this journey, for being always nice and sweet. I would like to thank all my colleagues from the Plant Research Centre for all your help, encouragement, and support.

I would like to thank my family, especially my parents and my beloved partner, for all your love, support and accompany. LOVE YOU. ❤️

List of abbreviations

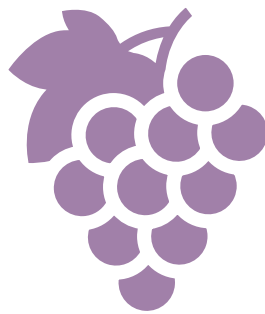|	
ABT	Average daily mean berry temperature
CMT	The correlations (by 'Pearson correlation') between average berry mass and TSS
DAA	Days after anthesis
DAV	Days after veraison
DPB	Dorsal porous bundles
EVS	Enclosed voids between two closed located seeds
EtOH	Ethanol
FDA	Fluorescein diacetate
GST	Growing season temperature
GTD_n (n=1,2,3,4)	Growing temperature days
HBT	Highest daily mean berry temperature
IVM	Irregular voids close to seed hilum as part of the OPB in the mesocarp
IVS	Isolated void in areas close to the stylar remnant
LBT	Lowest daily mean berry temperature
Micro-CT	Micro-computed tomography
O_2	Oxygen
OPB	Ovular porous bundles
PAI	Plant area index
PLT	Percentage of living tissue
SSM	The slope of the regression between amount of sugar per berry and berry mass on a log-scale
SSV	Scattered small voids with varied shapes in the mesocarp only before veraison
ST	Sponge tissue
STB	Sponge tissue in the brush area
STP	Sponge tissue in pedicel/receptacle
STT	Sponge tissue tube
TSS	Total soluble solids
$T_{(canopy\ air\ max\ daily)}$	Daily maximum canopy air temperature
$T_{(canopy\ air\ mean\ daily)}$	Daily mean canopy air temperature
VEI	Large void between endosperm and inner integument
VFS	Two voids in fossettes (seed folds)
VH	Void hook connected to OPB
VNB	Voids network in beak area
VPB	Ventral porous bundles
VSM	Voids between ovule (seeds) and ovary wall (mesocarp cells)
VSP	Vertical shoot positioned

Chapter 1

Literature review

Table of Contents

1. Introduction

Late-ripening berry shrinkage of *Vitis vinifera* L., was first reported by McCarthy (1997) in Shiraz (Syrah) and has also been called 'prolonged dehydration' (B. R. Bondada & Keller, 2012) or 'late-season dehydration' (Krasnow et al., 2010). It has caused increasing concern in a range of climates and regions worldwide, especially in warm regions in Australia. Concern arises from the significantly decreased yield and deterioration of grape quality, e.g., excess sugar accumulation, higher pH (B. R. Bondada & Keller, 2012), and poor colour and flavour development (e.g., lower terpenoids) (Shivashankara et al., 2013). Up to 30% yield loss has been reported for vines with shrivelled Shiraz berries (McCarthy, 1997, 1999; Tilbrook & Tyerman, 2008). Not surprisingly berry shrinkage can further impact final wine composition and sensory traits directly also influence yeast metabolism, with more dark fruit, and dead/stewed fruit characters and lower anthocyanins (Chou et al., 2018; Šuklje et al., 2016). Furthermore, wines with high alcohol may interfere with flavour perception and negatively impact a wine's aromatic complexity. The high alcohol levels in wine can also result in higher taxes or trade barriers in many countries, and rejection by consumers for health and safety reasons (Varela et al., 2015). Accompanying late-ripening berry shrinkage is the onset of cell death in the mesocarp (Fuentes et al., 2010; Krasnow et al., 2008; Pagay, 2018; Tilbrook & Tyerman, 2008, 2009). This phenomenon has been found to occur in many of the most important wine-making varieties, like Cabernet Sauvignon, Merlot, Chardonnay, and especially Shiraz (*ibid*). With more frequent and severe heat waves and droughts predicted in the future because of 'global warming' (Perkins et al., 2012; Webb et al., 2011), berry cell death and shrinkage are expected to be more frequent and severe (Bonada et al., 2013; Xiao, Liao, et al., 2018).

This study first reviews grape berry structure and development, with a focus on regulation of water uptake and loss at different stages. This is examined in the context of berry water loss (backflow to the vine and transpiration from the berry) and mesocarp cell death across different varieties. Then factors that may influence cell death and shrinkage are discussed, emphasising high temperature and hypoxia (Bonada et al., 2013; Xiao, Rogiers, et al., 2018; Xiao, Liao, et al., 2018). Ethanol is a product

of fermentation associated with hypoxia/anoxia in plant tissues and can be exacerbated by high temperature and drought stress (Gibbs & Greenway, 2003; Greenway & Gibbs, 2003; Kelsey & Westlind, 2017). Excessive ethanol accumulation as an indicator of berry cell death is also examined. The applications to monitor and ameliorate berry cell death and shrinkage are summarised, such as using rootstock of high drought tolerance, antitranspirants application.

2. Grape berry structure

A mature grape berry is made up of seeds and the pericarp including the endocarp, flesh mesocarp (flesh) and exocarp (skin) with each part having distinct cell structure and biochemical properties (Hardie et al., 1996) (Figure 1). The endocarp surrounding the locules has often been considered as part of the mesocarp. The single grape berry is developed from a single flower ovary consisting of four ovules. The ovary wall develops into the pericarp, and the fertilised ovules develop into seeds. One berry can contain up to four seeds, but the actual number of seeds in the berry is often fewer than four (Ristic & Iland, 2008).

2.1. Seeds

Grape seeds are located in the berry centre and comprise 2% to 6% of the berry mass depending on the variety (Mironeasa et al., 2010). The seed consists of three components: an embryo, an endosperm and the testa (seed coat); the testa contains an outer integument of three layers and an inner integument that surrounds an endosperm in which the embryo is enclosed (Pratt, 1971; Walker et al., 1999). Seed development corresponds to particular stages in berry development (Ristic & Iland, 2008). The weight and number of seeds can influence pericarp development due to their positive effects on pericarp cell division probably via hormones, especially gibberellins (Dry & Coombe, 2004; Ollat et al., 2002; Ristic & Iland, 2008).
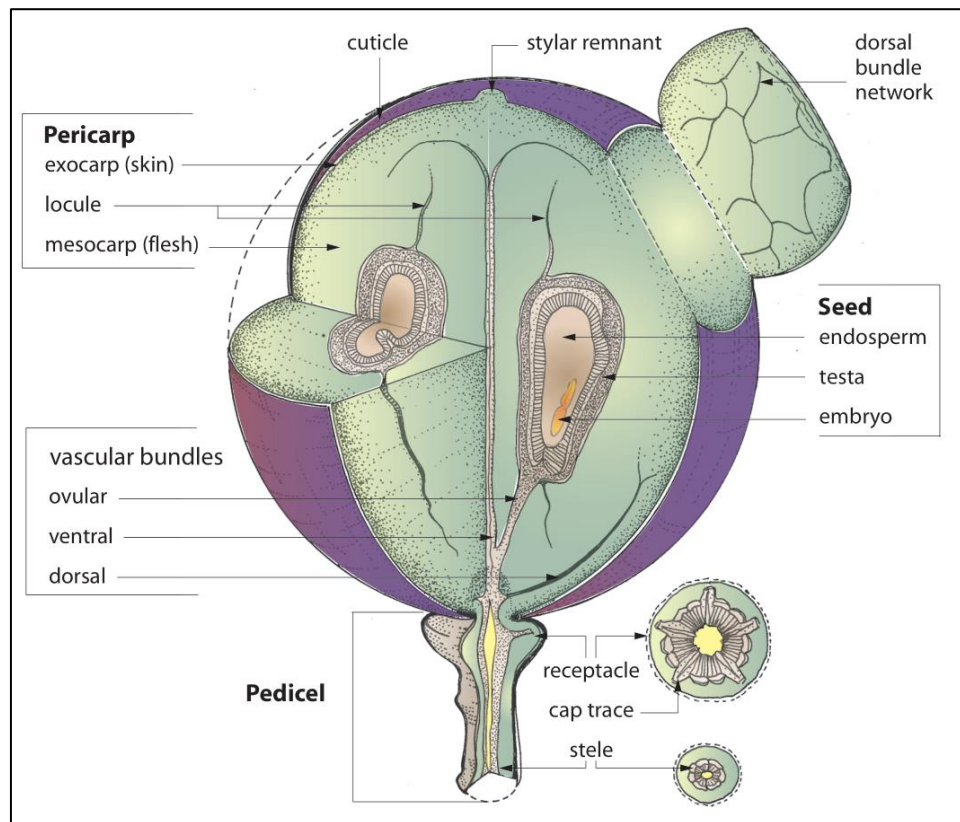
Figure 1 Structural components of the grape berry (Iland et al., 2011) (currently published by Patrick Iland Wine Promotions; originally published by The American Society of Enology and Viticulture; used with permission from the Patrick Iland Wine Promotions).

2.2. Mesocarp (flesh)

The berry mesocarp consists of 25 to 30 layers of highly vacuolated large parenchyma cells (Figure 1), making up approximately 80% of the berry mass (Hardie et al., 1996). Tissues exterior to and inside the peripheral vascular bundles of the pericarp are called outer mesocarp and inner mesocarp respectively (Considine & Knox, 1979).

2.3. Exocarp (skin)

The berry exocarp (skin) is a complex structure with multi-layers, consisting of several layers of underlying thick-walled cells and a layer of outer epidermis cells covered by the cuticle and epicuticular wax (Hardie et al., 1996) (Figure 1). The cuticle and outer wax layer play an essential role in controlling water movement between the epidermal cells and the ambient atmosphere and protecting the fruit against environmental factors, such as pests, radiation or mechanical impacts (Heywood, 1970; Riederer & Schreiber, 2001; Rogiers, Hatfield, Jaudzems, et al., 2004). When

present, stomata are the preferred sites of water loss, however there are very few stomata in post-veraison berry skins, and when present they become transformed during berry development into non-functional lenticels that are primarily filled with wax (Rogiers, Hatfield, Jaudzems, et al., 2004). Grape skin ranges from 5% to 18% of a fresh berry mass (Bioletti, 1938; Wilson et al., 1986).

2.4. Lenticels on the pedicel

Grape berries are attached to a cluster through their pedicels, the original flower stem (Figure 1). Lenticels (irregularly distributed opening holes) are very prominent on the surface of the grape pedicel consisting of loosely packed cells (Lendzian, 2006). The lenticels on pedicels are developed from stomata with analogous functions to stomata (Lendzian, 2006; Xiao et al., 2021). The lenticels on the pedicel likely provide the entry sites for low resistance gas exchange between the interior of berries and the atmosphere, for the exchange of water and gases, such as oxygen, carbon dioxide and other possible volatile organic compounds such as ethanol (Xiao et al., 2021; Xiao, Liao, et al., 2018).

2.5. Vascular system

Berry growth is supported by the vascular system through the pedicels to import carbon, sugar, and mineral nutrients. The vascular system continues from the pedicel to the inside of the berry and then branch in three directions, dividing into peripheral vasculature in the outer part of the mesocarp, central vascular (a large central strand in the columella) and ovular vasculature to the seeds as a hook (Figure 2) (Ollat et al., 2002; Xie et al., 2023). In contrast to the berry, the pedicel does not show solute accumulation during ripening (Coombe, 1992). Most of the resources for dry weight accumulation by the berry are provided by phloem. Phloem sap contains a higher solute content than xylem sap (15 to 25% w/v, compared to <0.4% w/v) (Pate, 1975).

Figure 2 Distribution of the vascular network in grape berry (Xie et al., 2023). (A) Peripheral vascular network viewed from the pedicel end of grape berry. (B) Peripheral vascular network view from the style of grape berry. (C) Peripheral vascular network from a side view. (D) Central vascular network after tissue clearing. (E) Ovular vasculature. (F) Ovular vasculature after tissue clearing. (Figure is used under a Creative Commons license, https://www.sciencedirect.com/science/article/pii/S2468014122000619)

2.6. Berry Composition

As for composition, the ripe grape berry is mainly comprised of water, sugar (glucose and fructose) and organic acids (mostly malate and tartrate), stored primarily in the mesocarp vacuoles (Tilbrook & Tyerman, 2006). Although thousands of other compounds have been found in grape berries, these three altogether make up about 99.5% of the mass of the juice (Tilbrook & Tyerman, 2006). At harvest maturity (20-25 °Brix of total soluble solids, TSS), there is approximately 75- 80% water content in berries depending on grape variety and desired wine style (Coombe, 1992; Tilbrook & Tyerman, 2006).

3. Grape berry development

After flowering, the development of berry mass generally follows a successive double-sigmoid pattern over time (Figure 3) (Coombe, 1976, 1992; Sadras & McCarthy, 2007). Three development phases are proposed based on this pattern: *Phase* 1, 'berry formation' from flowering to veraison, *Phase* 2 'berry maturation' from veraison to peak fresh mass, and *Phase* 3 'berry shrinkage' from peak fresh mass to harvest (Sadras & McCarthy, 2007). Several grape varieties such as Chardonnay and Grenache normally do not exhibit *Phase* 3 even though cell death can be detected in Chardonnay berry mesocarp (Fuentes et al., 2010; Sadras & McCarthy, 2007; Tilbrook & Tyerman, 2008, 2009). Each development phase has distinctive characteristics.

Phase 1 'berry formation' may occupy five-seven weeks where berries are rigid, green, and slow growing at this phase. Increase in size begins with a spate of cell division, then changes gradually to cell expansion, which later slows or ceases as the first sigmoid cycle ends (Coombe, 1976, 1992; Ollat et al., 2002). Acidity, cations, phenolics and some aroma compounds and their precursors accumulate during this phase. In contrast, almost no sugar accumulates as most translocated sugar is utilised as an energy source for growth and metabolism (Coombe & McCarthy, 2000; Tilbrook & Tyerman, 2006). Photosynthesis in the green berry also occurs in this phase (Breia et al., 2013). Seed development mostly happen during this stage with a steady increase in fresh and dry weight (Ristic & Iland, 2008). During this phase water influx into berries is via the xylem and phloem, but dominated via the xylem (Rogiers, Hatfield, Jaudzems, et al., 2004; Tyerman et al., 2008).
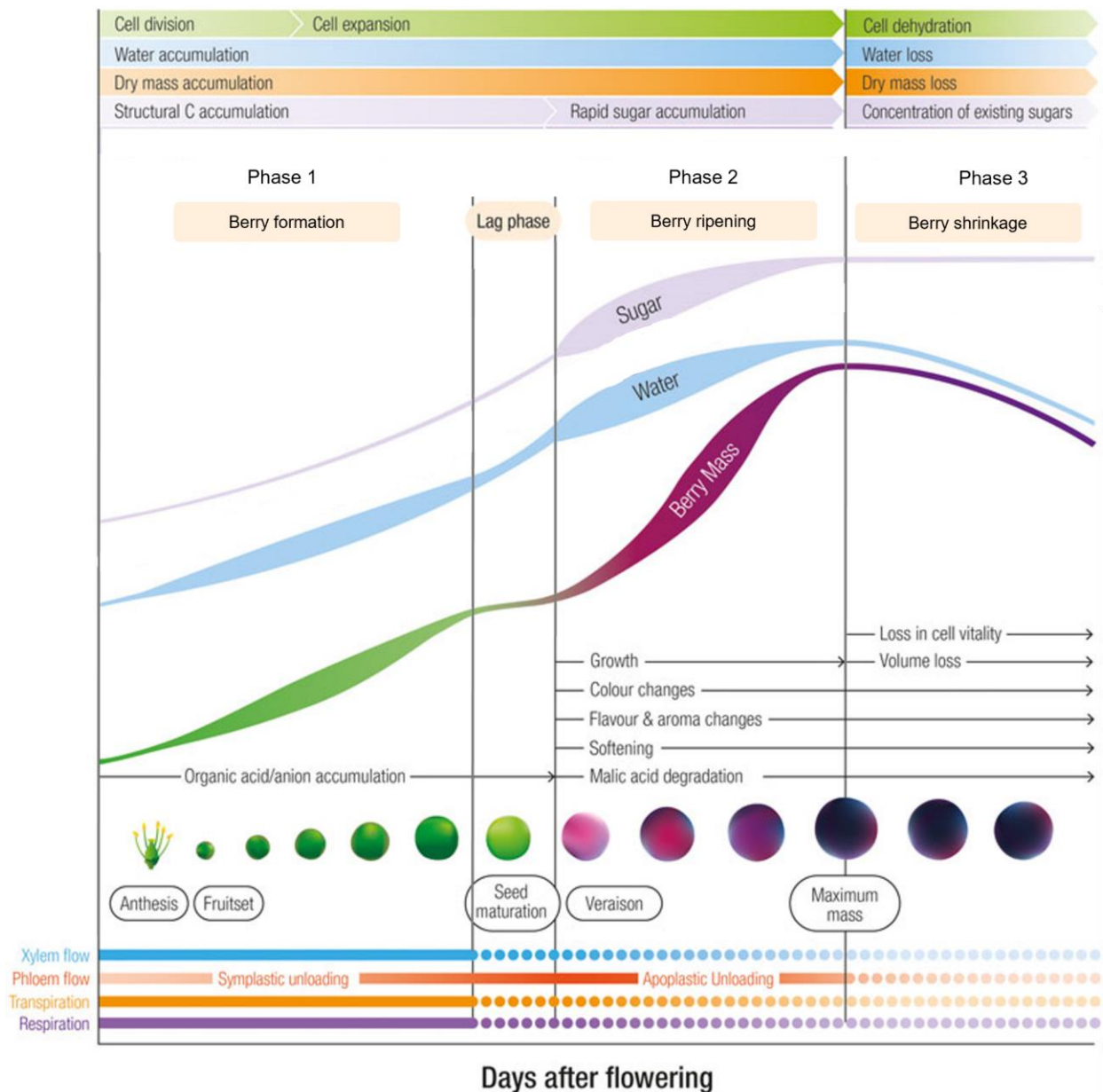
Figure 3 Summary of grape berry development stages with relative berry weight. Three phases can be identified based on changes in the rate of change of berry weight. *Phase* 1 (berry formation) is defined from flowering to veraison, *phase* 2 (berry maturation) starts from veraison to peak berry weight, *phase* 3 is indicated by cell death in mesocarp, and berry weight loss in some varieties such as Shiraz (Sadras & McCarthy, 2007; Tilbrook & Tyerman, 2008). Figure has been modified from Rogiers et al. (2017) and under the terms of the Creative Commons Attribution License (CC BY), https://www.frontiersin.org/journals/plant-science/articles/10.3389/fpls.2017.01629/full).

There is a lag phase between *Phase* 1 and *Phase* 2, lasting about one week. After that, *Phase* 2 'berry ripening' begins with 'veraison', termed by Coombe (1992) to generically describe a stage when dramatic changes in berry composition, structure and appearance take place (Coombe, 1992; Dry & Coombe, 2004). These events together mark the onset of berry ripening, e.g., the onset of berry softening, sugar accumulation, a decrease of tannin level in seeds and skins, accelerated berry growth and colour change of the berry skin for black grape varieties (Coombe, 1992; Dry & Coombe, 2004). Seeds reach full size and maximum fresh mass at the beginning of veraison, while maximum dry seed mass coincides with maximum berry mass later on (Ristic & Iland, 2008).

During *Phase* 2 'berry ripening', berry growth resumes intensely at the beginning but is only supported by cell expansion that slows gradually (Ollat et al., 2002). The accumulation of sugars in flesh and skins, potassium and phenolics in skins (including anthocyanins in black grapes) mainly happens in this phase (Coombe & McCarthy, 1997, 2000; Rogiers et al., 2017). Peak berry mass (and dry seed mass) is achieved at the end of this phase (Ristic & Iland, 2008; Sadras & McCarthy, 2007). Water inflow is dominated via the phloem, although the xylem is still functional (Fuentes et al., 2010; Rogiers et al., 2006; Tilbrook & Tyerman, 2006, 2009; Tyerman et al., 2008). Phloem unloading changes from a symplasmic to apoplasmic pathway during veraison in the hybrid grape (*Vitis vinifera* x *Vitis labrusca*), corresponding to an increase in cell wall invertases (Zhang et al., 2006). During this phase rapid sugar accumulation dominates the osmotic potential of berry cells, leading to more negative osmotic potential, high water uptake to the living cells of the berry, and a significant increase in berry volume and mass (Fuentes et al., 2010).

Phase 3 'berry shrinkage' only occurs in some grape varieties, typically Shiraz and Cabernet Sauvignon, late in ripening after peak mass (Fuentes et al., 2010; McCarthy, 1997, 1999; Rogiers et al., 2006; Tilbrook & Tyerman, 2006, 2009; Tyerman et al., 2008). It starts with a loss of fresh mass and volume, and then berry shrivel gradually becomes visible (*ibid*). Commercially desirable winemaking flavour ripeness and phenolic maturity are expected to take place during part of this

phase, which makes early harvest not really an alternative to avoid berry shrinkage (Coombe & McCarthy, 1997). Not enough is presently known about the phenomenon in Cabernet Sauvignon other than its association with warming conditions and berry exposure to determine the impacts on wine making and the timing of harvest (Krasnow et al., 2008; Pagay, 2018).

In addition to late-ripening shrinkage/shrivel disorder, there are several other ripening disorders related to loss of berry mass in *Vitis vinifera* L. These include sunburn, late-season bunch stem necrosis, and sugar accumulation disorder (SAD) (B. R. Bondada & Keller, 2012; Krasnow et al., 2010). Each of these have distinct morpho-anatomic features, shrivelling dynamics and berry composition at onset (B. R. Bondada & Keller, 2012; Krasnow et al., 2010).

4. Cause of late ripening grape berry shrinkage

4.1. Water loss

McCarthy and Coombe (1999) found that the loss of water rather than loss of dry matter accounted for most of the loss in Shiraz berry mass by calculating the components of berry mass during late ripening. It was further verified that nearly 90% of loss of mass was accounted for by water loss with some loss in dry mass accounted for by berry respiration (Rogiers et al., 2000).

Water movement from the berry back to the parent vine via the xylem vessels (backflow) along with transpiration could be a significant reason for water loss during berry shrinkage (Rogiers, Hatfield, Jaudzems, et al., 2004; Tilbrook & Tyerman, 2009; Tyerman et al., 2008). Backflow has been observed directly by dyes applied to the stylar end of post veraison berries that are subsequently observed in the xylem (Keller, 2006; Rogiers, Hatfield, & Keller, 2004; Tilbrook & Tyerman, 2009; Tyerman et al., 2008). By measuring the conductance for outflow from the berry and stem water potential, Tilbrook and Tyerman (2009) suggested that 30% of the weight loss of an average sized berry could be achieved after one week with a weight loss of 43 mg (approximately 7% of berry

volume) per day. Estimates of backflow for post veraison berries of Chardonnay based on hydraulic resistances of the berry and diurnal water potential gradients were between about 50 to 400 µL per day (Choat et al., 2009). More detailed investigation of the pedicel xylem and hydraulic conductance showed that water flow in both directions through the pedicel, although impeded during berry development by blockages and not air embolisms, could continue late into berry ripening (Knipfer et al., 2015).

Transpiration may also contribute to some extent, but weight loss during the late ripening of Shiraz berries was not the result of cuticle disruption or high transpiration rates alone (Rogiers, Hatfield, Jaudzems, et al., 2004). Grape berries cannot regulate transpiration regularly by stomata closure. The factors that determine transpiration rate are berry size and cuticular conductance, but predominantly vapour pressure deficit (VPD) (Y. Zhang & Keller, 2015). Water deficit can increase cuticular wax deposition in Gewürztraminer, but this did not change berry transpiration rates (Dimopoulos et al., 2020). Transpiration across the berry epidermis occurs throughout ripening but the rate progressively decreases dramatically after veraison (Rogiers et al., 2006; Rogiers, Hatfield, Jaudzems, et al., 2004; Scharwies & Tyerman, 2017; Y. Zhang & Keller, 2015). Even though transpiration rate of post veraison berries was only 16% of that of pre-veraison berries, transpiration could account for an average of 15 mg loss in fresh mass per berry per day (Rogiers, Hatfield, Jaudzems, et al., 2004). Another study also showed that transpiration could result in loss of 0.2 to 6% (3 to 100mg H_2O/day) of fresh berry mass daily (Y. Zhang & Keller, 2015).

Therefore, loss of berry mass and shrinkage can happen when loss of water from backflow along with transpiration continuously exceeds water uptake, which is dramatically decreased through both xylem and phloem late in ripening (McCarthy, 1999; Rogiers et al., 2006; Rogiers, Hatfield, Jaudzems, et al., 2004; Scharwies & Tyerman, 2017; Tilbrook & Tyerman, 2009; Tyerman et al., 2008; Y. Zhang & Keller, 2015). Berry shrinkage during the day in a diurnal cycle is observed in pre-veraison grapes on water stressed vines and less so in post-veraison grapes indicating that net water uptake can be

less than water loss on a daily basis but over time may be on average increasing or stable (Greenspan et al., 1996).

4.2. Water backflow and berry cell death

As living cells in the grape berry often have an intact semi-permeable cell membrane and large negative osmotic potential from high concentrations of dissolved solutes, water extraction from the berry would require relatively negative water potentials developed in the vine (Fuentes et al., 2010; Krasnow et al., 2008; Tilbrook & Tyerman, 2008).

Berry cell death in the mesocarp late in ripening was observed and also correlated with loss of mass (shrivel) in Shiraz. Berries with more dead cells tended to have more loss of mass (Bonada et al., 2013; Fuentes et al., 2010; Krasnow et al., 2008). Specifically, mesocarp cells in grape berries are mostly fully vital during 'berry formation' and early stages of 'berry maturation' (Bonada et al., 2013; B. Bondada, 2014; Tilbrook & Tyerman, 2009). At this stage, water inflow via the phloem is large, and the negative water/osmotic potential in the cell sap is effective in enabling cell expansion so that berry mass increases on average. However, a considerable osmotic potential in the apoplast will reduce the gradient for osmotic uptake of water and measurements suggest that solute content of the apoplast can be high (Keller & Shrestha, 2014). When cell death occurs, loss of berry cell vitality and membrane integrity will reduce or nullify the osmotic potential driving force so that berries are not able to balance xylem and apoplast tensions generated in the vine by leaf transpiration. Then large amounts of backflow can potentially occur when berries are still well connected hydraulically to the vine, as they are in Shiraz (Fuentes et al., 2010; Tilbrook & Tyerman, 2008, 2009).

The results from other varieties, Thompson seedless and Chardonnay, are consistent with this view (Tilbrook & Tyerman, 2009). Thompson seedless maintained nearly 100% vitality for all cells through development and well beyond full sugar ripeness. Thus very negative xylem pressure from the vine can be counteracted by the high osmotic pressure of berry cells (Tilbrook & Tyerman, 2008), and no berry mass loss and shrinkage occur even with high hydraulic conductance back to the vine.

Interestingly, Chardonnay also showed a similar cell death pattern to Shiraz but with almost no berry mass loss or shrinkage (Tilbrook & Tyerman, 2009). The possible reason is that Chardonnay is able to reduce hydraulic conductance to the vine during the period when cell death occurs in contrast to that of Shiraz (Tilbrook & Tyerman, 2009). In this way, Chardonnay could stop water flow back from the berry to the vine and almost entirely prevent berry shrinkage. Furthermore, a reduction in mesocarp cell viability during late ripening decreased the susceptibility of berries to splitting in response to wetting, confirming the loss of osmotic viability of the mesocarp cells (Clarke et al., 2010).

In conclusion, loss of berry mass appears to depend on the following processes occurring together: 1) Loss of berry cell vitality and loss of membrane semi-permeability, 2) Sufficient hydraulic conductivity for water to move back from berries via the xylem to the parent vine, 3) Decrease of water inflow into berries by phloem, 4) continued berry transpiration.

5. Berry cell death

In plants, cell death means the end of homeostasis in cells and often involves the loss of cell membrane integrity (Noodén, 2004), loss of function of cytosol or autolysis of vacuoles (Thomas et al., 2003). The causes of plant cell death are diverse and can be influenced by various biotic and abiotic factors that affect the plant's physiology and metabolism.

Cell death in late ripening grape berries has been clearly demonstrated in several varieties, most often in Shiraz, where decreased membrane integrity is observed in the large mesocarp cells using vital dyes (Krasnow et al., 2008; Tilbrook & Tyerman, 2009; Tyerman et al., 2008) and electrolyte leakage across the berry observed using electrical impedance (Caravia et al., 2015). It mainly occurs in the mesocarp and usually starts from the locule area surrounding the seeds within the inner mesocarp (Fuentes et al., 2010).

The cause of grape berry cell death remains unknown. It is different from normal berry cell senescence (Woo et al., 2018), which occurs at a very late time often beyond harvest and in the 'abscission zone'(the berry-pedicel indentation), and not the area of the mesocarp around the seeds. Also, no invading pathogenic microorganism has so far been reported to be related to berry mesocarp cell death. Exposure to light and wind seems not to influence cell death and berry shrivel (Clarke & Rogiers, 2019). However, some studies have revealed factors that can influence cell death, for example, high temperature, water stress and hypoxia inside the grape berry (Bonada et al., 2013; Krasnow et al., 2008; Xiao, Liao, et al., 2018).

5.1. Heatwave impacts

Heatwaves may play an important role in grape berry cell death. Both high temperature and water deficit were observed to induce and/or increase cell death and shrinkage in Shiraz and Chardonnay berries (Bonada et al., 2013; Xiao, Liao, et al., 2018). These authors also demonstrated a correlation between cell death and thermal time after anth]esis (°C d) with rapid cell death tending to occur after approximately 1000 (°C d) from anthesis. An application like overhead shading was reported to significantly ameliorate berry cell death and shrinkage through decreased heat stress (Caravia et al., 2016). More generally, even a few minutes of high-temperature exposure can lead to cellular damage (Hulands et al., 2014; Krasnow et al., 2010; Wahid et al., 2007). After long-term exposure, moderate temperatures can also cause berry injury or death (Wahid et al., 2007). The lethal temperature limit for most plant tissues is widely recognised as 1 minute at 60°C (Agee 1993, Dickinson and Johnson 2004, Michaletz and Johnson 2007). Black grape bunch temperatures could reach about 15 °C above ambient temperature when in direct light (Ponce de León & Bailey, 2021); in Australia, the maximum ambient temperature during a heatwave can easily be over 45 °C.

Berry shrinkage and cell death could be more serious in the future under the influence of 'global warming' from its dual impacts on grapevines. Firstly, vine phenology has moved earlier because of 'global warming', which is causing the critical maturation period to shift into warmer and drier

periods of the growing season (Bonada et al., 2013; Caravia et al., 2016; Petrie & Sadras, 2008; Webb et al., 2011). In addition, frequent and severe higher temperatures and droughts are predicted to occur in the future in many wine regions around the world, especially warm regions in Australia (Perkins et al., 2012; Webb et al., 2011).

5.2. Hypoxia influence

A link was found between mesocarp cell death and hypoxia/anoxia in the grape berry (Xiao, Rogiers, et al., 2018; Xiao, Liao, et al., 2018). Both grape berry internal oxygen concentration and cell vitality decline with fruit ripeness, and the minimum oxygen concentration even decreased to near zero (*ibid*). Also, the central mesocarp areas between the central axis and the grape berry skin had the lowest oxygen concentration ($[O_2]$) and the highest level of cell death (*ibid*). Moreover, when covering chardonnay berry pedicles with silicone grease to block oxygen diffusion into the berry via the obvious lenticels, hypoxia occurred in the centre of the berry, cell death increased, and ethanol accumulation increased (*ibid*). This also indicated the occurrence of alcoholic fermentation inside the berry due to hypoxia. In contrast Ruby seedless, a table grape variety not displaying cell death and berry shrivel, appeared to have more oxygen and less hypoxia inside berries, although steep $[O_2]$ gradients and hypoxia still existed (Xiao, Rogiers, et al., 2018). Consistent with this view, another study found that when water stress was applied to Shiraz, the internal $[O_2]$ decreased, while berry cell death and ethanol accumulation increased (Xiao, Liao, et al., 2018). On the other hand, hypoxia may also interact with heatwaves to accelerate berry cell death. High temperature accelerates O_2 consumption in cells where respiration rate essentially doubles for every 10 °C increase (approx.) in temperature (Atkin, 2003; Geigenberger, 2003).

5.3. Respiration

Mitochondrial respiration is a metabolic process of interlinked enzyme- and membrane-dependent reactions (Scafaro et al., 2021). It is central to plant physiology and occurs in the mitochondria during the day and the night in all parts of plants. Plants utilise aerobic respiration to provide energy from

sugars that is transiently stored in adenosine triphosphate (ATP) for all cellular processes, including metabolism, catabolism, and maintaining membrane structures and functions (Bailey-Serres & Voesenek, 2008; Gibbs & Greenway, 2003; Greenway & Gibbs, 2003). Respiration also plays a central role in the synthesis and recycling of primary metabolites such as nitrogenous compounds, amino acids and growth regulatory factors (Scafaro et al., 2021). In its absence, death will occur (Scafaro et al., 2021).

It has been long recognized that respiration is temperature sensitive; respiration rate essentially doubles for every 10 °C increase (approx.) in temperature (Atkin, 2003; Geigenberger, 2003). While excessive heat can inactivate respiratory enzymes and make membranes become overly fluid. Such changes can ultimately lead to the total breakdown of the respiration system (Scafaro et al., 2021).

Mitochondrial respiration uses oxygen as a terminal electron acceptor and pyruvate supplied by carbohydrate breakdown via glycolysis, which also produces a small amount of ATP (Bailey-Serres & Voesenek, 2008; Geigenberger, 2003). When O_2 concentrations drop to low levels (hypoxia) or are completely depleted (anoxia), oxidative respiration stops due to the lack of the terminal electron acceptor (O_2). At the same time, cytoplasmic pH drops, and the activity of the two fermentation enzymes pyruvate decarboxylase and alcohol dehydrogenase, increases. These can also metabolise accumulating pyruvate allowing glycolysis to produce a small amount ATP needed to maintain cell-membrane integrity and minimal functions, with ethanol produced in the cell's cytoplasm (*ibid*). Therefore, ethanol synthesis as a by-product is physiologically linked to anaerobic respiration.

6. Ethanol accumulation as an indicator of cell death

Ethanol synthesis from alcoholic fermentation, has been reported to increase in response to various stresses, including heat and drought (Bashir et al., 2022; Fan et al., 2011; Kelsey & Westlind, 2017; Matsui et al., 2022), mostly as a consequence of disruption of aerobic respiration, due in part to low

oxygen concentration, disruption to mitochondrial membrane function and enzyme activity (Kelsey & Westlind, 2017). The concentrations of ethanol accumulated reflected the degree of heat-induced fruit injury in apples (Fan et al., 2005) and in tree stems and woody tissues (Kelsey & Westlind, 2017). When the temperature rises above a threshold (such as 50°C), all the enzyme-regulated activities, including the production of ethanol involving pyruvate decarboxylase and alcohol dehydrogenase are likely to be inhibited (Kelsey & Westlind, 2017; Seidel, 1986). Hypoxia occurred in the centre of Chardonnay berries when oxygen diffusion into the berry was blocked by covering the obvious lenticels with silicone grease (Xiao, Rogiers, et al., 2018). Cell death increased, and ethanol accumulation increased, indicating the occurrence of alcoholic fermentation inside the berry due to hypoxia (*ibid*). Therefore, ethanol accumulation can be used as an indicator of berry stress due to hypoxia and/or heat stress at less extreme temperatures (< 50 °C).

Generally, ethanol synthesis from alcoholic fermentation does not result in ethanol accumulation to toxic levels although a high concentration in cells could disturb cell function by damaging lipid bilayers and increasing membrane permeability (Saltveit, 1989) and impair mitochondrial membrane function (Romieu et al., 1992). Even a concentration of 390 mM ethanol failed to simulate flooding injury in peas (Jackson et al., 1982). Total ethanol accumulation under anaerobic conditions could range from 15 to 150 mM in cottonwood roots and leaves (Chen et al., 2020). The maximum ethanol concentration ([EtOH]) reported in Chardonnay berries was 32.5 mM when lenticels were blocked (Xiao, Rogiers, et al., 2018). When berries were kept in an anaerobic atmosphere from several hours to several days at 30 °C, up to about 195 mM and 220 mM were observed in two studies respectively (Saltveit & Ballinger, 1983; Tesnière et al., 1994).

7. Porosity and gas exchange in grape berries (Micro-CT)

Steep oxygen gradients and hypoxia are common in many fruits under ambient oxygen concentrations, like in apples and pears (Cukrov, 2018). In grape berries, the $[O_2]$ gradients and hypoxia have only been studied in one dimension, with $[O_2]$ measured in one position in the very middle of the berry (Xiao, Rogiers, et al., 2018). For Shiraz, the variety that is prone to cell death, $[O_2]$ was only measured to a maximum depth of 1.5 mm from inside the berry skin to avoid the fragile electrode tip hitting the seeds (*ibid*). A two-dimensional $[O_2]$ distribution mapping within grape berries at different development stages remains to be elaborated.

Many factors can influence the internal $[O_2]$ in fruit, including the length of the transport pathway, the conductivity for gas transport of the tissue, and the oxygen consumption rate of the cells (Burg & Burg, 1965; Cameron & Yang, 1982; Ho et al., 2008; Ho, Verlinden, Verboven, & Nicolaï, 2006; Ho, Verlinden, Verboven, Vandewalle, et al., 2006; Lammertyn et al., 2001; Schotsmans et al., 2003). Plants do not have an active distribution system to transport O_2 in fruits; O_2 transport depends on passive transport according to Fick's law of diffusion, the movement of O_2 from high to low concentration drives the diffusion process (*ibid*). The conductivity of the tissue within fruits is to a large extent dependent on the porosity of the tissue (gas volume/tissue volume) (Cukrov, 2018). Tissue with higher porosity tends to have enhanced efficiency of O_2 diffusion (W. Armstrong, 1980; Cukrov, 2018). Like other fruit, grape berry mesocarp can be regarded as a porous medium with air spaces distributed in between the cells and gas transport goes mainly through the air spaces (Herremans et al., 2015; Ho et al., 2008; van Dongen & Licausi, 2015).

As mentioned previously, O_2 uptake and other gas exchange in fruits is primarily determined by tissue microstructure, which can be visualised and quantified by X-ray micro-computed tomography (Micro-CT). In general, 3-dimensional (3D) Micro-CT imaging is a non-destructive imaging method utilizing X-rays allowing the rapid digitisation of the 3D structure of a sample (Keklikoglou et al., 2021).

Although Micro-CT has been widely used in plant physiology for decades, only a few reports have studied the voids in grape berries and flowers (Xiao et al., 2021; Xiao, Rogiers, et al., 2018). They demonstrated that the porous network of the berry pedicel junction might provide an important pathway for gas exchange inside grape berries, including oxygen transfer (*ibid*). However, these studies only scanned berries at later development stages and under relatively low resolution. As the oxygen concentration showed variety and development stage differences, it would be worthwhile studying grape berry microstructure of different varieties at different development stages.

8. Applications to monitor and ameliorate berry mass loss and cell death

8.1. Monitoring berry mass and shrinkage

Loss of Shiraz berry mass was observed well before visible shrivel was observed, and before desirable wine-making flavour ripeness and phenolic maturation were achieved (McCarthy, 1997; McCarthy & Coombe, 1999; Sadras & McCarthy, 2007). With the predicted impacts of global warming, it would be helpful to monitor the onset of berry shrinkage and to be able to predict its onset for grape growers.

Sadras and McCarthy (2007) developed one allometric model of sugar per berry with fresh berry mass rather than time to indicate the onset of shrinkage. Allometric or scaling analysis deals with the differential growth rates of the organs of plants and animals (e.g., leaf vs root, liver vs heart) or process (e.g., body size vs metabolic rate) (McConnaughay & Coleman, 1999). Sadras and McCarthy (2007) demonstrated that the slope of the regression between the amount of sugar per berry and berry mass on a log-log scale was greater than 1 in *Phase* 2 (berry ripening) while smaller than 1 in *Phase* 3 (shrinkage), based on the relative rate of sugar accumulation per berry and the relative rate of fresh mass accumulation in the two phases. However, like other methods using time or change in mass as predictors of berry shrinkage, the determination of the onset of shrinkage relies on continuous data collection during the whole of berry development and is lagged to some extent, especially when sugar

accumulation compensates for water loss. Therefore, a better method for prediction of berry shrinkage that is less technically time consuming would be useful for the industry.

Utilising the significant variation in time of berry development that can naturally occur in the vineyard, a single date sampling using an allometric model of total soluble solids and berry fresh mass could be developed that may indicate progression from *Phase* 2 to *Phase* 3. Uneven ripening in *Vitis vinifera* commonly occurs between berries within a bunch, between bunches within a vine, between vines within the vineyard, and between vineyards although differences decrease throughout berry development, although they may become more synchronised at late stages (Amerine & Roessler, 1958; C. E. J. Armstrong et al., 2023; Deloire et al., 2019; Previtali et al., 2021; Shahood et al., 2020). A variation could arise at any time during the development of the ovary/berry, from initiation of the floral primordia before budburst to berry senescence (*ibid*). A one-time sampling method at a predicted time based on climatic conditions from veraison and previous history for the vineyard may be a more time efficient method to monitor the onset of berry shrinkage and to make decisions regarding irrigation and final harvest.

8.2. Techniques to ameliorate heat stress

There are many techniques to ameliorate heat stress by decreasing heat on berries in the field, for example, trellis design and use of foliage wires, irrigation strategy, and chemical sprays, i.e., sun protection agents (e.g., Kaolin) (Dry, 2009). In the establishment of new vineyards, rootstocks and scion varieties with better heat and drought tolerance may be used, as well as row orientation, which is being done in the Coonawarra to help control berry shrivel in Cabernet Sauvignon (*ibid*). Some vineyard interventions to alleviate heat stress such as over-head shading (Caravia et al., 2016) or in-canopy micro sprinklers (Caravia et al., 2017) are reported to mitigate cell death and loss of berry mass. However, the impact of other techniques on cell death and shrinkage in grape berries is still not understood.

8.2.1. Canopy orientation and Rootstock

In the case of vine rows aligned in a north-south direction, it was observed that berry clusters located on the western side of the vines, especially those directly exposed to the afternoon sun, generally exhibited higher average temperatures compared to clusters facing east ((Ponce de León & Bailey, 2021; Smart & Sinclair, 1976; Spayd et al., 2002).

The adoption of rootstocks in viticulture began as a response to the extensive devastation of European vineyards following the accidental introduction of grape phylloxera during the mid-19th century (Ordish, 1972). Rootstocks have since been developed for other traits such as drought tolerance, lime tolerance, salt tolerance, and influence on scion vigour and fruit maturity (Galet, 1998; Pongrácz, 1983). Drought-tolerant rootstocks with high vigour may have decreased berry cell death and less late ripening shrinkage under water stress and high temperatures with a combination of better water uptake and larger canopy size (Bonilla et al., 2015; De la Fuente et al., 2007; Dry & Coombe, 2005). It was noted that Shiraz scion grafted onto the drought-tolerant rootstock Ramsey showed a delayed shrinkage compared to when grafted on rootstock 101-14 Mgt (Rogiers, Hatfield, & Keller, 2004). Similarly, Singh (2010) observed that Thompson Seedless scion grafted onto the Schwarzmann rootstock, which has lower drought tolerance, was more susceptible to cell death and berry collapse compared to when it was grafted onto Ramsey. The impact of drought-tolerant rootstock and canopy orientation on cell death and shrinkage in Shiraz berries is still not understood.

8.2.2. Application of anti-transpirants

The antitranspirants, Di-1-p-menthene ($C_{20}H_{34}$) (also known as Pinolene) and Kaolin ($A_{l4}Si_4O_{10}(OH)_8$) are two types of organic film-forming compounds applied to plants to improve water use efficiency, and both were considered to be inactive from a biochemical point of view (Brillante et al., 2016; Cantore et al., 2009; Mphande et al., 2023). Pinolene is an emulsifiable terpenic polymer derived from the distillation of pine resins. After spraying, it forms a flexible, glossy and clear film that acts as a physical barrier to limit plant transpiration and water loss (Palliotti et al.,

2010). Pinolene was also observed to reduce Shiraz leaf transpiration and water loss from Merlot bunches in Australia (Fahey, 2018), but its influence on cell death remains unknown. Kaolin is a non-abrasive, non-toxic white clay-based aluminium silicate with excellent reflective properties (Cantore et al., 2009; Mphande et al., 2023). Kaolin can be dissolved into water and sprayed on the leaf or berry, leaving a thin deposit on the surface that can reflect UV and infrared radiation to reduce leaf and berry surface temperature (*ibid*). The effect of direct treatment on Shiraz bunches has not been reported and it is not known how antitranspirants may affect berry oxygen concentrations and cell death.

9. Scope and aims of this thesis

This thesis presented an opportunity to explore the mechanisms of grape berry cell death and berry shrivel, and to determine how they may be linked. The focus was on Shiraz berries for which three seasons of berry development measurements were taken on field-grown vines on different rootstocks to test the hypothesis that rootstock and bunch position may affect cell death and shrinkage. Detailed berry microstructure (porosity) using micro-CT was performed to understand how oxygen was distributed inside berries as measured in greater detail using oxygen microelectrodes. Based on the variations in temperature between the three seasons, and ethanol accumulation resulting from hypoxia and heat stress, it was possible to build a better predictive model of cell death. To add further insight into the physiological mechanisms of berry cell death and shrinkage different varieties were compared that were known to have variation in cell death and shrinkage. The study allowed investigation of applications to ameliorate berry shrinkage and dell death, and to develop methods of prediction and monitoring.

Research aims/ objectives

Chapter 2: a) Directly measure and map $[O_2]$ distribution in 2-dimensions at greater resolution than previously attained in different grape varieties at different development stages in order to determine the source of oxygen and direction of oxygen diffusion; b) Investigate the porosity of grape berries by high resolution Micro-CT; c) Further explore the link between variety, mesocarp cell death, hypoxia, and porosity.

Chapter 3: a) Test the influences of rootstocks (of different drought tolerance and vigour) and bunch orientation (east versus west, for north south vine rows) on Shiraz berry shrinkage and cell death; b) Identify the physiological cause of berry mesocarp cell death by exploring the correlation between temperature, ethanol accumulation and berry mesocarp cell death across different grape varieties; c) Develop one easy model to monitor berry development at different phases by allometric analysis between berry sugar and fresh mass accumulation.

Chapter 4: Identify the effects of two film-forming antitranspirant coatings, Kaolin and Pinolene, on berry cell death and loss of mass in Shiraz and Grenache, by testing their impacts on $[O_2]$, ethanol concentration [EtOH] and bunch temperature. It was hypothesised that both treatments may block oxygen uptake into berries by virtue of their impermeable barrier nature, as well as water loss resulting in a more complicated response in berry cell death and berry shrivel.

10. Significance/contribution to the discipline

Understanding the microstructure and oxygen distribution of grape berries will add valuable information to berry physiology and help understand the trigger of cell death in berries of some grape varieties. Models to predict cell death and berry shrinkage will help growers to better monitor the berry ripening process to produce fruit with balanced development and water retention. Kaolin and Pinolene spray were tested to provide useful information on effectiveness of this method for reducing adverse effects caused by heatwaves.

11. References

Amerine, M. A., & Roessler, E. B. (1958). Methods of determining field maturity of grapes. *American Journal of Enology and Viticulture*, *9*(1), 37–40. https://doi.org/10.5344/ajev.1958.9.1.37

Armstrong, C. E. J., Previtali, P., Boss, P. K., Pagay, V., Bramley, R. G. V., & Jeffery, D. W. (2023). Grape heterogeneity index: Assessment of overall grape heterogeneity using an aggregation of multiple indicators. *Plants*, *12*(7), Article 7. https://doi.org/10.3390/plants12071442

Armstrong, W. (1980). Aeration in higher plants. In H. W. Woolhouse (Ed.), *Advances in Botanical Research* (Vol. 7, pp. 225–332). Academic Press. https://doi.org/10.1016/S0065-2296(08)60089-0

Atkin, O. (2003). Thermal acclimation and the dynamic response of plant respiration to temperature. *Trends in Plant Science*, *8*(7), 343–351. https://doi.org/10.1016/S1360-1385(03)00136-5

Bailey-Serres, J., & Voesenek, L. A. C. J. (2008). Flooding stress: Acclimations and genetic diversity. *Annual Review of Plant Biology*, *59*(1), 313–339. https://doi.org/10.1146/annurev.arplant.59.032607.092752

Bashir, K., Todaka, D., Rasheed, S., Matsui, A., Ahmad, Z., Sako, K., Utsumi, Y., Vu, A. T., Tanaka, M., Takahashi, S., Ishida, J., Tsuboi, Y., Watanabe, S., Kanno, Y., Ando, E., Shin, K.-C., Seito, M., Motegi, H., Sato, M., … Seki, M. (2022). Ethanol-mediated novel survival strategy against drought stress in plants. *Plant and Cell Physiology*, *63*(9), 1181–1192. https://doi.org/10.1093/pcp/pcac114

Bioletti, F. (1938). Outline of ampelography for the vinifera grapes in California. *Hilgardia*, *11*(6), 227–293.

Bonada, M., Sadras, V. O., & Fuentes, S. (2013). Effect of elevated temperature on the onset and rate of mesocarp cell death in berries of Shiraz and Chardonnay and its relationship with berry shrivel: Thermal shift on mesocarp cell death and shrivel. *Australian Journal of Grape and Wine Research*, *19*(1), 87–94. https://doi.org/10.1111/ajgw.12010

Bondada, B. (2014). Structural and compositional characterization of suppression of uniform ripening in grapevine: A paradoxical ripening disorder of grape berries with no known causative clues. *Journal of the American Society for Horticultural Science*, *139*(5), 567–581. https://doi.org/10.21273/JASHS.139.5.567

Bondada, B. R., & Keller, M. (2012). Not all shrivels are created equal—Morpho-anatomical and compositional characteristics differ among different shrivel types that develop during ripening of grape (*Vitis vinifera* L.) berries. *American Journal of Plant Sciences*, *03*(07), 879–898. https://doi.org/10.4236/ajps.2012.37105

Bonilla, I., Toda, F. M. de, & Martínez-Casasnovas, J. A. (2015). Unexpected relationships between vine vigor and grape composition in warm climate conditions. *OENO One*, *49*(2), Article 2. https://doi.org/10.20870/oeno-one.2015.49.2.87

Boss, P. K., Buckeridge, E. J., Poole, A., & Thomas, M. R. (2003). New insights into grapevine flowering. *Functional Plant Biology*, *30*(6), 593–606. https://doi.org/10.1071/fp02112

Breia, R., Vieira, S., da Silva, J. M., Gerós, H., & Cunha, A. (2013). Mapping grape berry photosynthesis by chlorophyll fluorescence imaging: The effect of saturating pulse intensity in different tissues. *Photochemistry and Photobiology*, *89*(3), 579–585. https://doi.org/10.1111/php.12046

Brillante, L., Belfiore, N., Gaiotti, F., Lovat, L., Sansone, L., Poni, S., & Tomasi, D. (2016). Comparing kaolin and pinolene to improve sustainable grapevine production during drought. *PLOS ONE*, *11*(6), e0156631. https://doi.org/10.1371/journal.pone.0156631

Burg, S. P., & Burg, E. A. (1965). Gas exchange in fruits. *Physiologia Plantarum*, *18*(3), 870–884. https://doi.org/10.1111/j.1399-3054.1965.tb06946.x

Cameron, A. C., & Yang, S. F. (1982). A simple method for the determination of resistance to gas diffusion in plant organs. *Plant Physiology*, *70*(1), 21–23. https://doi.org/10.1104/pp.70.1.21

Cantore, V., Pace, B., & Albrizio, R. (2009). Kaolin-based particle film technology affects tomato physiology, yield and quality. *Environmental and Experimental Botany*, *66*(2), 279–288. https://doi.org/10.1016/j.envexpbot.2009.03.008

Caravia, L., Collins, C., Petrie, P. R., & Tyerman, S. D. (2016). Application of shade treatments during Shiraz berry ripening to reduce the impact of high temperature: Shade reduces impact of high temperature on Shiraz. *Australian Journal of Grape and Wine Research*, *22*(3), 422–437. https://doi.org/10.1111/ajgw.12248

Caravia, L., Collins, C., & Tyerman, S. D. (2015). Electrical impedance of Shiraz berries correlates with decreasing cell vitality during ripening: Impedance of Shiraz berries and cell vitality. *Australian Journal of Grape and Wine Research*, *21*(3), 430–438. https://doi.org/10.1111/ajgw.12157

Caravia, L., Pagay, V., Collins, C., & Tyerman, S. d. (2017). Application of sprinkler cooling within the bunch zone during ripening of Cabernet Sauvignon berries to reduce the impact of high temperature. *Australian Journal of Grape and Wine Research*, *23*(1), 48–57. https://doi.org/10.1111/ajgw.12255

Chen, Y., Althiab Almasaud, R., Carrie, E., Desbrosses, G., Binder, B. M., & Chervin, C. (2020). Ethanol, at physiological concentrations, affects ethylene sensing in tomato germinating seeds and seedlings. *Plant Science*, *291*, 110368. https://doi.org/10.1016/j.plantsci.2019.110368

Choat, B., Gambetta, G. A., Shackel, K. A., & Matthews, M. A. (2009). Vascular function in grape berries across development and its relevance to apparent hydraulic isolation. *Plant Physiology*, *151*(3), 1677–1687. https://doi.org/10.1104/pp.109.143172

Chou, H.-C., Šuklje, K., Antalick, G., Schmidtke, L. M., & Blackman, J. W. (2018). Late-season Shiraz berry dehydration that alters composition and sensory traits of wine. *Journal of Agricultural and Food Chemistry*, *66*(29), 7750–7757. https://doi.org/10.1021/acs.jafc.8b01646

Clarke, S. J., Hardie, W. J., & Rogiers, S. Y. (2010). Changes in susceptibility of grape berries to splitting are related to impaired osmotic water uptake associated with losses in cell vitality: Fruit splitting in the ripening grape berry. *Australian Journal of Grape and Wine Research*, *16*(3), 469–476. https://doi.org/10.1111/j.1755-0238.2010.00108.x

Clarke, S. J., & Rogiers, S. Y. (2019). The role of fruit exposure in the late season decline of grape berry mesocarp cell vitality. *Plant Physiology and Biochemistry*, *135*, 69–76. https://doi.org/10.1016/j.plaphy.2018.11.025

Considine, J. A., & Knox, R. B. (1979). Development and histochemistry of the pistil of the grape, *Vitis vinifera*. *Annals of Botany*, *43*(1), 11–22. https://doi.org/10.1093/oxfordjournals.aob.a085602

Coombe, B. G. (1976). The development of fleshy fruits. *Annual Review of Plant Physiology*, *27*(1), 207–228. https://doi.org/10.1146/annurev.pp.27.060176.001231

Coombe, B. G. (1992). Research on development and ripening of the grape berry. *American Journal of Enology and Viticulture*, *43*(1), 101–110. https://doi.org/10.5344/ajev.1992.43.1.101

Coombe, B. G., & McCarthy, M. G. (1997). Identification and naming of the inception of aroma development in ripening grape berries. *Australian Journal of Grape and Wine Research*, *3*(1), 18–20. https://doi.org/10.1111/j.1755-0238.1997.tb00111.x

Coombe, B. G., & McCarthy, M. G. (2000). Dynamics of grape berry growth and physiology of ripening. *Australian Journal of Grape and Wine Research*, *6*(2), 131–135. https://doi.org/10.1111/j.1755-0238.2000.tb00171.x

Cukrov, D. (2018). Progress toward understanding the molecular basis of fruit response to hypoxia. *Plants (Basel, Switzerland)*, *7*(4), E78. https://doi.org/10.3390/plants7040078

De la Fuente, M., Linares, R., Baeza, P., & Lissarrague, J. R. (2007). Efecto del sistema de conducción en climas semiáridos sobre la maduración, composición de la baya y la exposición de los racimos en *Vitis vinifera* L. cv. Syrah. *Revista Enología*, *4*(4), 1–9.

Deloire, A., Pellegrino, A., & Ristic, R. (2019). Grape sampling: Spatial distribution of berry fresh mass, seed number and sugar concentration on grapevine clusters of Shiraz: Discussion of potential consequences for sampling to monitor vineyard ripening. *Wine & Viticulture Journal*, *34*(2). https://doi.org/10.3316/informit.389267107371643

Dimopoulos, N., Tindjau, R., Wong, D., Matzat, T., Haslam, T., Song, C., Gambetta, G., Kunst, L., & Castellarin, S. D. (2020). Drought stress modulates cuticular wax composition of the grape berry (*Vitis vinifera* L.). *Journal of Experimental Botany*, *71*. https://doi.org/10.1093/jxb/eraa046

Dry, P. R. (2009). Bunch exposure management. In *Technical booklet*. Grape and Wine Research and Development Corporation.

Dry, P. R., & Coombe, B. G. (2004). Grapevine phenology. In *Viticulture Volume I - Resources, 2nd Edition* (pp. 150–166).

Dry, P. R., & Coombe, B. G. (2005). *Viticulture. Volume 1, Resources* (2nd ed., repr. with alterations). Winetitles.

Fahey, D. J. (2018). *Manipulating winegrapes with antitranspirants* (DPI 1702; p. 22). NSW Department of Primary Industries | Plant Systems.

Fan, L., Song, J., Forney, C. F., & Jordan, M. A. (2011). Fruit maturity affects the response of apples to heat stress. *Postharvest Biology and Technology*, *62*(1), 35–42. https://doi.org/10.1016/j.postharvbio.2011.04.007

Fan, L., Song, J., Forney, C., & Jordan, M. (2005). Ethanol production and chlorophyll fluorescence predict breakdown of heat-stressed apple fruit during cold storage. *Journal of the American Society for Horticultural Science. American Society for Horticultural Science*, *130*. https://doi.org/10.21273/JASHS.130.2.237

Fuentes, S., Sullivan, W., Tilbrook, J., & Tyerman, S. (2010). A novel analysis of grapevine berry tissue demonstrates a variety-dependent correlation between tissue vitality and berry shrivel: Variety-dependent berry vitality and shrivel. *Australian Journal of Grape and Wine Research*, *16*(2), 327–336. https://doi.org/10.1111/j.1755-0238.2010.00095.x

Galet, P. (1998). *Grape varieties and rootstock varieties*. [Translated from the French by J. Smith] Oenoplurimédia.

Geigenberger, P. (2003). Response of plant metabolism to too little oxygen. *Current Opinion in Plant Biology*, *6*(3), 247–256. https://doi.org/10.1016/S1369-5266(03)00038-4

Gibbs, J., & Greenway, H. (2003). Review: Mechanisms of anoxia tolerance in plants. I. Growth, survival and anaerobic catabolism. *Functional Plant Biology: FPB*, *30*(3), 353. https://doi.org/10.1071/PP98095_ER

Greenspan, M. D., Schultz, H. R., & Matthews, M. A. (1996). Field evaluation of water transport in grape berries during water deficits. *Physiologia Plantarum*, *97*(1), 55–62. https://doi.org/10.1111/j.1399-3054.1996.tb00478.x

Greenway, H., & Gibbs, J. (2003). Review: Mechanisms of anoxia tolerance in plants. II. Energy requirements for maintenance and energy distribution to essential processes. *Functional Plant Biology: FPB*, *30*(10), 999–1036. https://doi.org/10.1071/PP98096

Hardie, W. J., O'brien, T. P., & Jaudzems, V. G. (1996). Morphology, anatomy and development of the pericarp after anthesis in grape, *Vitis vinifera* L. *Australian Journal of Grape and Wine Research*, *2*(2), 97–142. https://doi.org/10.1111/j.1755-0238.1996.tb00101.x

Herremans, E., Verboven, P., Verlinden, B. E., Cantre, D., Abera, M., Wevers, M., & Nicolaï, B. M. (2015). Automatic analysis of the 3-D microstructure of fruit parenchyma tissue using X-ray micro-CT explains differences in aeration. *BMC Plant Biology*, *15*(1), 264. https://doi.org/10.1186/s12870-015-0650-y

Heywood, V. H. (1970). The cuticles of plants. *Micron (1969)*, *2*(4), 454. https://doi.org/10.1016/0047-7206(70)90020-8

Ho, Q. T., Verboven, P., Verlinden, B. E., Lammertyn, J., Vandewalle, S., & Nicolaï, B. M. (2008). A continuum model for metabolic gas exchange in pear fruit. *PLOS Computational Biology*, *4*(3), e1000023. https://doi.org/10.1371/journal.pcbi.1000023

Ho, Q. T., Verlinden, B. E., Verboven, P., & Nicolaï, B. M. (2006). Gas diffusion properties at different positions in the pear. *Postharvest Biology and Technology*, *41*(2), 113–120. https://doi.org/10.1016/j.postharvbio.2006.04.002

Ho, Q. T., Verlinden, B. E., Verboven, P., Vandewalle, S., & Nicolai, B. M. (2006). A permeation-diffusion-reaction model of gas transport in cellular tissue of plant materials. *Journal of Experimental Botany*, *57*(15), 4215–4224. https://doi.org/10.1093/jxb/erl198

Hulands, S., Greer, D. H., & Harper, J. I. (2014). The interactive effects of temperature and light intensity on *Vitis vinifera* cv. 'Semillon' grapevines. II. Berry ripening and susceptibility to sunburn at harvest. *European Journal of Horticultural Science*, *79*(1), 1–7.

Iland, I., P., Dry, P., Proffitt, T., & Tyerman, S. (2011). *The grapevine: From the science to the practice of growing vines for wine*. Patrick Iland Wine Promotions.

Jackson, M. B., Herman, B., & Goodenough, A. (1982). An examination of the importance of ethanol in causing injury to flooded plants. *Plant, Cell & Environment*, *5*(2), 163–172. https://doi.org/10.1111/1365-3040.ep11571590

Keklikoglou, K., Arvanitidis, C., Chatzigeorgiou, G., Chatzinikolaou, E., Karagiannidis, E., Koletsa, T., Magoulas, A., Makris, K., Mavrothalassitis, G., Papanagnou, E.-D., Papazoglou, A. S., Pavloudi, C., Trougakos, I. P., Vasileiadou, K., & Vogiatzi, A. (2021). Micro-CT for biological and biomedical studies: A comparison of imaging techniques. *Journal of Imaging*, *7*(9), Article 9. https://doi.org/10.3390/jimaging7090172

Keller, M. (2006). Ripening grape berries remain hydraulically connected to the shoot. *Journal of Experimental Botany*, *57*(11), 2577–2587. https://doi.org/10.1093/jxb/erl020

Keller, M., & Shrestha, P. M. (2014). Solute accumulation differs in the vacuoles and apoplast of ripening grape berries. *Planta*, *239*(3), 633–642. https://doi.org/org/10.1007/s00425-013-2004-z

Kelsey, R. G., & Westlind, D. J. (2017). Physiological stress and ethanol accumulation in tree stems and woody tissues at sublethal temperatures from fire. *BioScience*, *67*(5), 443–451. https://doi.org/10.1093/biosci/bix037

Knipfer, T., Fei, J., Gambetta, G. A., McElrone, A. J., Shackel, K. A., & Matthews, M. A. (2015). Water transport properties of the grape pedicel during fruit development: Insights into xylem anatomy and function using microtomography. *Plant Physiology*, *168*(4), 1590–1602. https://doi.org/10.1104/pp.15.00031

Krasnow, M., Matthews, M., & Shackel, K. (2008). Evidence for substantial maintenance of membrane integrity and cell viability in normally developing grape (*Vitis vinifera* L.) berries throughout development. *Journal of Experimental Botany*, *59*(4), 849–859. https://doi.org/10.1093/jxb/erm372

Krasnow, Matthews, M. A., Smith, R. J., Benz, J., Weber, E., & Shackel, K. A. (2010). Distinctive symptoms differentiate four common types of berry shrivel disorder in grape. *California Agriculture*, *64*(3), 155–159. https://doi.org/10.3733/ca.v064n03p155

Lammertyn, J., Franck, C., Verlinden, B. E., & Nicolaï, B. M. (2001). Comparative study of the O_2, CO_2 and temperature effect on respiration between 'Conference' pear cell protoplasts in suspension and intact pears. *Journal of Experimental Botany*, *52*(362), 1769–1777. https://doi.org/10.1093/jexbot/52.362.1769

Lendzian, K. J. (2006). Survival strategies of plants during secondary growth: Barrier properties of phellems and lenticels towards water, oxygen, and carbon dioxide. *Journal of Experimental Botany*, *57*(11), 2535–2546. https://doi.org/10.1093/jxb/erl014

Matsui, A., Todaka, D., Tanaka, M., Mizunashi, K., Takahashi, S., Sunaoshi, Y., Tsuboi, Y., Ishida, J., Bashir, K., Kikuchi, J., Kusano, M., Kobayashi, M., Kawaura, K., & Seki, M. (2022). Ethanol induces heat tolerance in plants by stimulating unfolded protein response. *Plant Molecular Biology*, *110*(1), 131–145. https://doi.org/10.1007/s11103-022-01291-8

McCarthy, M. G. (1997). The effect of transient water deficit on berry development of cv. Shiraz (*Vitis vinifera* L.). *Australian Journal of Grape and Wine Research*, *3*(3), 2–8. https://doi.org/10.1111/j.1755-0238.1997.tb00128.x

McCarthy, M. G. (1999). Weight loss from ripening berries of Shiraz grapevines (*Vitis vinifera* L. cv. Shiraz). *Australian Journal of Grape and Wine Research*, *5*(1), 10–16. https://doi.org/10.1111/j.1755-0238.1999.tb00145.x

McCarthy, M. G., & Coombe, B. G. (1999). Is weight loss in ripening grape berries cv. Shiraz caused by impeded phloem transport? *Australian Journal of Grape and Wine Research*, *5*(1), 17–21. https://doi.org/10.1111/j.1755-0238.1999.tb00146.x

McConnaughay, K. D. M., & Coleman, J. S. (1999). Biomass allocation in plants: Ontogeny or optimality? A test along three resource gradients. *Ecology*, *80*(8), 2581–2593. https://www.jstor.org/stable/177242

Mironeasa, S., Leahu, A., Codina, G., Silviu-Gabriel, S., & Mironeasa, C. (2010). Grape seed: Physicochemical, structural characteristic and oil content. *Journal of Agroalimentary Process and Technologies*, *16*(1), 1–6.

Mphande, W., Farrell, A. D., & Kettlewell, P. S. (2023). Commercial uses of antitranspirants in crop production: A review. *Outlook on Agriculture*, *52*(1), 3–10. https://doi.org/10.1177/00307270231155257

Noodén, L. D. (2004). *Plant cell death processes edited by Larry D. Noodén.* Boston.

Ollat, N., Carde, J.-P., Gaudillère, J.-P., Barrieu, F., Diakou-Verdin, P., & Moing, A. (2002). Grape berry development: A review. *OENO One*, *36*(3), Article 3. https://doi.org/10.20870/oeno-one.2002.36.3.970

Ordish, G. (1972). *The great wine blight.* JM Dent & Sons.

Pagay, V. (2018). *Is berry shrivel in Cabernet Sauvignon influenced by climate and does this potentially affect characteristics of the resulting wine?* (UA 1702). the University of Adelaide. https://limestonecoastwine.com.au/library/64-is-berry-shrivel-in-cabernet-sauvignon-influenced-by-climate-and-does-this-potentially-affect-characteristics-of-the-resulting-wine/

Palliotti, A., Poni, S., Berrios, J. G., & Bernizzoni, F. (2010). Vine performance and grape composition as affected by early-season source limitation induced with anti-transpirants in two red *Vitis vinifera* L. cultivars. *Australian Journal of Grape and Wine Research*, *16*(3), 426–433. https://doi.org/10.1111/j.1755-0238.2010.00103.x

Pate, J. S. (1975). Exchange of solutes between phloem and xylem and circulation in the whole plant. In M. H. Zimmermann & J. A. Milburn (Eds.), *Transport in Plants I* (pp. 451–473). Springer Berlin Heidelberg. https://doi.org/10.1007/978-3-642-66161-7_19

Perkins, S. E., Alexander, L. V., & Nairn, J. R. (2012). Increasing frequency, intensity and duration of observed global heatwaves and warm spells. *Geophysical Research Letters*, *39*(20), 2012GL053361. https://doi.org/10.1029/2012GL053361

Petrie, P. R., & Sadras, V. O. (2008). Advancement of grapevine maturity in Australia between 1993 and 2006: Putative causes, magnitude of trends and viticultural consequences. *Australian Journal of Grape and Wine Research*, *14*(1), Article 1. https://doi.org/10.1111/j.1755-0238.2008.00005.x

Ponce de León, M. A., & Bailey, B. (2021). A 3D model for simulating spatial and temporal fluctuations in grape berry temperature. *Agricultural and Forest Meteorology*, *306*, 108431. https://doi.org/10.1016/j.agrformet.2021.108431

Pongrácz, D. P. (1983). *Rootstocks for grape-vines.* David Philip.

Pratt, C. (1971). Reproductive Anatomy in cultivated grapes—A review. *American Journal of Enology and Viticulture*, *22*(2), 92–109. https://doi.org/10.5344/ajev.1971.22.2.92

Previtali, P., Dokoozlian, N., Capone, D., Wilkinson, K., & Ford, C. (2021). Exploratory study of sugar and C_6 compounds in single berries of grapevine (*Vitis vinifera* L.) cv. Cabernet Sauvignon throughout ripening. *Australian Journal of Grape and Wine Research*. https://doi.org/10.1111/ajgw.12472

Riederer, M., & Schreiber, L. (2001). Protecting against water loss: Analysis of the barrier properties of plant cuticles. *Journal of Experimental Botany*, *52*(363), 2023–2032. https://doi.org/10.1093/jexbot/52.363.2023

Ristic, R., & Iland, P. (2008). Relationships between seed and berry development of *Vitis vinifera* L. cv Shiraz: Developmental changes in seed morphology and phenolic composition. *Australian Journal of Grape and Wine Research*, *11*, 43–58. https://doi.org/10.1111/j.1755-0238.2005.tb00278.x

Rogiers, S. Y., Coetzee, Z. A., Walker, R. R., Deloire, A., & Tyerman, S. D. (2017). Potassium in the grape (*Vitis vinifera* L.) berry: Transport and function. *Frontiers in Plant Science*, *8*, 1629. https://doi.org/10.3389/fpls.2017.01629

Rogiers, S. Y., Greer, D. H., Hatfield, J. M., Orchard, B. A., & Keller, M. (2006). Solute transport into Shiraz berries during development and late-ripening shrinkage. *American Journal of Enology and Viticulture*, *57*(1), 73–80. https://doi.org/10.5344/ajev.2006.57.1.73

Rogiers, S. Y., Hatfield, J. M., Jaudzems, V. G., White, R. G., & Keller, M. (2004). Grape berry cv. Shiraz epicuticular wax and transpiration during ripening and preharvest weight loss. *American Journal of Enology and Viticulture*, *55*(2), 121–127. https://doi.org/10.5344/ajev.2004.55.2.121

Rogiers, S. Y., Hatfield, J. M., & Keller, M. (2004). Irrigation, nitrogen, and rootstock effects on volume loss of berries from potted Shiraz vines. *Vitis*, *43*(1), 1–6. https://doi.org/10.5073/vitis.2004.43.1-6

Rogiers, S. Y., Keller, M., Holzapfel, B. P., & Virgona, J. M. (2000). Accumulation of potassium and calcium by ripening berries on field vines of *Vitis vinifera* (L) cv. Shiraz. *Australian Journal of Grape and Wine Research*, *6*(3), 240–243. https://doi.org/10.1111/j.1755-0238.2000.tb00184.x

Romieu, C., Tesniere, C., Than-Ham, L., Flanzy, C., & Robin, J.-P. (1992). An examination of the importance of anaerobiosis and ethanol in causing injury to grape mitochondria. *American Journal of Enology and Viticulture*, *43*(2), 129–133. https://doi.org/10.5344/ajev.1992.43.2.129

Sadras, V. O., & McCarthy, M. G. (2007). Quantifying the dynamics of sugar concentration in berries of *Vitis vinifera* cv. Shiraz: A novel approach based on allometric analysis. *Australian Journal of Grape and Wine Research*, *13*(2), 66–71. https://doi.org/10.1111/j.1755-0238.2007.tb00236.x

Saika, H., Matsumura, H., Takano, T., Tsutsumi, N., & Nakazono, M. (2006). A point mutation of Adh1 gene is involved in the repression of coleoptile elongation under submergence in rice. *Breeding Science*, *56*(1), 69–74. https://doi.org/10.1270/jsbbs.56.69

Saltveit, M. E. (1989). Effect of alcohols and their interaction with ethylene on the ripening of epidermal pericarp discs of tomato fruit. *Plant Physiology*, *90*(1), 167–174. https://doi.org/10.1104/pp.90.1.167

Saltveit, M. E., & Ballinger, W. E. (1983). Effects of anaerobic nitrogen and carbon dioxide atmospheres on ethanol production and postharvest quality of 'Carlos' grapes. *Journal of the American Society for Horticultural Science*, *108*(3), 462–465. https://doi.org/10.21273/JASHS.108.3.462

Scafaro, A. P., Fan, Y., Posch, B. C., Garcia, A., Coast, O., & Atkin, O. K. (2021). Responses of leaf respiration to heatwaves. *Plant, Cell & Environment*, *44*(7), 2090–2101. https://doi.org/10.1111/pce.14018

Scharwies, J. D., & Tyerman, S. D. (2017). Comparison of isohydric and anisohydric (*Vitis vinifera* L. cultivars reveals a fine balance between hydraulic resistances, driving forces and transpiration in ripening berries. *Functional Plant Biology*, *44*(3), 324. https://doi.org/10.1071/FP16010

Schotsmans, W., Verlinden, B. E., Lammertyn, J., & Nicolaï, B. M. (2003). Simultaneous measurement of oxygen and carbon dioxide diffusivity in pear fruit tissue. *Postharvest Biology and Technology*, *29*(2), 155–166. https://doi.org/10.1016/S0925-5214(02)00251-X

Seidel, K. W. (1986). Tolerance of seedlings of ponderosa pine. Douglas-fir, grand fir, and engelmann spruce for high temperatures. *Northwest Science.*, *60*(1).

Shahood, R., Torregrosa, L., Savoi, S., & Romieu, C. (2020). First quantitative assessment of growth, sugar accumulation and malate breakdown in a single ripening berry. *OENO One*, *54*(4), Article 4. https://doi.org/10.20870/oeno-one.2020.54.4.3787

Shivashankara, K. S., Laxman, R. H., Geetha, G. A., Roy, T. K., Srinivasa Rao, N. K., & Patil, V. S. (2013). Volatile aroma and antioxidant quality of 'Shiraz' grapes at different stages of ripening. *International Journal of Fruit Science*, *13*(4), 389–399. https://doi.org/10.1080/15538362.2013.789235

Singh, D. (2010). *Causes and prevention of table grape berry collapse*. Horticulture Australia Ltd.

Smart, R. E., & Sinclair, T. R. (1976). Solar heating of grape berries and other spherical fruits. *Agricultural Meteorology (Netherlands)*, *17*(4), 241–259. https://doi.org/doi:10.1016/0002-1571(76)90029-7

Spayd, S., Tarara, J., Mee, D. L., & Ferguson, J. C. (2002). Separation of sunlight and temperature effects on the composition of *Vitis vinifera* cv. Merlot berries. *American Journal of Enology and Viticulture*, *53*(5), 171–182. https://doi.org/10.5344/ajev.2002.53.3.171

Šuklje, K., Zhang, X., Antalick, G., Clark, A. C., Deloire, A., & Schmidtke, L. M. (2016). Berry shriveling significantly alters Shiraz (*Vitis vinifera* L.) grape and wine chemical composition. *Journal of Agricultural and Food Chemistry*, *64*(4), 870–880. https://doi.org/10.1021/acs.jafc.5b05158

Tesnière, C., Romieu, C., Dugelay, I., Nicol, M. Z., Flanzy, C., & Robin, J. P. (1994). Partial recovery of grape energy metabolism upon aeration following anaerobic stress. *Journal of Experimental Botany*, *45*(1), 145–151. https://doi.org/10.1093/jxb/45.1.145

Thomas, H., Ougham, H. J., Wagstaff, C., & Stead, A. D. (2003). Defining senescence and death. *Journal of Experimental Botany*, *54*(385), 1127–1132. https://doi.org/10.1093/jxb/erg133

Tilbrook, J., & Tyerman, S. (2006). *Water, sugar and acid: How and where they come and go during berry ripening*. Australian Society of Viticulture and Oenology Seminar (2006 : Mildura, Vic.). https://www.semanticscholar.org/paper/Water%2C-sugar-and-acid%3A-how-and-where-they-come-and-Tilbrook-Tyerman/16c552dc41efba382364ac16876a1467499ddc78

Tilbrook, J., & Tyerman, S. D. (2008). Cell death in grape berries: Varietal differences linked to xylem pressure and berry weight loss. *Functional Plant Biology*, *35*(3), 173. https://doi.org/10.1071/FP07278

Tilbrook, J., & Tyerman, S. D. (2009). Hydraulic connection of grape berries to the vine: Varietal differences in water conductance into and out of berries, and potential for backflow. *Functional Plant Biology*, *36*(6), 541. https://doi.org/10.1071/FP09019

Tyerman, S. D., Tilbrook, J., Pardo, C., Kotula, L., Sullivan, W., & Steudle, E. (2008). Direct measurement of hydraulic properties in developing berries of *Vitis vinifera* L. cv Shiraz and Chardonnay. *Australian Journal of Grape and Wine Research*, *10*(3), 170–181. https://doi.org/10.1111/j.1755-0238.2004.tb00020.x

van Dongen, J. T., & Licausi, F. (2015). Oxygen sensing and signaling. *Annual Review of Plant Biology*, *66*(1), 345–367. https://doi.org/10.1146/annurev-arplant-043014-114813

Varela, C., Dry, P. r., Kutyna, D. r., Francis, I. l., Henschke, P. a., Curtin, C. d., & Chambers, P. j. (2015). Strategies for reducing alcohol concentration in wine. *Australian Journal of Grape and Wine Research*, *21*, 670–679. https://doi.org/10.1111/ajgw.12187

Wahid, A., Gelani, S., Ashraf, M., & Foolad, M. (2007). Heat tolerance in plants: An overview. *Environmental and Experimental Botany*, *61*(3), 199–223. https://doi.org/10.1016/j.envexpbot.2007.05.011

Walker, R., Chen, Z., Técsi, L., Famiani, F., Lea, P., & Leegood, R. (1999). Phosphoenolpyruvate carboxykinase plays a role in interactions of carbon and nitrogen metabolism during grape seed development. *Planta*, *210*, 9–18. https://doi.org/10.1007/s004250050648

Webb, L. B., Whetton, P. H., & Barlow, E. W. R. (2011). Observed trends in winegrape maturity in Australia. *Global Change Biology*, *17*(8), 2707–2719. https://doi.org/10.1111/j.1365-2486.2011.02434.x

Wilson, B., Strauss, C. R., & Williams, P. J. (1986). The distribution of free and glycosidically-bound monoterpenes among skin, juice, and pulp fractions of some white grape varieties. *American Journal of Enology and Viticulture*, *37*(2), 107–111. https://doi.org/10.5344/ajev.1986.37.2.107

Woo, H. R., Masclaux-Daubresse, C., & Lim, P. O. (2018). Plant senescence: How plants know when and how to die. *Journal of Experimental Botany*, *69*(4), 715–718. https://doi.org/10.1093/jxb/ery011

Xiao, Rogiers, S. Y., Sadras, V. O., & Tyerman, S. D. (2018). Hypoxia in grape berries: The role of seed respiration and lenticels on the berry pedicel and the possible link to cell death. *Journal of Experimental Botany*, *69*(8), 2071–2083. https://doi.org/10.1093/jxb/ery039

Xiao, Stait-Gardner, T., Willis, S. a., Price, W. S., Moroni, F. J., Pagay, V., Tyerman, S. D., Schmidtke, L. M., & Rogiers, S. Y. (2021). 3D visualisation of voids in grapevine flowers and berries using X-ray micro computed tomography. *Australian Journal of Grape and Wine Research*, *27*(2), 141–148. https://doi.org/10.1111/ajgw.12480

Xiao, Z., Liao, S., Rogiers, S. Y., Sadras, V. O., & Tyerman, S. D. (2018). Effect of water stress and elevated temperature on hypoxia and cell death in the mesocarp of Shiraz berries: Berry hypoxia and death under water/heat stress. *Australian Journal of Grape and Wine Research*, *24*(4), 487–497. https://doi.org/10.1111/ajgw.12363

Xie, Z., Fei, T., Forney, C. F., Li, Y., & Li, B. (2023). Improved maceration techniques to study the fruit vascular anatomy of grape. *Horticultural Plant Journal*, *9*(3), 481–495. https://doi.org/10.1016/j.hpj.2022.06.008

Zhang, X. Y., Wang, X.-L., Wang, X.-F., Xia, G.-H., Pan, Q.-H., Fan, R.-C., Wu, F.-Q., Yu, X.-C., & Zhang, D.-P. (2006). A Shift of Phloem Unloading from Symplasmic to Apoplasmic Pathway Is Involved in Developmental Onset of Ripening in Grape Berry. *Plant Physiology*, *142*(1), 220–232. https://doi.org/10.1104/pp.106.081430

Zhang, Y., & Keller, M. (2015). Grape berry transpiration is determined by vapor pressure deficit, cuticular conductance, and berry size. *American Journal of Enology and Viticulture*, *66*(4), 454–462. https://doi.org/10.5344/ajev.2015.15038

Chapter 2

2D oxygen distribution mapping and 3D Micro-CT analysis of grape

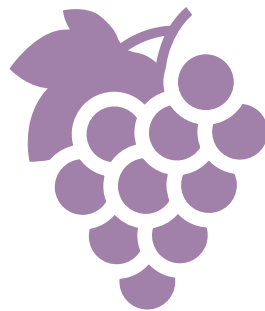**berries: Exploring the hypoxia link to mesocarp cell death across varieties**

Table of Contents

Note: All the Micro-CT Figures are in the PowerPoint file (From Figure 5 to Figure 13)

2D oxygen distribution mapping and 3D Micro-CT analysis of grape berries: Exploring the hypoxia link to mesocarp cell death across varieties

1. Introduction

Onset and rate of cell death in berry mesocarp of *Vitis vinifera* L. is variety dependent; very typical in Shiraz and becoming more common in Cabernet Sauvignon, while it rarely occurs in Grenache (Fuentes et al., 2010; Krasnow et al., 2008; Tilbrook & Tyerman, 2008). It correlates with late-ripening berry shrinkage, a common phenomenon in warm wine-growing regions (Bondada & Keller, 2012; Fuentes et al., 2010; Keller, 2006; Keller et al., 2015; Tilbrook & Tyerman, 2008). This can be manifested in grapes as excess sugar accumulation, lower anthocyanins, poor flavour development (e.g., lower terpenoids) (Shivashankara et al., 2013), and in wines, more dead/stewed fruit characters (Chou et al., 2018; Šuklje et al., 2016).

The cause of cell death in the berry mesocarp remains elusive, except for environmental factors such as heat stress and water stress, hypoxia in the grape berry has been reported to be related to it (Bonada et al., 2013; Krasnow et al., 2008; Xiao, Liao, et al., 2018; Xiao, Rogiers, et al., 2018). Hypoxia is often described as when the oxygen concentration limits aerobic respiration, usually between 1% and 5% of saturation (Loreti & Perata, 2020; Sasidharan et al., 2017), i.e., between about 2.7 µmol/L to 13.6 µmol/L. In grape berries, though [O_2] measurements were only conducted in one dimension from the very middle of the berry, steep oxygen concentration ([O_2]) gradients were observed from both the berry centre axis and the berry skin towards the mesocarp interior where the lowest [O_2] and even hypoxia often occurred (Xiao, Rogiers, et al., 2018). The central mesocarp areas between the central axis and the grape berry skin also had the highest level of cell death (Fuentes et al., 2010; Krasnow et al., 2008; Tilbrook & Tyerman, 2008). Besides, in Shiraz, although internal [O_2] was only measured to a maximum depth of 1.5 mm from the berry skin towards the berry centre, [O_2] and cell death were closely correlated where both grape berry internal [O_2] and cell vitality declined with fruit ripeness (Xiao, Rogiers, et al., 2018). In contrast, Ruby seedless, a table grape variety not displaying cell death

and berry shrivel, appeared to have more oxygen and less hypoxia inside berries, although steep [O_2] gradients and hypoxia still existed (Xiao, Rogiers, et al., 2018). So far only limited one-dimension of [O_2] profiles have been reported in grape berries. A better understanding of the cell death process linked to berry shrinkage may be revealed by combining higher resolution (two-dimension) of [O_2] profiles and berry microstructure at different development stages while also comparing different varieties with different degrees of cell death.

The [O_2] distribution within fruit and other plant organs is largely dependent on cell microstructure and features such as air spaces, oxygen diffusion barriers and structures such as lenticels (Armstrong et al., 2006; Raven, 1996). Plants do not have an active distribution system to transport oxygen in fruits. Oxygen uptake for fruit tissue mainly depends on passive transport according to Fick's law of diffusion, the concentration of O_2 ([O_2]) from high concentration to low concentration drives the diffusion process (Burg & Burg, 1965; Cameron & Yang, 1982; Ho et al., 2006, 2008; Lammertyn et al., 2001; Schotsmans et al., 2003). The efficiency of O_2 transport within fruits is to a large extent dependent on the porosity of the tissue (gas volume/tissue volume), where the air spaces between cells provide a low resistant pathway for diffusion (Cukrov, 2018; Ho et al., 2008; Rajapakse et al., 1990; van Dongen & Licausi, 2015).

Grape berry microstructure can be visualised and quantified by X-ray micro-computed tomography (Micro-CT). In general, Micro-CT imaging is a non-destructive imaging technique using X-rays allowing the rapid digitisation of the 3D structure of a sample with a relatively high resolution to 3 μm or less (Keklikoglou et al., 2021). Specifically, a rotating specimen is placed between an X-ray source and an X-ray detector, and a series of radiographs (projection images) of this specimen can be generated. Subsequently, these projection images are reconstructed into grey-scale cross-section images. The local density of the specimen structure is related to the attenuation coefficient of the X-rays that pass through the specimen, which affects the intensity of the grayscale value of a pixel of the reconstructed CT images. Low density structures have low X-ray attenuation, resulting in lower

greyscale intensity (darker), and *vice versa*. From these reconstructed CT images, the anatomical features can be revealed from simple image analyses, e.g., density, porosity and thickness, to advanced morphometric analysis and 3D visualisation of the specimen (Keklikoglou et al., 2021).

Although Micro-CT has been widely used in plant physiology for decades, only a few reports have studied the voids in grape berries and flowers (Xiao et al., 2021; Xiao, Rogiers, et al., 2018). Their results revealed that the lenticels (irregularly distributed opening holes) on the pedicel and porous network of the receptacle-berry junction might provide an important pathway for oxygen transfer in to berries (Xiao et al., 2021; Xiao, Rogiers, et al., 2018). These studies only scanned berries at later development stages and under relatively low resolution (50 μm), therefore some microstructure may have been overlooked, especially in early development stages.

The aims of this study were as follows: a) to directly measure and map [O_2] distribution at a greater resolution than previously attained in different grape varieties at different development stages, b) to investigate the porosity of grape berries by high resolution Micro-CT, c) to further explore the link between grape variety, berry mesocarp cell death, hypoxia and porosity.

2. Materials and methods

2.1. Experimental Site and vineyard

The samples (grape berries) were harvested from the Coombe Vineyard and Alverstoke Vineyard at Waite Campus of the University of Adelaide, South Australia (34°58'03.12" S and 138°38'00.21" E) during 2020-21 for oxygen profiles, and 2021-22 season for Micro-CT and respiration rate. The climate for Adelaide is classified as hot Mediterranean with wet winters and hot and dry summers, described as warm/hot with mean January temperature ranges from 21 °C to 25 °C (Smart & Dry, 1980). The soil type is classified as DR2.23 hard pedal red duplex with 8% clay content from 0 to 110 cm and 60% clay content at 300–690 cm (Litchfield, 1951); no stone layer or water table was present within this depth.

All vines are own-rooted, with rows (3 m spacing) north-south oriented under drip irrigation. Irrigation regimes were approximately 0.9 to 1.1 ML/ha of water per season for Shiraz and Cabernet Sauvignon, 1.5 ML/ha per season for Chardonnay, while no irrigation was provided for Grenache for the last 8 seasons. All other vineyard managements were the same for all varieties in this study. All vines have been trained in a two-wire vertical shoot positioned (VSP) trellis system and spur pruned (two buds), carrying approximately 40 shoots per vine.

2.2. [O_2] Profiles in berries

2.2.1. Berry sampling and preparation

In the 2020-21 season, berries of *V. vinifera* L. varieties Shiraz (clone BVRC12, planted in 1990), Grenache (clone 137, planted in 2000), Chardonnay (clone, I10V1, planted in 2004), and table grapes Ruby Seedless and Flame seedless (planted in 1990) were sampled. Only a few samples were taken from the table grape varieties during the season. All varieties except for the table grape varieties were sampled weekly during ripening from about 80 to 110 days after anthesis (DAA). Every time, about 5 to 10 berries were randomly sampled from about ten labelled bunches. Berries were collected from the middle of the bunches and cut from pedicels with scissors to avoid possible damage to berries. Berries were then placed in a polystyrene box with an ice pack while transporting from the field to the lab (approx. 30 mins). All the sampled berries were normally collected from the outward side of the bunch for easy operation. Individual berries were equilibrated to room temperature (about 22 °C) before measurements. Berry mass, length, and diameter were measured before oxygen measurements. Total soluble solids (TSS) and berry mesocarp temperature were measured after oxygen measurement by a digital refractometer (Model PR101, Atago, Tokyo, Japan) and IR thermometer (Fluke 568; Fluke Corporation, Everett, WA, USA) with a type-K thermocouple bead probe (Fluke 80PK-1). Also, cell vitality of some berries was estimated by fluorescein diacetate (FDA) vital staining after oxygen measurements as described in Tilbrook and Tyerman (2008) (also see Chapter 3, 2.4). All oxygen measurements were conducted on the same day of berry sampling.

2.2.2. [O_2] measurements

The internal berry [O_2] was determined mostly as described in Xiao, Rogiers et al. (2018). Berry [O_2] was measured using the micro profiling system from Unisense A/S (Aarhus, Denmark), which consists of a Clark-type O_2 microelectrode with a tip diameter of 25 μm (OX-25; Unisense A/S, Aarhus, Denmark), a motorized micromanipulator for positioning the electrode, and the related software (the Unisensor) (https://unisense.com/products/microprofiling-system/). The microelectrodes were calibrated in a zero O_2 solution (0.1 M NaOH, 0.1 M $C_6H_7NaO_6$) and an aerated Milli-Q water (saturation, 272 μmol/l at 22 °C), as 100% O_2 solution. The two dimensional [O_2] profiles of the berry were mapped in the very middle longitude section between the seeds, where the berry mesocarp cell vitality by FDA is often measured (Tilbrook & Tyerman, 2008).

Before O_2 measurements, the berry structure, especially the location of the seeds was checked using a LED light (iPhone) to avoid hitting the seeds with the fragile microsensor tip. A straight line was then drawn (using a fine mark pen) on the skin between seeds in the very middle of the berry from berry junction to berry stylar end (Figure 1, yellow line). The [O_2] profiles were measured from several spots along this line. On each spot, [O_2] was taken from the skin with steps of between 100 to 500 μm (known exactly) towards the centre of the berry. The motorized micromanipulator can automatically move downward and upward (z-axis, in and out of the berry placed on a horizontal holding platform) with each depth recorded by the software (Unisensor). Each measurement was applied for a 10 s duration at each depth. Between each position, a 20 s waiting time was applied to ensure stable signals. The position of each profile in the berry along the longitudinal axis was determined by the distance from the berry/pedicel junction recorded by the Vernier calliper on the x-axis of the motorized micromanipulator. The depths into the berry from the skin were recorded by the Unisensor software (z-axis) with the motorized micromanipulator.

To map [O_2] distributions, [O_2] profiles on each of 8 berries from 4 different varieties was measured along the longitudinal axis every 1 mm or 2 mm step along the drawn straight line (from berry junction to berry stylar end). To compare [O_2] distribution in different varieties (Shiraz, Grenache and Chardonnay) during development, [O_2] profiles from about 5 berries (replicates) for each variety at each development stage were measured. [O_2] profiles in these berries were measured at only three spots on the longitudinal straight line due to time constraints (Figure 1): a) berry centre, b) at the middle point between berry centre and the pedicel junction, c) at the middle point between berry centre and the stylar remnant. For variety comparison, berry length and radius were normalised to 1 when presenting data to enable comparison between berries of different size.
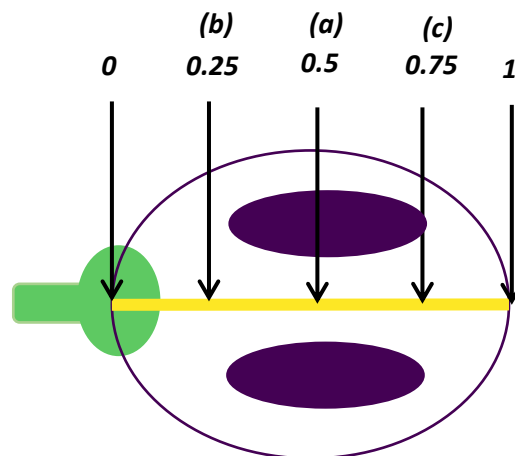
Figure 1 Illustration of the three locations for [O_2] measurements to compare differences between varieties. a) at the berry centre, b) at the middle point between the berry centre and the pedicel junction, c) at the middle point between berry centre and the stylar remnant.

2.3. Respiration rate

To examine how internal [O_2] profiles may relate to berry respiration rates, an oxygen sensor (Vernier, Beaverton, USA) (https://www.vernier.com/product/go-direct-o2-gas-sensor/) was used for respiration measurements of Shiraz and Grenache berries in the 2021-22 season. Temperature dependence of berry respiration of Shiraz and Grenache berries at two different maturations (about 20 °Brix and 27 °Brix) were determined at 15, 23, 35 and 45 °C. There were 4 replicates with 200

grams of berries (with pedicels on) for each replicate. This sensor measures gaseous oxygen concentration and air temperature. Berries were put in a container with a volume of approx. 600 ml with the oxygen sensor attached to it. The container with berries in was then submerged in a temperature-controlled water bath to regulate temperature and to limit oxygen leakage during measurements. After respiration measurements, total berry mass and TSS for each replicate were measured. The respiration rate per gram of berry was then determined from the oxygen consumption rate and total berry mass in the container.

2.4. Statistical analysis of [O_2] and respiration rate

Data analysis of [O_2] profiles and respiration rate, visualisation, and statistics were performed using R (R Foundation for Statistical Computing, Vienna, Austria) and RStudio software version 1.4.1717 (https://www.rstudio.com/) and associated packages. Generative additive models and interpolation were applied to smooth data during a single berry [O_2] distribution analysis.

At different temperatures (23, 35 and 45 °C), differences in respiration rate between different varieties (Shiraz versus Grenache) and different development stages (about 20 °Brix versus about 27 °Brix) were tested by two-way ANOVA (Figure 14-A). Since no data was collected at 15 °C for berries at late-stage ripening (about 27 °Brix), differences in respiration rate between Shiraz and Grenache at 15 °C were tested by t-test. The relationships between temperature (X) and respiration rate (Y) were then fitted by an exponential growth equation Y=Y0*exp(k*X) (Figure 14-B).

2.5. Micro-CT imaging and image processing

2.5.1. Berry sampling and preparation

In the 2021-22 season, berries of *V. vinifera* L. varieties Shiraz (clone BVRC12, planted in 1990), Grenache (clone 137, planted in 2000), Chardonnay (clone I10V1, planted in 2000), and Cabernet Sauvignon (clone 125, planted in 2000) were sampled every week or two weeks from before veraison until after normal harvest date. Sampling took place in the morning at about 9 am. When sampling, bunches on the vine were first immersed in Milli-Q water and several small branch bunches were cut

from the peduncle in water to avoid air ingress to the xylem vessels, which would show as empty voids in CT images. During transportation to the laboratory (approx. 1 hour), the stems of these small bunches were also kept in water. At the laboratory, in order to avoid cavitation in the vascular system and dehydration, berries were cut from pedicels under Milli-Q water. During X-ray CT scanning, the very end of the berry pedicel was put in a filtered (2 μm) sucrose solution, the osmolarity of the sugar concentration of which was similar to the predicated berry juice. The sucrose solution was scanned together with the berry and later used as the zero-porosity reference. Seeds from some scanned berries were removed and scanned separately under the same settings. On each sampling date, 2 to 4 berries were cut from these small bunches from each variety and scanned. In total 58 Shiraz berries, 45 Grenache berries, 32 Cabernet Sauvignon berries and 34 Chardonnay berries were scanned during the whole season. All micro-CT scans were conducted on the same day of berry sampling. After CT scanning, berry mass was determined and TSS of juice was measured with a digital refractometer (Model PR101, Atago, Tokyo, Japan).

2.5.2. X-ray micro-tomography

Grapes were scanned with a Skyscan 1076 (Bruker micro-CT, Kontich, Belgium) at the micro-CT facility at Adelaide Microscopy, where whole berries had 2-D projections acquired at 70 kV, 200 μA, Al 0.25 mm filter, 0.2° rotation step, double averaging and 7.04 μm pixel size or 3.48×10^{-7} mm^3 voxel size. In total, around 1000 projection images (8-bit bitmap) were captured per berry with an average of two scans per projection and an exposure time of 740 ms per exposure, resulting in about 60 minutes scanning time for each scan for one or two berries.

2.5.3. Micro-CT image processing and analysis

The projection images were then reconstructed into cross-section grey scale images (8-bit bitmap) using NRecon (bruker-microct.com). Fine tuning of the reconstruction parameters was set using NRecon to ensure that artefact removal could be done accurately. The parameters used in this study were as follows: 1) A ring artefact reduction was used to remove noise that is basically due to rotation

of the sample (level 20, software specific value) and, 2) 'beam hardening correction' to remove artefacts caused by the density or the attenuation coefficient of the sample (level 30, software specific value). Smoothing was also applied to reduces noise with a gaussian filter of 2 pixels. Subsequently, CT-Analyzer (bruker-microct.com) was used to facilitate segmentation of different structures based on different grayscale intensities. The grayscale intensity of the reconstructed images ranges from 0 to 255. The reconstructed images with different grayscale intensity were translated into porosity values using a simple interpolation method due to a linear porosity-grayscale relationship, bright regions are of higher density and dark regions are of lower density. Grayscale values of sucrose solution (as 0% porosity) and air (as 100% porosity) were used as reference values. The 3-D microstructural geometric image of different structures was generated using CTVox (bruker-microct.com).

2.5.4. Voids/low density quantification in the pedicel and brush area

For each berry, a cuboid volume as a region of interest (ROI) was delineated in the pedicel-brush area but with lenticels on the pedicel excluded as the lenticel were hard to separate with the background when delineate ROI. This ROI corresponded to complex variations in porosity and was likely a key area restricting O_2 diffusion. Cross-sections through the ROI were taken at 7.04 µm steps and the porous area of void/low density were measured (segmentation method in Table 1).

Table 1 Task list in CT-Analyser for voids and low-density tissue.

Structure	Separation steps in CT-Analyser
voids/air space	Global threshold: **0-50** Despeckle: remove 2d (Dimension) speckle less than 5 pixels Morphological operations: closing in 2d, 1 radius of square kernel
Low density	Filter: Gaussian blur, 2d, 1 radius, round kernel (twice) Global threshold: **50-75** Morphological operations: closing in 2d (Dimension), 1 radius of square kernel Despeckle: remove 3d speckle: less than 100 voxels

3. Results

3.1. Oxygen distribution map

The [O_2] distributions in two dimensions from several varieties are shown in Figure 2-A as generated heatmaps from the individual profiles in units of μmol L^{-1} (log10 scale). These were generated at 1 mm or 2 mm intervals from the berry pedicel junction to the stylar remnant and smoothed with a generalized additive model in R. Some general distribution patterns can be seen from these heatmaps even though they are from different varieties at different development stages. The [O_2] profiles in all berries tended to be symmetrically distributed with respect to the central axis with steep [O_2] gradients between different regions of the berry (Figure 2-A). In the berry central longitudinal axis (especially at the pedicel junction/brush area) and areas close to the berry skin (especially in the stylar end), the [O_2] was highest at around 300 μmol L^{-1}, then sharply decreased towards the mesocarp interior to almost 0 μmol L^{-1}. The hypoxic regions (less than 13.6 μmol L^{-1}) in the berry mesocarp were common but varied between berries, from a small oval shape to larger half circle area covering almost the whole mesocarp (Figure 2-A). The regions of low cell vitality (white) (Figure 2-B) matched the 2d [O_2] profiles shown in Figures 2-A. This generally occurred around the seed locule in the mesocarp interior.

To compare [O_2] distribution in Shiraz, Grenache, and Chardonnay at different stages, averaged data from 5 berries are summarised in the heatmaps shown in Figure 3, also with a Log10 scale of [O_2] in units of μmol L^{-1}. These measurements occurred over a TSS range from 16 °Brix to 26 °Brix. Although [O_2] was only measured at three locations along the longitudinal axis of each berry (Figure 1), the O_2 distribution pattern was consistent with that from single berries at 1mm or 2 mm steps shown in Figure 2-A. Also, all varieties showed a decrease in internal [O_2] and an increase in hypoxic longitudinal-sectional area as TSS increased (Figure 3). At a similar TSS, Shiraz and Chardonnay seem to have similar [O_2] levels, that were more severely hypoxic than for Grenache.
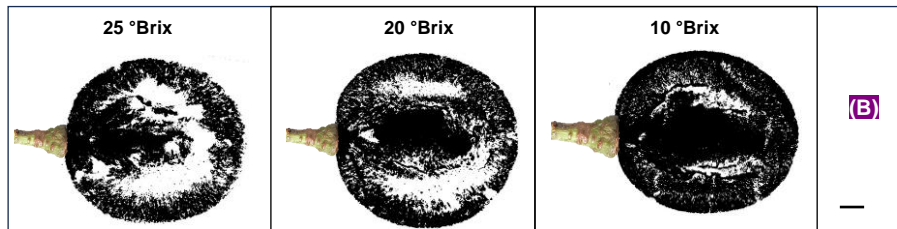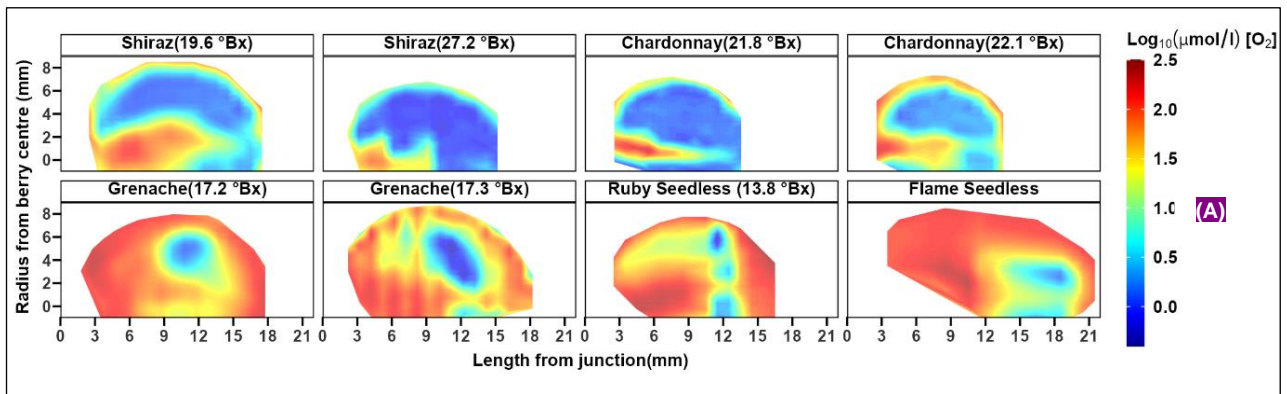
Figure 2 (A) Heatmaps with Log10 scale of (μmol L^{-1}) [O_2] from 8 single berries from different varieties (Shiraz and Grenache, Chardonnay, Ruby Seedless and Flame Seedless). [O_2] on several berries was measured every 1 mm step along the straight line from berry junction to berry end (Figure 1, the yellow line), with steps of between 100 to 500 μm from the skin toward the berry centre. Generative additive models and interpolation by R were applied to smooth the data. **(B)** Three examples of Shiraz berries of different stages showing area of berry cell death in the mesocarp (white), modified from FDA images. Scale bar = 1 mm.
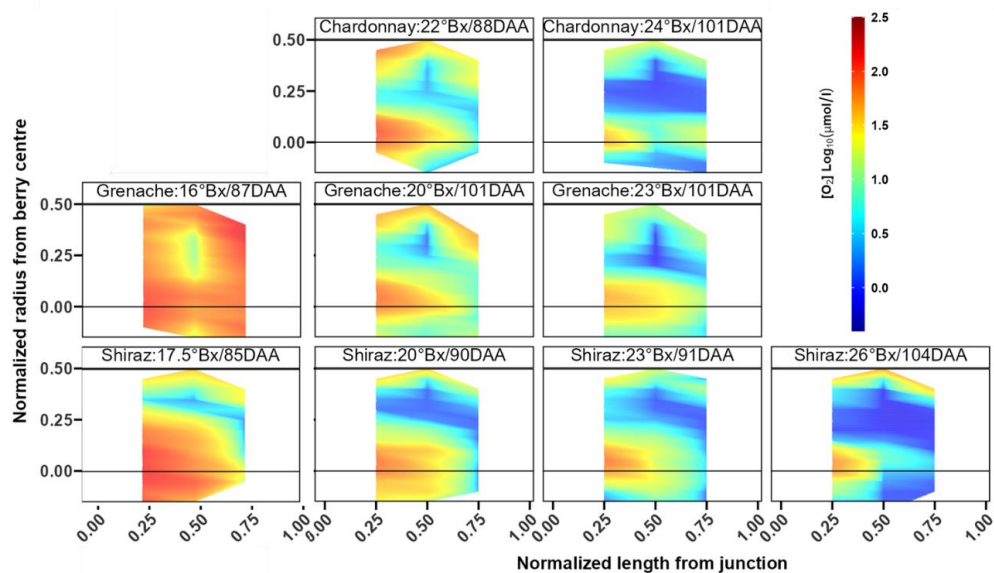
Figure 3 Heatmaps (with interpolation) with Log10 scale of (μmol L^{-1}) [O_2] for grape berries at different development stages for Chardonnay, Grenache and Shiraz (average data from five berries). Berry length and berry diameter were normalized to 1 for comparison since Grenache has on average large berries than Shiraz. Interpolation by R was applied to smooth the data (note variation cannot be shown on a heat map).

Figure 4 demonstrates two examples of cell vitality staining with FDA in the Shiraz berry's longitudinal section with superimposed [O₂] profiles from the same berries. With the high spatial resolution (i.e., 100 - 200µm) used in these measurements, there was also an [O₂] peak between the berry skin and mesocarp interior between 100 to 500 µm from the berry surface (Figure 4).

x: Distance to berry centre (mm)
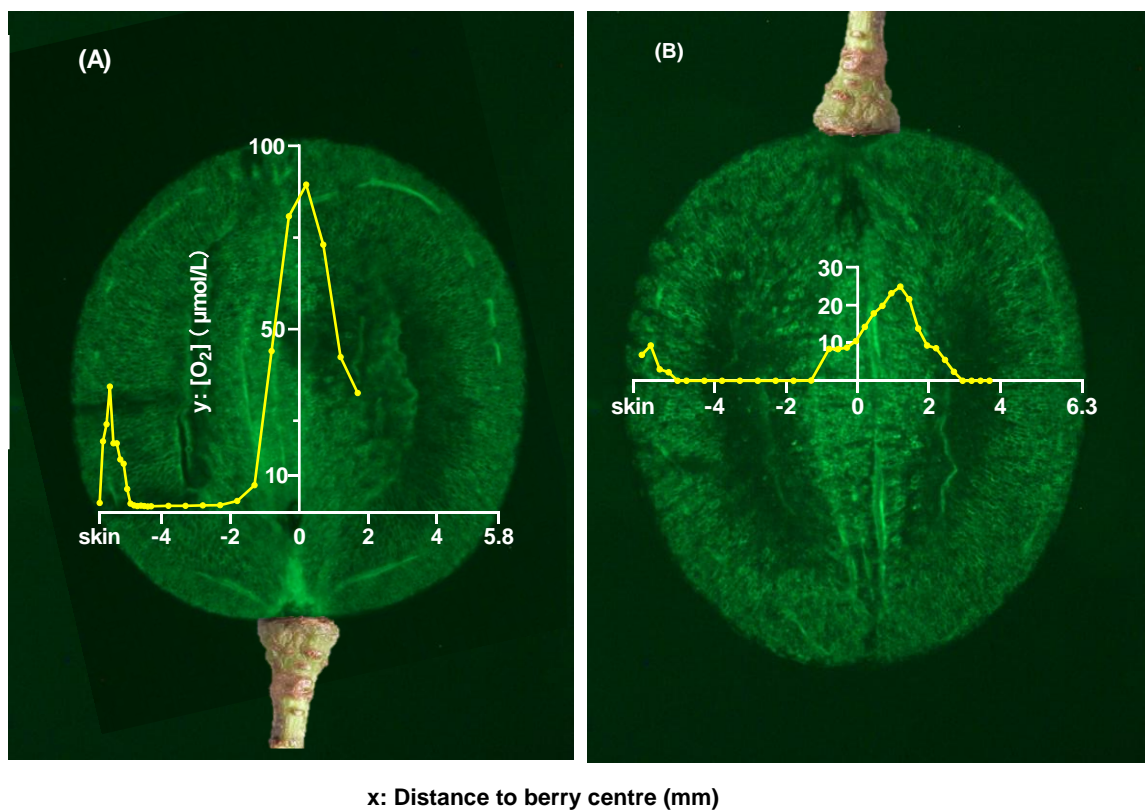
Figure 4 Example [O₂] profiles of Shiraz berries with FDA staining showing location of cell death from the same berries. Berries were sampled on 31st Jan 2021 with 21.4 °Brix and 13th Feb 2021 with 27.2 °Brix for berry (A) and berry (B) respectively. [O₂] was measured from the exact locations where the x axis is located in the images, i.e., at the middle point between the berry centre and the pedicel junction for berry(A), and at the berry centre for berry (B). The dark area in the berries indicates cell death. Note the bright areas (high vitality) where the vascular tissue is located. Pedicels are shown for orientation purposes, not actual representation.

3.2. Micro-CT imaging of grape berries during development

Compared with porosity references (air and sucrose solution), significant contrasts were found between 5 different structures in the berry with distinct grey scale intensities (0-255) (Figure 5): 1) voids or air apace (grey scale intensity below 50), 2) low density structures (grey scale intensity between 50 and 75), 3) berry tissue or water filled void (grey scale intensity between 75 and 120), 4) berry skin (grey scale intensity between 125 and 145), 5) very bright crystal structures in the endocarp and outer mesocarp, with grey scale intensity above about 170. The berry skin was obviously denser (brighter) than the mesocarp cell region, especially after veraison (Figure 9, 10, 11). No obvious void/low density openings were observed on the berry skin in all varieties. However, under a resolution of 7.04 micrometres, intercellular structures in grape berries cannot be revealed here. (All the Micro-CT Figures are in the PowerPoint file (From Figure 5 to Figure 13)).

The two major low-density structures in the berry, voids and low-density regions, seldomly existed alone, but were often intertwined (Figure 5, 'Sponge Tissue'). Therefore a "Sponge Tissue" (ST) was defined that is a combination of voids and low-density regions for ease of discussion. The voids and Sponge Tissue (ST) in the pedicel, mesocarp and seeds are categorised separately in Table 2 (Figure 6, 7, 9, 10, 11, 12, 13). Since this study focussed on the porous properties of grape berries, structures of grey scale intensity above 75 were combined as non-void structures (Figure 5).

Therefore, to make 3D models, only 3 global thresholds were defined to separate different structures, i.e., the voids or air space (grey scale intensity below 50), low-density structures (grey scale intensity between 50 and 75), and non-void structures (grey scale intensity above 75) (Figure 5). A brief recipe of segmentation of voids and low-density structures on CT-Analyzer is listed in Table 1. The area of interest was defined as the whole berry excluding the lenticels on the pedicel for the reasons outlined above. After segmentation, a 3-D microstructural geometric image of different structures was generated with different colour rendering modules to distinguish the different structures.

Table 2 Summary of voids and Sponge Tissue (ST) in different parts (pedicel, mesocarp/endocarp and seeds) of Shiraz berries (Figure 6, 7, 9, 10, 11, 12, 13). Figures 6,7 and 8 show results for the porous structures in the pedicel-brush area. Figure 9,10,11 show the porous structures in Shiraz at different stages from pre-veraison (about 5 °Brix) to shrivel (over 30 °Brix) with 3D videos. Figure 12 -A, B, C shows examples (3D model images) of Sponge Tissue structure in Shiraz berries. Figure 12-D shows an example of the voids network in ventral porous bundles (VPB) in Grenache at late stage with grey scale imaging in longitude section. Figure 13 shows the voids in the area close to the stylar end in different varieties.

Locations	Porosity type		
In pedicel	ST and/or voids	Lenticels (Figure 6,7)	
	ST	ST in pedicel/receptacle, STP (Figure 6, 7, 9, 10, 11)	
In mesocarp (endocarp)	ST	ST in the brush area, STB (Figure 6, 7, 9, 10, 11)	
		ST tube (STT) (Figure 9,10,11,12)	dorsal porous bundles, DPB
			ovular porous bundles, OPB
			ventral porous bundles, VPB
	Voids	voids between ovule (seeds) and ovary wall (mesocarp cells), VSM (Figure 9-CD)	
		scattered small voids (SSV) with varied shapes in the mesocarp only before veraison (Figure 9-B)	
		irregular voids close to seed hilum as part of the OPB in the mesocarp, IVM (Figure 10, 11)	
		enclosed voids between two closed located seeds, EVS (Figure 10-A6)	
		isolated void in areas close to the stylar remnant, IVS (Figure 13)	
In seeds	Voids	void hook connected to OPB, VH (Figure 10,11)	
		voids network in beak area, VNB (Figure 10)	
		two voids in fossettes (seed folds), VFS (Figure 10,11)	
		large void between endosperm and inner integument, VEI (Figure 11)	

3.2.1. Sponge Tissue (ST) in the pedicel-brush region

Figure 6 shows the detailed porous structure as sequential cross sections from pedicel to the brush region in a Shiraz berry (5 °Brix) via a gif movie (Figure 6-ABC). Figure 7-A shows some examples of the pedicel-brush area in Shiraz at different development stages with greyscale images of longitudinal slices. Figure 7-B shows the detailed porous structure as sequential longitudinal sections in this region in a Grenache berry (5 °Brix) via a gif movie. Figure 8 demonstrates the area of porous regions as a function of distance to the junction of the pedicel-brush area at different development stages (TSS, different colours) in different varieties.

The voids and/or low-density holes (lenticels) (Figure 6-D, the green arrow) can be observed on the pedicel surface and were directly connected to the Sponge Tissue in the pedicel (STP). The STP extended into the berry via the brush area through the pedicel junction, referred to here as Sponge Tissue in the brush (STB) (Figure 6, 7, 8). The longitudinal cross-sectional area of the Sponge Tissue in the brush (STB) (Figure 7, 8-A), and especially the STB cross sectional area normalised to berry mass (Figure 8-B), showed a decreasing trend with berry development in all varieties. There was a dramatic decrease occurring at veraison and reaching a minimum in berries that were over 25 °Brix. In shrivelled Shiraz berries when TSS was over 30 °Brix (Figure 7) the area was very much reduced. In the brush area (positive values on the x-axis in Figure 8), there was an obvious constriction (pinch-point) where the cross-sectional area of the porous region dips in both Shiraz and Grenache (the red arrows in Figure 8). This occurs at about 0.5 mm from the berry-pedicel junction in Grenache while it was about 1 mm in Shiraz (Figure 8). Grenache also shows a second constriction at about 1.5 mm that corresponds to those also seen in Cabernet Sauvignon and Chardonnay but appears to be absent in Shiraz. The differences in this structure between Shiraz and Grenache are also demonstrated in Figure 7. The main constriction is likely to extended for longer in Shiraz than in Grenache, and the minimum area per berry mass seems larger in Grenache than in Shiraz when TSS was lower than about 25 °Brix. In Chardonnay and Cabernet Sauvignon, there were two constrictions in the porous structure in the brush area. In Cabernet Sauvignon there was a sharp constriction at less than 0.5 mm

from the junction then a broad constriction at 1 mm that dramatically reduced in area after veraison. Chardonnay showed a similar pattern to Cabernet Sauvignon but with a less broad constriction at 1-1.2 mm from the junction.

In the pedicel-brush centre, there was a non-void tissue (grey scale between 75 and 120) (Figure 6, 7) surrounded by Sponge Tissue in both pedicel and the brush area. This non-void tissue was a solid cylinder in the pedicel and had around 8 non-void solid protrusions extended to surroundings in the receptacle (Figure 6C-(9), 7). When extended into the brush area, the non-void cylinder tissue split into two branches at the pedicel-berry junction.

3.2.2. The dorsal porous bundles (DPB) and the ventral porous bundles (VPB)

Immediately after the split at the berry-pedicel junction, many tiny tissue branches extended from the non-void cylinder tissue, penetrating the surrounding Sponge Tissue then extending to the berry tissue in the berry periphery (Figure 6C-(16-18), 7). Interestingly, these tiny tissue branches were normally not solid but were often with Sponge Tissue tubes (STT) inside them. There were also in total up to 4 Sponge Tissue tubes (STT) in the two split branches. These Sponge Tissue tubes (STT) normally originated from Sponge Tissue at the berry-pedicel junction area or in the brush (STP) and spread to 3 directions: they extended to the mesocarp periphery (referred to as the dorsal porous bundles, DPB) (Figure 9,10), to the berry centre between the seeds (referred as ventral porous bundles, VPB) (Figure 10) and to the seeds (referred as the ovular porous bundles, OPB) (Figure 6C-(24), 10, 11).

The dorsal porous bundles (DPB) and the ventral porous bundles (VPB) could extend to the berry stylar end and sometimes connected there (Figure 12-A, B, C). Also, the dorsal porous bundles (DPB) and the ventral porous bundles (VPB) showed great variation between berries even at similar development stages. It is challenging to quantify the size of the tiny DPB and VPB and compare between different TSS, especially with the often-occurring ring artefacts. However, it seemed that the dorsal porous bundles (DPB) and the ventral porous bundles (VPB) network decreased with berry development in Shiraz, and even disappeared in shrivelled Shiraz (Figure 9,10,11), while in Grenache,

these networks, especially the dorsal porous bundles (DPB) were still visible in more ripe berries (Figure 12-D).

3.2.3. The ovular porous bundles (OPB) and voids in seeds

Considering the ovular porous bundles (OPB, Figure 10), a maximum of 4 small branches of the OPB traversed the split non-void branches foremost to the seed and then connected with an irregular void (IVM) located close to the seed hilum (Figure 9, 10, 11). The OPB with the IVM were often observed even until late in ripening for all varieties. The ovular porous bundles (OPB) ended at the seed hilum during the berry formation phase when there were almost no voids or Sponge Tissue (ST) inside the seeds (Figure 9). After veraison, if there was a well-developed seed, ovular porous bundles (OPB) could be observed to be connected to the void hook (VH) inside the seeds through the hilum. This void hook (VH) inside seeds went along the raphe, normally initiated from the seed hilum, along the ridge of the keel and over though the notch furthest to the dorsal side, where it ended with the large irregular voids in the chalaza area (Figure 10, 11). This void hook (VH) was often observed even until late ripening in all varieties.

Apart from the void hook (VH) inside the seed, there were other voids observed inside seeds after veraison. A void network on the seed beak area (VNB) was often observed (Figure 10-B2, C). From about 15 °Brix, a sail-like void (VFS) started to develop symmetrically in each of the two fossettes till late harvest (Figure 10, 11). Their (VFS) volume increased with time and reached full size at about 25 °Brix. After about 25 °Brix, there was another void appearing in seeds between the inner integument and endosperm, referred to as VEI (Figure 11). The volume of the VEI increased with time, but was only observed in varieties with berry shrinkage, i.e., Shiraz and Cabernet Sauvignon, not in Grenache and Chardonnay. It should be noted that the void network on the seed beak area (VNB), the sail-like voids (VFS) and void between the seed inner integument and endosperm (VEI) appeared to be in isolation from each other and from the void hook (VH) (Figure 10, 11).

3.2.4. Voids in the mesocarp

Although there was no hollow structure inside seeds before veraison, there were large voids surrounding the seeds and connected to the Sponge Tissue in the brush area (SPB) (Figure 9). These voids were located between seeds and mesocarp/endocarp cells (referred to as VSM), with decreased size and different shapes occurring during berry development, changing from larger intact ones surrounding the seeds to smaller helmet-like networks along the ravine of the seed and then disappearing after veraison (Figure 9, 10, 11). Scattered small voids (SSV) with varied shapes in the mesocarp were also observed at this stage that decreased with development and disappeared at the end of veraison (Figure 9). When two seeds were closely located, a long strip-like void (EVS) was enclosed between the seeds (Figure 10-A6). Furthermore, the seed coats after veraison had higher density than normal berry tissue while they were of similar density to berry tissue before veraison (Figure 9, 10, 11).

A small isolated but obvious void (VSR) was located close to the stylar scar connecting the atmosphere and the berry interior (Figure 13). This was consistently observed in Grenache, Shiraz and Chardonnay at all development stages, but rarely in Cabernet Sauvignon. It was relatively larger and elongated in Grenache compared to the small ellipse shaped voids in Shiraz and Chardonnay (Figure 13).

3.3. Respiration rate differences between Shiraz and Grenache

The respiration rates of Shiraz and Grenache berries at different temperature and ripeness were measured during the 2021-22 season (Figure 14) in order to determine if the large differences observed in the degree of hypoxia within the berries could be associated with differences in respiration rates. However, there was no significant differences between the two varieties at each ripeness stage (TSS) (Figure 14-A). In both cases the respiration rate increased exponentially with temperature ($R^2 > 0.85$), roughly doubling for every 10 °C increase of temperature (estimated doubling is between approximately 8 and 11°C) (Figure 14-B).
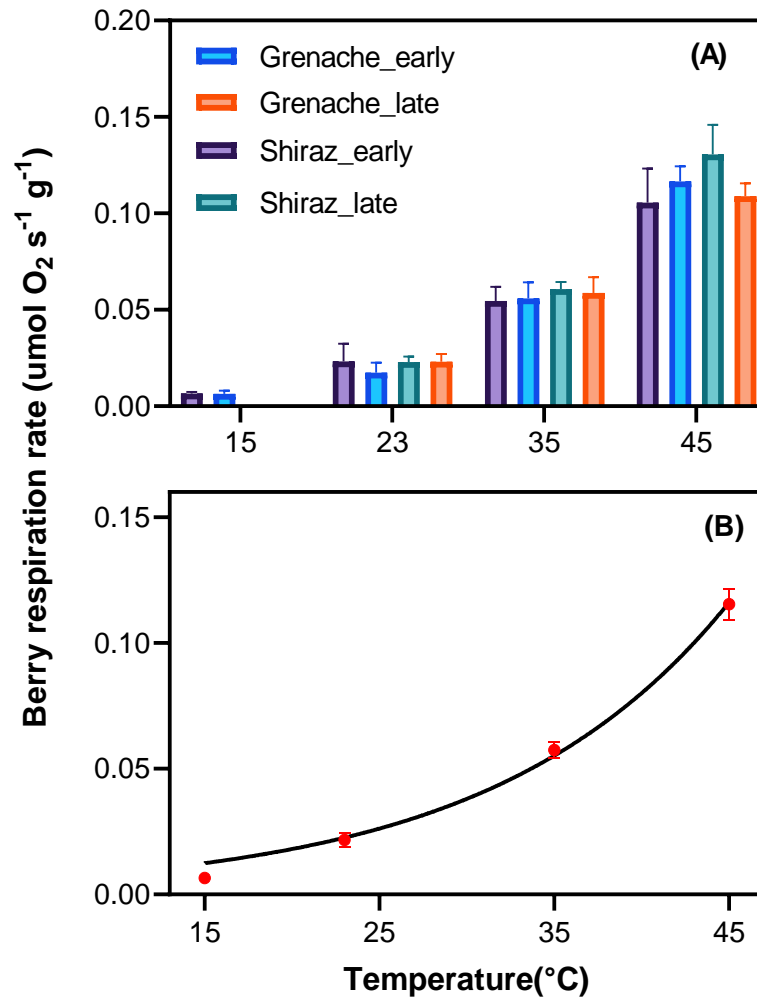
Figure 14 Berry respiration rates as a function of incubation temperature comparing Grenache and Shiraz berries at different stages of development (early and late). (A) Respiration rate of Shiraz and Grenache berries at different stages (TSS in early stage was 20 °Brix, TSS in late stage was 27 °Brix) (mean ± SEM, n = 4). Each replicate included about 200 gm of berries. There is no difference between Shiraz and Grenache nor between different ripeness (two-way ANOVA (temperature of 23, 35 and 45 °C) and T-test (temperature of 15°C)). (B) Combined data from the two varieties at different stages to examine the relationship between temperature and respiration rate. An exponential equation (Y=Y0*exp(k*X)) was fitted between temperature (X) and respiration rate (Y), red values are mean ± SEM (n = 8 at 15 °C, n= 16 at 23,35 and 45 °C).

4. Discussion

Combining results from [O_2] profiles with micro-CT during different development stages enables a better understanding of the O_2 diffusion pathways in grape berries. Examination of different varieties with berry development may provide clues as to why some varieties are more prone to cell death than others if cell death is a result of hypoxia/anoxia.

The porosity microstructure of grape berries changed with berry development from before veraison to late harvest in all varieties. Regions of low density (from Micro-CT) are assumed to be equivalent to high porosity and which largely determine the gas exchange pattern, including oxygen transfer. Each development phase displayed distinctive microstructures, both in mesocarp and seeds. Generally, voids and Sponge Tissue (ST) in the brush area, i.e., the STB (Figure 6, 7, 8) and the Sponge Tissue Tube (DPB, OPB and VPB) (Figure 9, 10, 11), showed a decreasing trend with berry development in all varieties in this study, with a dramatic decrease occurring at veraison, and where the Sponge Tissue Tubes almost disappeared in shrivelled Shiraz berries (Figure 11). This is consistent with the decreased [O_2] and increasing extent of hypoxic regions during advancement of ripening (Figure 2, 3). On the contrary, in the seeds for all varieties examined, there were almost no hollow structures before veraison, while after veraison, different types of voids in seeds were gradually revealed with time (Figure 9, 10, 11).

On the other hand, very bright crystal structures in the endocarp and outer mesocarp were observed, with grey scale intensity above about 170. It is reported that there are two types of crystals distributed in grape berries (Hardie et al., 1996). One is druses of calcium oxalate that were present in most endocarp cells and confined to that tissue. The other type is raphides consisting of calcium tartrate that are distributed in an apparently unordered array throughout the outer mesocarp (Hardie et al., 1996).

4.1. Oxygen entry sites for grape berries

Gas exchange between fruit and the atmosphere is often considered to be via diffusion through openings (lenticels and/or stomata) in the skin, while the skin is often regarded as a gas diffusion barrier because of different impermeable layers of tissues (aqueous, cuticular, and waxy layers) (Cukrov, 2018). In grape berries, the lenticels (irregularly distributed opening holes) on the pedicel likely provided the entry sites for low resistance gas exchange between the interior of berries and the atmosphere (Xiao et al., 2021; Xiao, Rogiers, et al., 2018). Grape (Shiraz) berry skin is reported to have very low gas permeability because of the thick waxy cuticle and lack of lenticels and stomata (Rogiers et al., 2004). The mature berry skin tended to have higher density than the mesocarp from Micro-CT imaging in this study with no obvious stomata or lenticels, indicating that berry skin had even lower gas conductivity than berry mesocarp. Also, with $[O_2]$ measured every 100 µm (Figure 4), a peak of $[O_2]$ between the skin and the mesocarp interior was consistently observed, which also indicated the higher $[O_2]$ in the periphery of the mesocarp was not likely to be a result of O_2 diffusing (permeating) across the berry skin, but possibly from the dorsal porous bundles (DPB) network in the mesocarp periphery (see below). This peak was not evident in the $[O_2]$ heatmaps, maybe because most data was collected or summarised at a 500 µm step resolution in Figure 2 and Figure 3. The direct measurements of gas permeability of grape berry skin require further investigation.

This study also discovered another entry site for O_2 uptake into grape berries, located at the stylar remnant as a macroscopic void (VSR) in most grape berries at all stages (Figure 13). An increase in $[O_2]$ close to the stylar remnant was also consistent with this (Figure 2). However, this site probably does not provide as much O_2 access compared to the lenticels on the pedicel since it had a small volume and no other porous structures extended from it for further delivery to the mesocarp. The VSR was observed in most berries of Grenache, Shiraz and Chardonnay, while it was rarely observed in Cabernet Sauvignon (Figure 13). The VSR in Grenache was larger and longer than that of other varieties, perhaps associated with the larger berry size, which probably accounts for the higher $[O_2]$ in the stylar end of the Grenache berry (Figure 2, 3). Xiao et al. (2021) mentioned that no voids could

be observed closer to the stylar remnant. This is possibly because of the lower spatial resolution (50 μm) and limited sample sizes used in that study. Berries were scanned under 7.04 μm resolution in this study.

4.2. Oxygen diffusion inside berries at different development phases

The pathways of oxygen diffusion inside berries are likely to change with berry development because the size and shape of porous structures observed in this study change with time. After flowering, berry mass generally follows a successive double-sigmoid pattern over time with three distinct phases (Sadras and McCarthy, 2007, Coombe, 1976), *Phase* 1, 'berry formation' from flowering to veraison; *Phase* 2 'berry maturation' from veraison to peak fresh mass; and for some varieties like Shiraz and Cabernet Sauvignon, there is a *Phase* 3 'berry shrinkage' from peak fresh mass to harvest. Grenache and table grapes do not have a *Phase* 3 and tend not to show berry shrivel (Fuentes et al., 2010; Krasnow et al., 2008; Tilbrook & Tyerman, 2008).

In *Phase* 1 (berry formation), the berry initiates from an ovary in which large voids exist between the ovary wall (develops into mesocarp) and the ovules (develop into seeds) (Xiao et al., 2021). These voids between seeds and mesocarp/endocarp cells (VSM) were obvious in berries before veraison in this study (Figure 9). With berry development, both the ovary wall and ovule expand with cell division and enlargement (Ollat et al., 2002). Most of the VSM were gradually filled and decreased with time to almost disappear at the end of veraison in seeded berries, except the ones (EVS) enclosed between two seeds where mesocarp/endocarp cells may not have access (Figure 10-A6). For seedless varieties, where seeds do not develop properly, there could be some spare space after mesocarp cell development. This could be the reason why some studies observed a significant number of macroscopic voids in mature seedless berries (Xiao et al., 2021).

Before veraison, the porosity in the brush area is also large with a high volume of Sponge Tissue (STB) (Figure 6, 7, 8). Seed coat lignification is not complete in this phase (Cadot et al., 2006), and was also indicated by lower density on CT scans than that after veraison in my study. The seed coat

was also reported to act as a pathway for transport and site for conversion of acids and sugars from the pericarp into the embryo sac in early development (Werker et al., 1979). Therefore, before berry veraison, the pathway for O_2 diffusion to seeds is likely to be from lenticels on the pedicel, via Sponge Tissue in the pedicel (STP), Sponge Tissue in the brush (STB), the voids between seeds and mesocarp/endocarp cells (VSM), ultimately to the seed coat surface and to directly enter seeds though the seed coat. Mesocarp cells are also likely to acquire O_2 through this pathway at this stage. Although no [O_2] profiles were collected on berries at this stage, the [O_2] in the berry would be expected to be higher than that at later stages because of the presence of this obvious diffusion pathway.

The Sponge Tissue Tube (SST) system, including the dorsal porous bundles (DPB), ventral porous bundles (VPB) and ovular porous bundles (OPB), could be the most important pathway for oxygen delivery, especially after veraison, when the voids (VSM) between seeds and mesocarp/endocarp cells were mostly filled (Figure 9,10,11,12). From the Sponge Tissue in the pedicel and brush area, the dorsal porous bundles (DPB), ventral porous bundles (VPB) and ovular porous bundles (OPB) may be responsible for the delivery of oxygen into the berry centre, mesocarp periphery and seeds respectively (Figure 9, 10). From these obvious Sponge Tissue (DPB, VPB and OPB), oxygen would then need to diffuse into the interior of mesocarp cells through the liquid phase of the apoplast and then cell membrane to the cells' cytoplasm (mitochondria) (Ho et al., 2009). This final cellular diffusion pathway is of high diffusional resistance, though some aquaporins could be involved since those located in the cell membrane of root cells have been proposed to facilitate O_2 diffusion (Cukrov, 2018; Ho et al., 2009; Zwiazek et al., 2017). A steep [O_2] gradient towards the mesocarp interior (between the berry centre axis and berry skin) may occur with even zero [O_2] often occurring in all varieties even at relatively early development stages. Therefore, cell death is more likely to commences in the mesocarp interior (Figure 2-B). Steep [O_2] gradients in fruits toward the core of the fruit are very common, for example in pear or apple (Cukrov, 2018).

As berries become ripe, gas exchange (oxygen uptake, carbon dioxide and ethanol removal) may be greatly impeded due to the decreased porosity in the brush area (STB) and decreased size of the pathway to the mesocarp (DPB and VPB), especially in Shiraz berries. This may explain the decreased $[O_2]$ in Shiraz berries with time, and therefore increased cell vitality. On the other hand, although Grenache is normally a larger berry than Shiraz which also imposes additional requirements for O_2 diffusion since the surface area to volume ratio is smaller. Grenache seems able to retain porous structures within the berry with development, resulting in higher gas exchange efficiency and minimal cell death.

4.3. Oxygen diffusion into seeds after veraison

After veraison, when seed coat lignification has completed as indicated by a dense seed coat and almost filled voids surrounding the seed, seeds are likely to develop a void hook (VH) (Figure 10,11) connecting the ovular porous bundles (OPB) for oxygen uptake, and/or other gas exchange, such as volatile ethanol and carbon dioxide release. This pathway could directly supply oxygen to most of the seeds as it almost extended to the whole seed along the seed raphe on the ventral side to the chalaza on the dorsal side.

Other structural voids developed inside seeds after veraison, i.e., the porous network on the beak (VNB) (Figure 10-B2, C) and the two fossettes (VFS) (Figure 10-B2, B4, C) on the seed ventral face during ripening and the large void between endosperm and inner integument (VEI) during late ripening (Figure 11-D). As they had no connections to the void hook (VH) (Figure 9, 10, 11) or the porous network outside the seeds, it seems they do not provide much function in gas exchange for seeds. The VFS was also reported by Xiao et al. (2021) with no gas transfer function suggested. On the other hand, the large void between the endosperm and seed coat (VEI), was only observed in varieties that are prone to berry shrivel, such as Shiraz and Cabernet Sauvignon. This may indicate that the endosperm also shrivels as the berry loses mass.

4.4. The Sponge Tissue system for gas exchange and the vascular bundles

The Sponge Tissue system for gas exchange (DPB, VPB and OPB) co-located with the likely position of vascular bundles, which supply water, nutrients and sugar to the berry. These start from the pedicel, then branch in three directions, dividing into peripheral vasculature, central vascular and ovular vasculature to the seeds as a hook (Xie et al., 2023) (Chapter 1- Figure 3). In this study, a non-void tissue cylinder was evident in the pedicel and brush area that split in the berry centre and periphery, with non-void solid protrusions extending to surroundings in the receptacle (Figure 6C-(9)). These correlate with the location of the vascular tissue (xylem and phloem). The aeration system (especially the VPB and DPB) seems to be located inside this non-void tissue (possible vascular system) as an aeration void tube but can only be visualized in the brush area. It is difficult to separate the non-void tissue (possible vascular system) from the mesocarp tissue when connected due to similar density in CT scans. This possible link between the vascular system and the aeration system needs further investigation.

The identified and complex Sponge Tissue system in the brush region is unlikely to be the result of cavitation and embolism within collocated xylem vessels because the pedicels were cut under water and were kept in solution during the whole scan procedure to avoid embolisms and dehydration. Also, the diameter of the voids is larger than would be expected for xylem. Furthermore, the peak in [O_2] profile near the skin (Figure 4) would correlate with the peripheral vascular bundles and DPB.

5. Conclusion

Gas exchange including oxygen uptake in grape berries is likely to be highly dependent on the porous gas-filled microstructure, especially in the brush region, which changes though different development stages. These are likely to influence berry cell death and berry shrivel depending on the variety since significant differences were observed between varieties that show greater cell death versus those that show little cell death. Gas exchange pathways for seeds was also different before and after veraison. Before veraison oxygen could directly diffuse into seeds through the seed coat, which was surrounded by voids connected to the sponge structure in the brush area and in the pedicel. After veraison, when

the voids surrounding the seeds were filled, a hooked tube-like void was visible inside the seed that connected the seed interior to the porous network in the brush area and pedicel. This is likely to provide oxygen for seed development.

For mesocarp, prior to veraison, the porous gas pathway (VSM) could also provide oxygen for mesocarp cells. Apart from that, a porous bundle-like network (DPB and VPB) extending from the spongy structure in the brush area is likely to be the major pathway for gas exchange for mesocarp cells, especially after veraison. However, these porous networks only extended to the berry centre and the mesocarp periphery. Oxygen diffusion to other mesocarp parts may then be confined to the liquid phases with high diffusion resistance, and therefore incurring steep [O_2] gradients towards the mesocarp interior. This may account for the common hypoxia in all varieties even at relatively early development stages. This situation may deteriorate with berry development as both the porosity in the brush area and in the bundle networks decreased with time, leading to decreased [O_2] with time in berry mesocarp. Other gas exchange, besides O_2 may be influenced by these changes including carbon dioxide and volatile (e.g., ethanol) release, which may also cause stress on cells and contribute to cell death for Shiraz. Grenache seems better at retaining the porous structures during development compared to Shiraz, which could be one of the reasons that Grenache had higher [O_2] and much less cell death than Shiraz.

6. References

Armstrong, J., Jones, R. E., & Armstrong, W. (2006). Rhizome phyllosphere oxygenation in Phragmites and other species in relation to redox potential, convective gas flow, submergence and aeration pathways. *New Phytologist*, *172*(4), 719–731. https://doi.org/10.1111/j.1469-8137.2006.01878.x

Bonada, M., Sadras, V. O., & Fuentes, S. (2013). Effect of elevated temperature on the onset and rate of mesocarp cell death in berries of Shiraz and Chardonnay and its relationship with berry shrivel: Thermal shift on mesocarp cell death and shrivel. *Australian Journal of Grape and Wine Research*, *19*(1), 87–94. https://doi.org/10.1111/ajgw.12010

Bondada, B. R., & Keller, M. (2012). Not all shrivels are created equal—Morpho-anatomical and compositional characteristics differ among different shrivel types that develop during ripening of grape (*Vitis vinifera* L.) berries. *American Journal of Plant Sciences*, *03*(07), 879–898. https://doi.org/10.4236/ajps.2012.37105

Burg, S. P., & Burg, E. A. (1965). Gas exchange in fruits. *Physiologia Plantarum*, *18*(3), 870–884. https://doi.org/10.1111/j.1399-3054.1965.tb06946.x

Cadot, Y., Miñana-Castelló, M. T., & Chevalier, M. (2006). Anatomical, histological, and histochemical changes in grape seeds from *Vitis vinifera* L. cv Cabernet franc during fruit development. *Journal of Agricultural and Food Chemistry*, *54*(24), 9206–9215. https://doi.org/10.1021/jf061326f

Cameron, A. C., & Yang, S. F. (1982). A simple method for the determination of resistance to gas diffusion in plant organs. *Plant Physiology*, *70*(1), 21–23. https://doi.org/10.1104/pp.70.1.21

Chou, H.-C., Šuklje, K., Antalick, G., Schmidtke, L. M., & Blackman, J. W. (2018). Late-season Shiraz berry dehydration that alters composition and sensory traits of wine. *Journal of Agricultural and Food Chemistry*, *66*(29), 7750–7757. https://doi.org/10.1021/acs.jafc.8b01646

Cukrov, D. (2018). Progress toward understanding the molecular basis of fruit response to hypoxia. *Plants (Basel, Switzerland)*, *7*(4), E78. https://doi.org/10.3390/plants7040078

Fuentes, S., Sullivan, W., Tilbrook, J., & Tyerman, S. (2010). A novel analysis of grapevine berry tissue demonstrates a variety-dependent correlation between tissue vitality and berry shrivel: Variety-dependent berry vitality and shrivel. *Australian Journal of Grape and Wine Research*, *16*(2), 327–336. https://doi.org/10.1111/j.1755-0238.2010.00095.x

Hardie, W. J., O'brien, T. P., & Jaudzems, V. G. (1996). Morphology, anatomy and development of the pericarp after anthesis in grape, *Vitis vinifera* L. *Australian Journal of Grape and Wine Research*, *2*(2), 97–142. https://doi.org/10.1111/j.1755-0238.1996.tb00101.x

Ho, Q. T., Verboven, P., Mebatsion, H. K., Verlinden, B. E., Vandewalle, S., & Nicolaï, B. M. (2009). Microscale mechanisms of gas exchange in fruit tissue. *New Phytologist*, *182*(1), 163–174. https://doi.org/10.1111/j.1469-8137.2008.02732.x

Ho, Q. T., Verboven, P., Verlinden, B. E., Lammertyn, J., Vandewalle, S., & Nicolaï, B. M. (2008). A continuum model for metabolic gas exchange in pear fruit. *PLOS Computational Biology*, *4*(3), e1000023. https://doi.org/10.1371/journal.pcbi.1000023

Ho, Q. T., Verlinden, B. E., Verboven, P., & Nicolaï, B. M. (2006). Gas diffusion properties at different positions in the pear. *Postharvest Biology and Technology*, *41*(2), 113–120. https://doi.org/10.1016/j.postharvbio.2006.04.002

Keklikoglou, K., Arvanitidis, C., Chatzigeorgiou, G., Chatzinikolaou, E., Karagiannidis, E., Koletsa, T., Magoulas, A., Makris, K., Mavrothalassitis, G., Papanagnou, E.-D., Papazoglou, A. S., Pavloudi, C., Trougakos, I. P., Vasileiadou, K., & Vogiatzi, A. (2021). Micro-CT for biological and biomedical studies: A comparison of imaging techniques. *Journal of Imaging*, *7*(9), Article 9. https://doi.org/10.3390/jimaging7090172

Keller, M. (2006). Ripening grape berries remain hydraulically connected to the shoot. *Journal of Experimental Botany*, *57*(11), 2577–2587. https://doi.org/10.1093/jxb/erl020

Keller, M., Zhang, Y., Shrestha, P. M., Biondi, M., & Bondada, B. R. (2015). Sugar demand of ripening grape berries leads to recycling of surplus phloem water via the xylem. *Plant, Cell & Environment*, *38*(6), 1048–1059. https://doi.org/10.1111/pce.12465

Krasnow, M., Matthews, M., & Shackel, K. (2008). Evidence for substantial maintenance of membrane integrity and cell viability in normally developing grape (*Vitis vinifera* L.) berries throughout development. *Journal of Experimental Botany*, *59*(4), 849–859. https://doi.org/10.1093/jxb/erm372

Lammertyn, J., Franck, C., Verlinden, B. E., & Nicolaï, B. M. (2001). Comparative study of the O_2, CO_2 and temperature effect on respiration between 'Conference' pear cell protoplasts in suspension and intact pears. *Journal of Experimental Botany*, *52*(362), 1769–1777. https://doi.org/10.1093/jexbot/52.362.1769

Litchfield, W. H. (1951). Soil survey of the Waite Agricultural Research Institute. *CSIRO, Division of Soils, Divisional Report*, *2*, 51. https://doi.org/10.4225/08/58712dac56dd4

Loreti, E., & Perata, P. (2020). The many facets of hypoxia in plants. *Plants*, *9*(6), 745. https://doi.org/10.3390/plants9060745

Ollat, N., Carde, J.-P., Gaudillère, J.-P., Barrieu, F., Diakou-Verdin, P., & Moing, A. (2002). Grape berry development: A review. *OENO One*, *36*(3), Article 3. https://doi.org/10.20870/oeno-one.2002.36.3.970

Rajapakse, N. C., Banks, N. H., Hewett, E. W., & Cleland, D. J. (1990). Development of oxygen concentration gradients in flesh tissues of bulky plant organs. *Journal of the American Society for Horticultural Science*, *115*(5), 793–797. https://doi.org/10.21273/JASHS.115.5.793

Raven, J. A. (1996). Into the voids: The distribution, function, development and maintenance of gas spaces in plants. *Annals of Botany*, *78*(2), 137–142. https://doi.org/10.1006/anbo.1996.0105

Rogiers, S. Y., Hatfield, J. M., Jaudzems, V. G., White, R. G., & Keller, M. (2004). Grape berry cv. Shiraz epicuticular wax and transpiration during ripening and preharvest weight loss. *American Journal of Enology and Viticulture*, *55*(2), 121–127. https://doi.org/10.5344/ajev.2004.55.2.121

Sasidharan, R., Bailey-Serres, J., Ashikari, M., Atwell, B. J., Colmer, T. D., Fagerstedt, K., Fukao, T., Geigenberger, P., Hebelstrup, K. H., Hill, R. D., Holdsworth, M. J., Ismail, A. M., Licausi, F., Mustroph, A., Nakazono, M., Pedersen, O., Perata, P., Sauter, M., Shih, M.-C., … Voesenek, L. A. C. J. (2017). Community recommendations on terminology and procedures used in flooding and low oxygen stress research. *New Phytologist*, *214*(4), 1403–1407. https://doi.org/10.1111/nph.14519

Schotsmans, W., Verlinden, B. E., Lammertyn, J., & Nicolaï, B. M. (2003). Simultaneous measurement of oxygen and carbon dioxide diffusivity in pear fruit tissue. *Postharvest Biology and Technology*, *29*(2), 155–166. https://doi.org/10.1016/S0925-5214(02)00251-X

Shivashankara, K. S., Laxman, R. H., Geetha, G. A., Roy, T. K., Srinivasa Rao, N. K., & Patil, V. S. (2013). Volatile aroma and antioxidant quality of 'Shiraz' grapes at different stages of ripening. *International Journal of Fruit Science*, *13*(4), 389–399. https://doi.org/10.1080/15538362.2013.789235

Smart, R. E., & Dry, P. R. (1980). A climatic classification for Australian viticultural regions. *Annual Technical Issue*.

Šuklje, K., Zhang, X., Antalick, G., Clark, A. C., Deloire, A., & Schmidtke, L. M. (2016). Berry shriveling significantly alters Shiraz (*Vitis vinifera* L.) grape and wine chemical composition. *Journal of Agricultural and Food Chemistry*, *64*(4), 870–880. https://doi.org/10.1021/acs.jafc.5b05158

Tilbrook, J., & Tyerman, S. D. (2008). Cell death in grape berries: Varietal differences linked to xylem pressure and berry weight loss. *Functional Plant Biology*, *35*(3), 173. https://doi.org/10.1071/FP07278

van Dongen, J. T., & Licausi, F. (2015). Oxygen sensing and signaling. *Annual Review of Plant Biology*, *66*(1), 345–367. https://doi.org/10.1146/annurev-arplant-043014-114813

Werker, E., Marbach, I., & Mayer, A. M. (1979). Relation between the anatomy of the testa, water permeability and the presence of phenolics in the genus Pisum. *Annals of Botany*, *43*(6), 765–771. https://doi.org/10.1093/oxfordjournals.aob.a085691

Xiao, Stait-Gardner, T., Willis, S. a., Price, W. S., Moroni, F. J., Pagay, V., Tyerman, S. D., Schmidtke, L. M., & Rogiers, S. Y. (2021). 3D visualisation of voids in grapevine flowers and berries using X-ray micro computed tomography. *Australian Journal of Grape and Wine Research*, *27*(2), 141–148. https://doi.org/10.1111/ajgw.12480

Xiao, Z., Liao, S., Rogiers, S. Y., Sadras, V. O., & Tyerman, S. D. (2018). Effect of water stress and elevated temperature on hypoxia and cell death in the mesocarp of Shiraz berries: Berry hypoxia and death

under water/heat stress. *Australian Journal of Grape and Wine Research*, *24*(4), 487–497. https://doi.org/10.1111/ajgw.12363

Xiao, Z., Rogiers, S. Y., Sadras, V. O., & Tyerman, S. D. (2018). Hypoxia in grape berries: The role of seed respiration and lenticels on the berry pedicel and the possible link to cell death. *Journal of Experimental Botany*, *69*(8), 2071–2083. https://doi.org/10.1093/jxb/ery039

Xie, Z., Fei, T., Forney, C. F., Li, Y., & Li, B. (2023). Improved maceration techniques to study the fruit vascular anatomy of grape. *Horticultural Plant Journal*, *9*(3), 481–495. https://doi.org/10.1016/j.hpj.2022.06.008

Zwiazek, J. J., Xu, H., Tan, X., Navarro-Ródenas, A., & Morte, A. (2017). Significance of oxygen transport through aquaporins. *Scientific Reports*, *7*, 40411. https://doi.org/10.1038/srep40411

Chapter 3

Towards a model explaining cell death and berry shrinkage in Shiraz:

Comparing rootstocks and other varieties

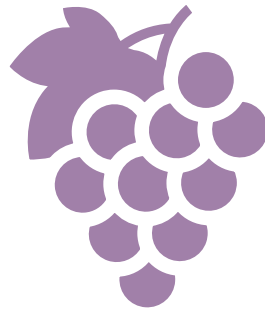# Table of Contents

Towards a model explaining cell death and berry shrinkage in Shiraz: comparing rootstocks and other varieties

1. Introduction

Late-ripening berry shrinkage and cell death of *Vitis vinifera* L. have caused increasing concerns worldwide, berry shrinkage normally becomes visible before desirable wine-making flavour ripeness and phenolic maturation are achieved, with significant adverse impacts on both grapes and resulting wines (McCarthy, 1997; McCarthy & Coombe, 1999; Sadras & McCarthy, 2007). Shrivelled berries tend to have excess sugar accumulation, higher pH (Bondada & Keller, 2012), lower anthocyanins and poor flavour development (e.g., lower terpenoids) (Shivashankara et al., 2013). Wines from shrivelled berries are likely to have deteriorated composition and sensory traits, including more alcohol, dark fruit and dead/stewed fruit characters (Chou et al., 2018; Šuklje et al., 2016). Besides, up to 30% yield loss has been reported for vines with shrivelled Shiraz berries (McCarthy, 1997; McCarthy & Coombe, 1999; Tilbrook & Tyerman, 2008). In the future under the influence of 'global warming' with more severe and frequent heat waves predicted (Perkins et al., 2012), berry shrinkage and cell death could be more serious (Bonada et al., 2013; Xiao, Liao, et al., 2018).

Generally, the development of grape berry mass follows a double-sigmoid pattern over time with three distinct development phases. *Phase* 1 'berry formation' from flowering to veraison, *phase* 2 'berry maturation' from veraison to peak fresh mass, and 'berry shrinkage' for *phase* 3 from peak fresh mass to harvest for some varieties such as Shiraz, but it rarely occurs in Grenache (Coombe, 1976, 1992; Sadras & McCarthy, 2007). Nearly 90% berry weight loss is in the form of water, and loss in dry weight could be accounted for by berry respiration (McCarthy & Coombe, 1999; Rogiers et al., 2000). Except for continued transpiration from berries, water flow back to the parent vine (backflow) was also reported to contribute to berry water loss (Keller, 2006; Rogiers, Hatfield, Jaudzems, et al., 2004; Tilbrook & Tyerman, 2009; Tyerman et al., 2008; Zhang & Keller, 2015). Backflow may be more prominent if berry cell death occurs in the mesocarp while berries are still well hydraulically

connected to the vine; a typical situation for Shiraz (Caravia et al., 2015; Fuentes et al., 2010; Tilbrook & Tyerman, 2008, 2009).

Sadras and McCarthy (2007) demonstrated that the slope of the regression between amount of sugar per berry and berry mass on a log-scale (SSM) was greater than 1 in *Phase* 2 while smaller than 1 in *Phase* 3, based on the allometric or scaling analysis, which deals with the differential growth rates of the organs of plants and animals (e.g., leaf vs root, liver vs heart) or process (e.g., body size vs metabolic rate) (McConnaughay & Coleman, 1999). This can be understood as the relative rate of sugar accumulation per berry in *Phase* 2 exceeding the relative rate of berry net accumulation of fresh mass. For *Phase* 3, a large reduction in berry mass offsets any change of sugar per berry. However, like other methods using time or change in mass as predictors of berry shrinkage, this method also relies on continuous data collection during the whole of berry development and is lagged to some extent, especially when sugar accumulation compensates for water loss. Utilising the significant variation in time of berry development that can naturally and commonly occur in the vineyard, between berries within a bunch, between bunches within a vine, and between vines within the vineyard (Amerine & Roessler, 1958; Armstrong et al., 2023; Deloire et al., 2019; Previtali et al., 2021; Shahood et al., 2020), a one-time sampling method on a single date sampling using an allometric model of sugar and berry mass data could be developed to monitor berry development.

The cause of berry cell death remains obscure. Several factors are reported to contribute to it, including heat stress, water stress and hypoxia inside the berries (Bonada et al., 2013; Caravia et al., 2015; Xiao, Liao, et al., 2018). Elevated temperature and water stress were found to induce and/or increase cell death and shrinkage in grape berries (Bonada et al., 2013; Caravia et al., 2015; Xiao, Liao, et al., 2018). For north-south oriented vine rows, berry clusters on the west side of vines, particularly for berries that are directly exposed to the afternoon sunlight, tended to have higher temperatures on average than that of east-facing clusters (Ponce de León & Bailey, 2021; Smart & Sinclair, 1976; Spayd et al., 2002), whether this temperature difference results in Shiraz berries on

the west side having more cell death and shrinkage remains unknown. Drought-tolerant rootstocks with high vigour (causing greater shading of clusters) may have decreased stress under water stress and high temperatures. The impact of varying drought-tolerant rootstocks on cell death and shrinkage in Shiraz berries is still not understood.

Cell death appears to be correlated with hypoxia in grape berries. For Shiraz berries, internal oxygen concentration [O_2] and cell vitality both declined with fruit ripeness (Xiao, Rogiers, et al., 2018; Xiao, Liao, et al., 2018). The mesocarp areas in the mid-section between the central axis and the berry skin had the lowest [O_2] and the highest level of cell death in Shiraz (Xiao, Rogiers, et al., 2018). In contrast, Ruby seedless, a table grape cultivar not displaying cell death and berry shrinkage, appeared to have high internal [O_2] and fewer hypoxic regions (Xiao, Rogiers, et al., 2018).

Ethanol synthesis from alcoholic fermentation (as a survival strategy), has been reported to increase in response to various stress, including heat, drought and hypoxia stress, mostly as a consequence of disruption of aerobic respiration, due in part to low oxygen concentration, disruption to mitochondrial membrane function and enzyme activity (Bashir et al., 2022; Fan et al., 2011; Kelsey & Westlind, 2017; Matsui et al., 2022). Hypoxia occurred in the centre of Chardonnay berries when oxygen diffusion into the berry was blocked by covering the obvious lenticels with silicone grease (Xiao, Rogiers, et al., 2018). Cell death increased, and ethanol accumulation increased, indicating the occurrence of alcoholic fermentation inside the berry due to hypoxia (Xiao, Rogiers, et al., 2018). The concentrations of ethanol accumulated reflected the degree of heat-induced fruit injury in apples (Fan et al., 2005) and in tree stems and woody tissues (Kelsey & Westlind, 2017). Therefore, ethanol accumulation can be used as an indicator of berry stress resulting from hypoxia and/or heat stress, at less extreme temperatures (e.g., 50 °C), above which the function of enzymes involved in ethanol synthesis (pyruvate decarboxylase and alcohol dehydrogenase) is inhibited (Kelsey & Westlind, 2017; Seidel, 1986). Generally, ethanol synthesis from alcoholic fermentation does not result in ethanol accumulation to toxic levels; even a concentration of 390 mM ethanol failed to simulate flooding

injury in peas (Jackson et al., 1982). The maximum ethanol concentration ([EtOH]) reported in Chardonnay berries was 32.5 mM when lenticels were blocked (Xiao, Rogiers, et al., 2018). When berries were kept in an anaerobic atmosphere for several hours to several days at 30 °C, up to about 195 mM and 220 mM were observed respectively in two studies (Saltveit & Ballinger, 1983; Tesnière et al., 1994).

This study aimed to a) identify the physiological cause of berry mesocarp cell death and shrinkage by exploring the correlation between temperature, ethanol accumulation, berry mesocarp cell death and berry shrinkage across different grape varieties, b) develop one easy model to monitor berry development at different phases by allometric analysis between berry sugar and fresh mass accumulation with one sampling, and c) test the influences of rootstocks (of different drought tolerance and vigour) and cluster orientation (east versus west) on Shiraz berry shrinkage and cell death.

2. Material and Methods

2.1. Experimental vineyard and climate

Samples of grape berries were taken from the Coombe Vineyard at Waite Campus of the University of Adelaide, South Australia (34°58'03.12" S and 138°38'00.21" E). The climate for Adelaide is classified as hot Mediterranean with wet winters and hot and dry summers, described as a warm to hot region with the mean January temperature (MJT) ranging from 21 °C to 25 °C (Smart & Dry, 1980). The soil type is classified as DR2.23 hard pedal red duplex with 8% clay content from 0 to 110 cm and 60% clay content at 300–690 cm (Litchfield, 1951); no stone layer or water table was present within this depth.

Most of the experiments were conducted over three consecutive growing seasons from 2018 to 2021. Seasonal temperature (station 23034), rainfall (station 23005) for growing seasons from 2018 to 2021 (Table 1) were sourced from the Australian Bureau of Meteorology website (Bureau of Meteorology,

www.bom.gov.au). Growing Season Temperature (GST) is the mean of monthly average temperatures for October to April, calculated from mean monthly maximum and minimum temperatures. Data from these stations were similar comparing to the local weather station in the vineyard.

2.2. Plant material

Experimental vines were *Vitis vinifera* L. cv. Shiraz (clone BVRC12) on own roots or different rootstocks (see below), Grenache (clone 137), Cabernet Sauvignon (clone 125), Chardonnay (clone I10V1). Vines of Grenache, Cabernet Sauvignon and Chardonnay are in one row respectively in the field. For Shiraz, own root (BVRC12) and four rootstocks of different drought resistances and vigour were selected, including Ruggeri 140, Ramsey, Schwartzmann and 420 A. According to Wine Australia Rootstock Selector Tool (https://www.grapevinerootstock.com/), Ruggeri 140 is classified as a high drought tolerant rootstock with moderate to high vigour, Ramsey as moderate to high drought tolerance with high vigour, Schwartzmann as low drought tolerance and moderate vigour, and 420 A as low to moderate drought tolerance and low to moderate vigour. Shiraz scions on different rootstocks and own roots are randomly located in 11 different rows in the field.

All Shiraz and Cabernet Sauvignon vines were planted in 1990, Grenache vines were planted in 2000, Chardonnay vines were planted in 2004, with rows (3 m spacing) north-south oriented under drip irrigation. Irrigation regimes were approximately 1.1 ML/ha of water per season for Shiraz and Cabernet Sauvignon, 1.5 ML/ha per season for Chardonnay, while no irrigation was provided for Grenache for the last 8 seasons. All other vineyard managements were the same for all varieties in this study. All vines have been trained in a two-wire vertical shoot positioned (VSP) trellis system and spur pruned to 2 buds.

There were 5 replications for each variety and Shiraz-rootstock combination where each replicate consisted of 3 or 4 adjacent vines. All berries were sampled from the west side of the canopy for Grenache and Cabernet Sauvignon, but from the east side for Chardonnay due to ease of access. For

Shiraz, berries were taken from each side of the canopy (east and west) as separate samples. Several healthy bunches were labelled for each replicate for cell vitality estimation (see 2.4) before veraison. Berries for the other estimations were from other unlabelled bunches.

Overall berry mass, total soluble solids (TSS) (see 2.3) and percentage of living tissue (PLT) in the mesocarp (see 2.4) for Shiraz were measured in three growing seasons in 2018-19, 2019-20, 2020-21. All 5 Shiraz rootstocks were examined in 2018-19 and 2019-20 seasons, while only 3 (Ramsey, 420 A, own roots) were examined in season 2020-21. The same measures were undertaken in the other three varieties (Chardonnay, Grenache, Cabernet Sauvignon) only in season 2020-21.

Overall berry samples for berry mass and TSS (see 2.3) were sampled approximately every week from two weeks before veraison until normal harvest date for wine making, lasting about 10 weeks, i.e., 10 samples per replication and rootstock for each season. Berry samplings for PLT (see 2.4) normally started two to three weeks later, resulting in about 7 samples per replicate and rootstock combination for each season. These two sets of measurements (overall berry mass/ TSS and PLT) for Shiraz were normally conducted in the early morning over two consecutive days, while for the other three varieties, they were done on the same day. All berries in this study were sampled from the outward side of the bunch. Berries were stored in one sealed plastic bag in groups and placed in a polystyrene box with an ice pack in to keep cool during transportation to the laboratory (approx. 30 mins).

2.3. Overall berry mass and total soluble solids

For all the varieties, for each sampling, 24 berries per replicate (5 replicates) were sampled randomly by hand (no pedicel attached) from 8 different unlabelled bunches, 3 berries per bunch, from proximal, mid, and base of the bunch respectively. Once samples were taken into the laboratory, total berry mass from each replicate was measured, berry number was counted, and the average single berry mass (berry mass$_{overall}$) was then calculated. Subsequently all 24 berries in one replicate were thoroughly squashed in the original sample bag (sealed PE plastic bag) by hand to get the juice. Juice

TSS ($TSS_{overall}$) (^{o}Brix) was then determined with a temperature compensated digital refractometer (Model PR101, Atago, Tokyo, Japan). Some juice was collected from the refractometer for ethanol concentration estimation (details see 2.5). Sugar per berry ($Sugar\ content_{overall}$) was taken as berry mass times TSS (Deloire, 2011).

2.4. Berry mesocarp percentage living tissue

For Grenache, Cabernet Sauvignon and Chardonnay, for each sampling, 4 berries were sampled per replicate. For Shiraz, there were 2 berries per replicate for each rootstock taken on each side of the canopy respectively. All berries were separated carefully from the pedicel by small scissors to avoid possible damage to berries. In total, there were approximately 100 berries in 2018-19 and 2019-20 season, 60 berries in 2020-21 season for Shiraz, and 20 berries each for Grenache, Cabernet Sauvignon and Chardonnay at each sampling. Measurement of percentage living tissue (PLT) for Shiraz was normally conducted over two consecutive days because of the large sample size.

Berry mesocarp PLT was estimated by fluorescein diacetate (FDA) vital staining on a half-cut berry, mostly as described in Tilbrook and Tyerman (2008). Briefly, a 2M sucrose solution was prepared (1 or 2 L volume) and stored in the 4 °C fridge for later use, 10 mL 4.8 mM FDA (SigmaAldrich, St Louis, MO, USA) solution (20 mg FDA dissolved in 10 mL acetone) was prepared and stored at room temperature with aluminium foil wrapping to avoid photolysis. On the day of measurement, several 50 ml stock solutions of sucrose of a range of osmolality were made based on predicated osmolarity of the berry juice, derived from TSS. These 50 ml stock solutions were diluted from the prepared 2M sucrose solution, with 5 µL of FDA solution added in to each 50 ml tube and well mixed. These 50 ml sucrose solutions were covered with aluminium foil during the whole process. After berries were taken into the laboratory from the field, single berry mass was first measured, then the berry was sectioned longitudinally between seeds with the help of a bright LED light shone through the berry in order to delimit seeds. One half of the berry was crushed for juice TSS (^{o}Brix) and juice ethanol concentration ([EtOH]) (details see 2.5). The other half for FDA staining was placed in one of 12

wells of a multi-well plate. About 2-3 ml of the prepared FDA solution of a similar osmolality (within 10%) was applied to completely submerge the sectioned berry. The plate was then covered with aluminium foil and incubated in the dark for at least 30 minutes. The half-berries were blotted, and the cross-section side was viewed under a Nikon SMZ 800 dissecting microscope (Nikon Co., Tokyo, Japan) at 0.5 x magnification under ultraviolet light. Images were obtained with the same gain and exposure settings (10 s exposure and 6.80 x gain) using a Nikon DS-5Mc (Tochigi Nikon Precision Co., Ltd, Otawara, Japan) colour-cooled digital camera and NIS-Elements F2.30 software. As there were often seeds included in the Shiraz images from the 2018-19 season, these images were also analysed using an ImageJ line transect procedure (Tilbrook & Tyerman, 2008) to exclude seeds. Image analysis in 2019-20 and 2020-21 seasons for all varieties was conducted by MATLAB 2017 based on Fuentes et al. (2010) with minimal modifications.

2.5. Berry ethanol concentration

Berry [EtOH] in juice was determined in two parts: a) [EtOH] in single berries in Shiraz from different rootstocks and b) average [EtOH] from a group berries (about 24 berries) in different varieties only on own root (Shiraz BVRC12, Grenache 137, Cabernet Sauvignon 125, Chardonnay I10V1).

a) Single berry [EtOH] in Shiraz

For juice [EtOH] estimation in single Shiraz berries, juice samples were collected from single Shiraz berries from 2019-20 season. In most cases the juice was collected during the PLT estimation process (see 2.4) from half-berries from 5 different rootstocks, the others were from single whole berries. After berry mass estimation, the whole berries were squashed for juice to measure TSS and then juice was stored in a 1.5 ml sealed Eppendorf tube with minimal headspace, kept on ice, and subsequently stored at -20 °C for later [EtOH] estimation.

b) Average [EtOH] to compare different varieties

The [EtOH] of grouped berries ([EtOH]$_{variety\ group}$) from the four varieties were examined to test for varietal differences during 2020-21 and 2021-22 season. Berries were taken from the west side of the canopy of Shiraz, Cabernet and Grenache, but from the east side of the Chardonnay canopy. Samples were taken irregularly and linked to forecast temperatures in order to sample before, during and after heatwaves. Roughly 10 to 20 samplings in total were performed during the season for each variety. There were 5 replicates for each variety on each sampling day with 24 berries per replicate. Berry sampling, average berry mass, TSS measurement, and the juice collection method were the same as outlined in 2.3. Juices were collected as detailed above before [EtOH] measurements. Some juices were from the overall berry mass/TSS measurements in 2.3.

On the day of [EtOH] estimation, juice samples were defrosted at room temperature and centrifuged to clarify. Juice samples in the 1.5 ml sealed Eppendorf tube were centrifuged at 14,000 rpm for 3 minutes. Care was taken to avoid loss of volatile ethanol from samples and lids were kept secured until the enzymic method was begun. After centrifugation (and dilution for some samples), berry [EtOH] was quantified with an enzymatic ethanol assay kit based on Xiao, Liao, et al. (2018) with minimal modifications following the manufacturer's instructions with standard curve included (Megazyme International Ireland, Wicklow, Ireland). All the pipette tips and Milli-Q water used for these estimations were autoclaved in advance. Two to three replicates were conducted for each sample estimation, and data with considerable variation were repeated later until two replicate values were reasonably close.

2.6. Canopy ambient temperature & berry temperature

The growing season of grape berries in the Southern hemisphere commences in September. During each growing season from the end of December to the following March, air temperature inside the canopy was recorded by temperature data loggers every 15 minutes with built-in sensors (Tiny Tag Transit 2 Data Logger thermometers, model TG-4080, Gemini Data Loggers, Chichester,

England). All the sensors have a reading resolution of 0.01°C according to the manufacturer's specifications. Sensors (Figure S1) were positioned on the east and west of the canopy at bunch level and were protected by two shells made of white Stevenson-type plastic funnels with holes drilled to allow air movement over the sensor but protecting the sensor from direct sunlight. There were about 50 sensors distributed in the field with each investigated roots stock and variety. Average values were calculated from all the sensors, then daily mean canopy air temperature $(T_{canopy\ air\ mean\ daily})$ and daily maximum canopy air temperature $(T_{canopy\ air\ max\ daily})$ were determined during each growing season.

The temperature of shaded berries is reported to be close to the ambient air temperature, while berries directly exposed to sunlight could reach over 15 °C above ambient air temperature (Ponce de León & Bailey, 2021; Smart & Sinclair, 1976; Spayd et al., 2002; Stoll & Jones, 2007). Therefore, for the modelling where temperature was an input to predict cell death, the daily mean canopy air temperature $(T_{canopy\ air\ mean\ daily})$ was defined as the lowest daily mean berry temperature (LBT), while the average daily mean berry temperature (ABT) and the highest daily mean berry temperature (HBT) were defined as $(T_{canopy\ air\ mean\ daily} + 2.5)$, and $(T_{canopy\ air\ mean\ daily} + 5)$, the ABT was used to fit the model to predict average PLT, and the LBT and HBT were used to simulate the PLT variation.

During a heatwave on one occasion when daily maximum air temperature was 40 °C at 16:30 (28th January 2020, Shiraz berries 19 days after veraison, TSS = ~ 18 °Brix), Shiraz berry mesocarp temperatures were measured when the bunches were exposed to the direct solar beam (at approx.16:00) using an IR thermometer (Fluke 568; Fluke Corporation, Everett, WA, USA) and with a type-K thermocouple bead probe (Fluke 80PK-1). Five Shiraz berries (exposed to sunlight) in the field were randomly chosen and berry mesocarp temperature was measured with the bead probe inserted inside the berry.

2.7. Stem water potential

Midday stem water potential measurements of different Shiraz rootstocks after veraison were carried out in 2019-20 (on 11/2/2020) and 2020-21(on 11/3/2021) season, and pre-dawn water potential in 2018-2019 (on 8/1/2019) season. The procedures followed that from Iland et al., (2011). In 2019-20 and 2020-21 season, stem water potential was measured on a sunny day between 11:00 and 13:00 (Australian CST) in order to determine if there were large variations across the vineyard or related to rootstock. For each replicate, one healthy and fully expanded leaf was selected from the mid – upper part of the canopy on each side (east and west) of the canopy. All selected leaves were fully exposed to sunlight and were enclosed in a foil covered zip-locked bag for 1 hour to prevent transpiration and equilibrate with the stem before measurements. The bagged leaves were placed in the pressure chamber as soon as possible (less than 5 seconds) after excision from the vine.

2.8. Plant area index and pruning mass per vine

Plant area index (PAI) is an important factor in the assessment of grapevine canopy architecture, which is often defined as the total one-side area of leaf tissue and woody structure (non-leaf material) per unit ground surface area (Breda, 2003). During 2018-19, and 2019-20 season, PAI of each Shiraz vine from different rootstocks was estimated at the Coombe vineyard using an iPhone App (VitiCanopy) (De Bei et al., 2016). PAI is referred to as LAI_e in their study (De Bei et al., 2016). One image per vine was taken using the front camera of the device with a 'selfie stick', to allow the operator to see the image to be taken on the screen and instantly judge its suitability for analysis. Upwardly direct photographs under the canopy for analysis were taken consistently at 20 cm from the trunk. The images were taken between 10:00 and 12:00 to avoid sun reflection. PAI of each vine was automatically estimated by the VitiCanopy APP with these images.

The pruning mass was also recorded in the three growing seasons at the Coombe vineyard by cutting all the canes to two nodes, and the values are presented as mass (kg) per vine.

2.9. Statistical analysis

The correlations (by 'Pearson correlation') between average berry mass (Berry mass$_{average\ Shiraz}$) and TSS (TSS$_{average\ Shiraz}$) and the slope of the regression between amount of sugar per berry and berry mass in a log-scale (Sadras & McCarthy, 2007) at each sampling date in the different development phases were tested by package 'ggplot' in R. To exclude the influence of initial cell divisions, i.e., to normalise to number of cells in the berry, outliers for each rootstock replicate with very high or very low 'berry mass at 15 °Brix' were excluded using the interquartile range (IQR) method (range = 1) (Barbato et al., 2011). For each rootstock replicate, the 'average berry mass at 15 °Brix' was calculated by simple linear regression between berry mass and TSS when TSS ranged between 10 to 18 °Brix. This is based on the assumption that berry cell division had finished while loss of berry mass had not yet started. Excluded vines were two Ramsey and one Ruggeri 140 replicates in 2018-19 season (high values), and two 420A replicates in 2020-21 season (one with low values, one with high values) (Figure S2). Cross-validation (Berrar, 2019) resampling was employed to tests the model of a smaller sample size. On each sampling date, all samples were randomly divided 5-fold in 2018-19 (46 samples in total) and 2019-20 season (50 samples in total), and 2-fold in 2020-21 season (26 samples in total) to get subsets of around 10 samples, repeated 100 times, i.e., around 500 subsets were created with 10 samples in each subset for 2018-19 and 2019-20 season, and 200 subsets for 2020-21 season. Then the model was tested with these subsets.

All data analysis, visualisation, and statistics were performed using R (R Foundation for Statistical Computing, Vienna, Austria) and RStudio software version 1.4.1717 (https://www.rstudio.com/) and associated packages.

3. Results

3.1. Seasonal conditions and Phenological stages

In 2018-19, 2019-20 and 2020-21 seasons, the average temperature during the growing season from September to April was 19.86 °C, 19.22 °C and 19.54°C while the mean January temperature was 24.55 °C, 21.95 °C and 22.25 °C respectively (Table 1). As for rainfall, the total precipitations were 159.4 mm, 196.8 mm and 236.0 mm respectively during the three seasons. Season 2018-19 was the driest and hottest season with only 0.2 mm and 13.2 mm rainfall in January and February respectively. Canopy air temperatures (from the sensors in Figure S1) in the west canopy side tended to be higher than that in the east side after 14:00 pm, up to 5 °C differences occurred at about 16:00 when daily maximum temperature was usually achieved (Figure S3). The physiology stages of different varieties from different seasons are summarised in Table 2. Veraison for Shiraz in season 2020-21was about 1 week earlier than the other two seasons.

Table 1 Climate conditions for the three seasons of the study. Growing season monthly mean temperature (°C), growing degree days (°C days), and monthly total rainfall (mm) in Coombe Vineyard from 2018-2021.

	Mean temperature (°C)			GDD (°C days)			Total rainfall (mm)		
	2018-2019	2019-2020	2020-2021	2018-2019	2019-2020	2020-2021	2018-2019	2019-2020	2020-2021
Sep	13.10	13.60	15.75	93.00	108.00	172.50	25.4	50.2	70.4
Oct	17.55	17.60	16.60	327.05	343.60	377.10	28.4	23.2	59.4
Nov	18.30	17.70	21.25	576.05	574.60	714.60	51.8	23.0	12.2
Dec	22.55	22.85	20.10	965.10	972.95	1,027.70	31.4	17.0	20.2
Jan	24.55	21.95	22.25	1,416.15	1,343.40	1,407.45	0.2	27.6	24.4
Feb	22.40	20.90	21.15	1,763.35	1,659.50	1,719.65	13.2	51.6	28.2
Mar	20.55	19.95	19.65	2,090.40	1,967.95	2,018.80	9.0	4.2	21.2
Apr	18.85	16.90	16.95	2,355.90	2,174.95	2,227.30	9.0	102.0	21.4
Average	19.86	19.22	19.54						
Total							**159.4**	**196.8**	**236.0**

Table 2 Key phenology stages during the study for each of the varieties. Dates of flowering (E-L stage 23) and veraison (E-L stage 34) for different varieties in Coombe Vineyard from 2018 to 2021.

Variety	Stage	2018-2019	2019-2020	2020-2021
Shiraz	Flowering	5 Nov 18	3 Nov 19	4 Nov 20
	Veraison	5 Jan 19	9 Jan 20	31 Dec 20
Grenache	Flowering			6 Dec 20
	Veraison			7 Jan 21
Chardonnay	Flowering			3 Nov 20
	Veraison			22 Dec 20
Cabernet Sauvignon	Flowering			8 Nov 20
	Veraison			1 Jan 21

3.2. Rootstock & canopy orientation impacts on Shiraz berry mass and TSS

Based on the different drought tolerance and vigour (see 2.2), Shiraz own root (BVRC12) and the four rootstocks were classified into two groups for analysis, Ramsey and Ruggeri 140 rootstocks were grouped as high drought tolerant and high vigour, while Shiraz on own roots, Schwartzmann and 420A were grouped as low drought tolerant and low vigour rootstocks. In each rootstock group (high and low drought tolerance/vigour), there were no significant differences of both berry mass and TSS between different rootstocks (all $p > 0.05$) in all season's sampling dates by two-way ANOVA (factors = rootstock, canopy orientation) and pairwise comparisons (default Bonferroni correction) using package 'BruceR' in R (Figure S4, S5). Therefore, data of different rootstocks in each group were combined for later analysis.

For comparison and analysis of the berry development parameters, TSS and mass, sampling dates in the three growing seasons were allocated into one of four groups according to berry development as 1) '*Phase* 1 berry formation' (days after veraison (DAV) between -15 to -7), 2) '*Phase* 2 berry ripening' (DAV between 0 to 14), 3) 'Around peak mass' (DAV between 19 to 35), 4) '*Phase* 3 berry shrinkage' (DAV between 40 to 50). Then the differences of berry mass and TSS between rootstock groups (high versus low drought tolerance/vigour) and canopy orientation (east versus west) at different development phases were checked by two-way ANOVA (factors = drought tolerance/vigour,

canopy orientation) (Figure 1, 2). No interactions from drought tolerant/vigour grouping and canopy

orientation in both TSS and berry mass were observed in all three seasons.
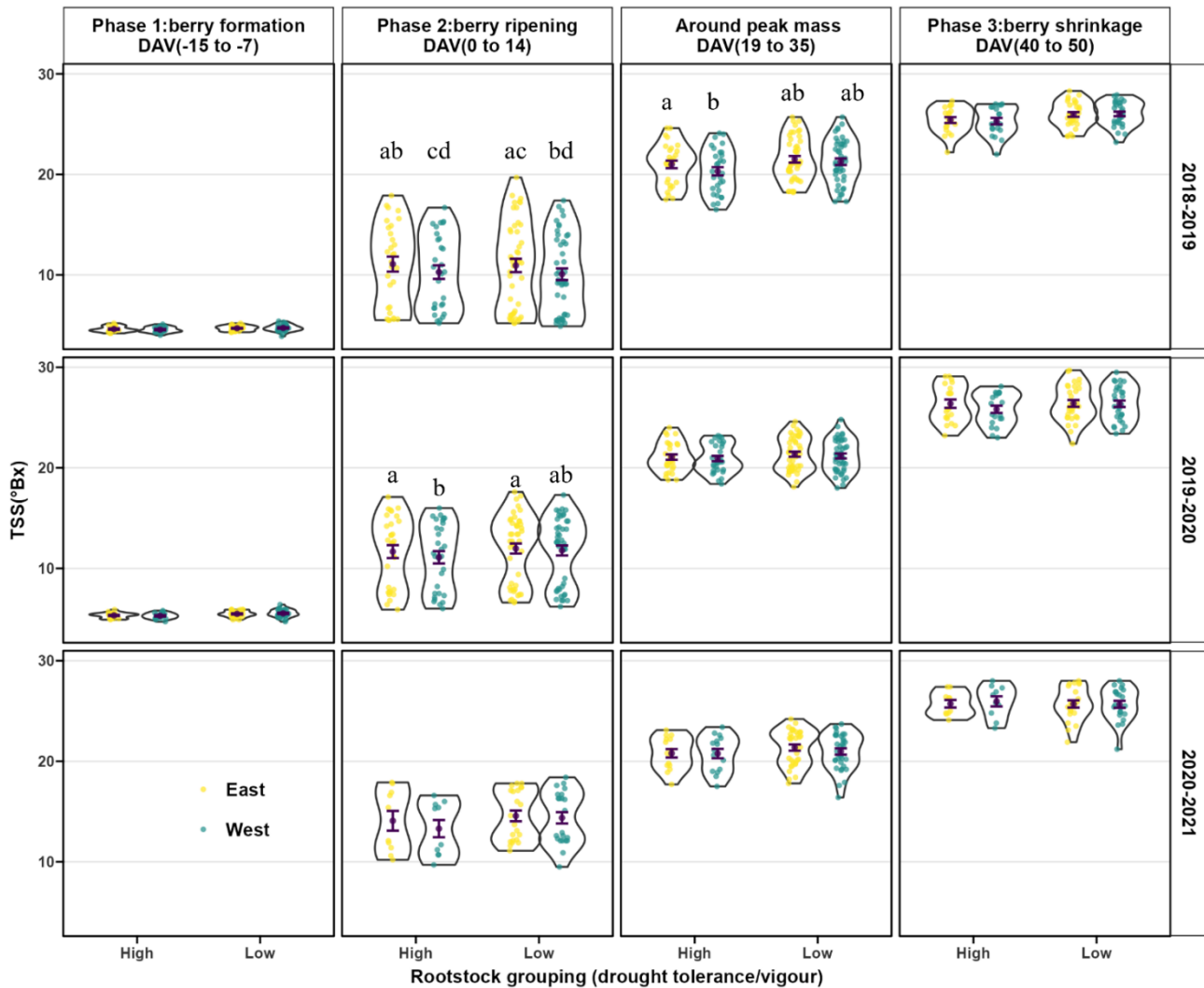
Figure 1 Comparison of berry TSS of Shiraz berries comparing rootstock cohorts and bunch orientation in the different phases of development over the three seasons of study. Cohorts of rootstocks are based on high and low drought tolerance/vigour. Violin plots with individual data are shown for east (yellow) and west (blue) orientations of bunches. Purple dots are mean ± SEM (n =10 to 45). Different letters indicate statistically significant differences ($p < 0.05$) in each subplot. No letters indicate no significant differences.
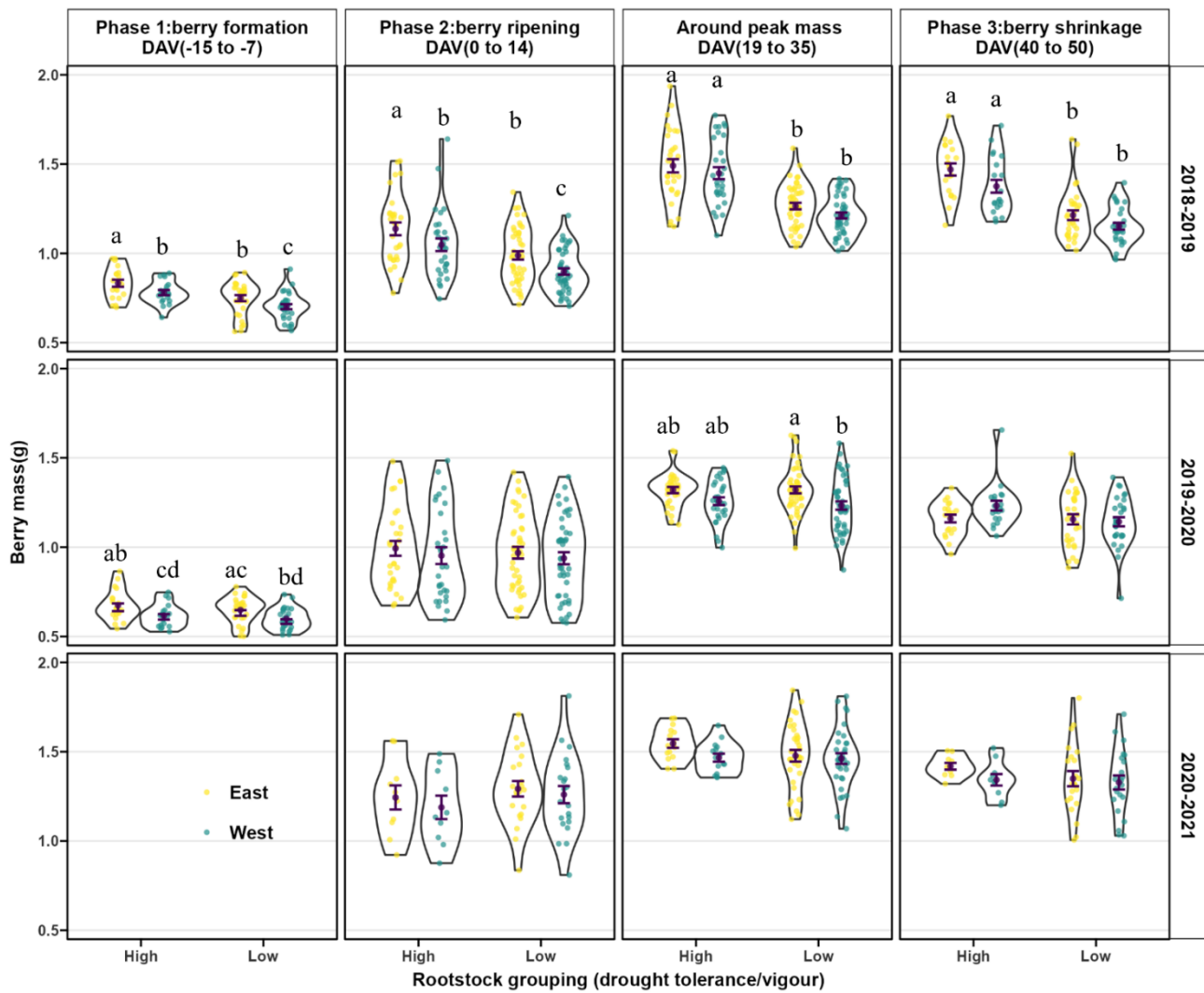
Figure 2 Comparison of Shiraz berry mass comparing rootstock cohorts and bunch orientation in the different phases of development over the three seasons of study. Violin plots with individual data are shown for east (yellow) and west (blue) orientated bunches. Purple dots are mean ± SEM (n =10 to 45). Different letters indicate statistically significant differences ($p < 0.05$) in each subplot. No letters indicate no significant differences.

In all development phases in each season, there was no significant effect of drought tolerant/vigour groupings on TSS (Figure 1). Berries on the east side tended to have slightly higher TSS than those on the west side, but only in season 2018-19 and 2019-20 and mostly in '*Phase* 2' (berry ripening).

In terms of berry mass, the effects of drought tolerance/vigour and canopy orientation were different in different growing seasons (Figure 2). In season 2018-19, both drought tolerant/vigour and canopy orientation are likely to influence berry mass. Specifically, in '*Phase* 1' and '*Phase* 2', berry mass was largest in Shiraz berries on the higher drought tolerant/vigour rootstocks on the east side, and lowest in the low drought tolerant/vigour rootstocks on the west side, while there were no significant differences between the other two combinations, i.e., berries on scions on the high drought tolerant/vigour on the west side and on the low drought tolerant/vigour on the east side. At 'around peak mass' and '*Phase* 3', no significant differences were found between east and west side of the canopy while high drought tolerant/vigour rootstocks tended to result in berries of higher mass on the scions.

In season 2019-20, no significant differences from drought tolerance/vigour, only canopy orientations had significant effects on berry mass. Berries in *Phase* 1 (2019-20 season) on the east had higher berry mass than that of the west side. In *Phase* 3 (2019-20 season), berries from east side also tended to have higher berry mass than that on the west side, but only in the low drought tolerant/vigour group. In the 2020-21 season, the significant impacts from both drought tolerance/vigour and canopy orientation on berry mass were not evident.

3.3. Rootstock & canopy orientation impacts on water potential, PAI and pruning mass per vine

As a check on heterogeneity within the trial for irrigation, no significant differences (one way ANOVA and T-test) were observed in stem water potentials measured during late ripening for different rootstock/scion combinations nor for different rootstock groupings near midday in 2019-20 and 2020-21 seasons (Figure 3-BC, S6-BC), also for predawn water potentials in 2018-19 season (Figure 3-A, S6-A). The predawn water potentials were about -0.42 to -0.12 MPa in 2020-21 season. The midday stem water potential in 2019-20 and 2020-21 season was about -0.81 to -1.25 MPa, no values lower than -1.5 MPa were observed.

The Plant area index (PAI) (Figure 3-DEF, S6-DEF) and pruning mass per vine (Figure 3-GH, S6-GH) for the different rootstock groupings (unpaired T test) and for rootstock/scion combinations (one way ANOVA) in different seasons were examined and tested for differences. As expected, the high drought tolerant/vigour rootstock groupings (Ramsey and Ruggeri 140) gave higher pruning mass per scion in 2018-19 and 2019-20 season (Figure 3-DEF), as well as higher PAI than the low drought tolerant/vigour rootstocks (Own root, Schwarzmann and 420A) but only in 2018-19 season (Figure 3-GH). Comparing different rootstocks (Figure S6-DEFGH), the high drought tolerant/vigour rootstocks (Ramsey and Ruggeri 140) sometimes gave higher pruning mass per scion as well as higher PAI than the less drought tolerant/vigour rootstocks (Own root, Schwarzmann and 420A), but this was inconsistent between seasons.
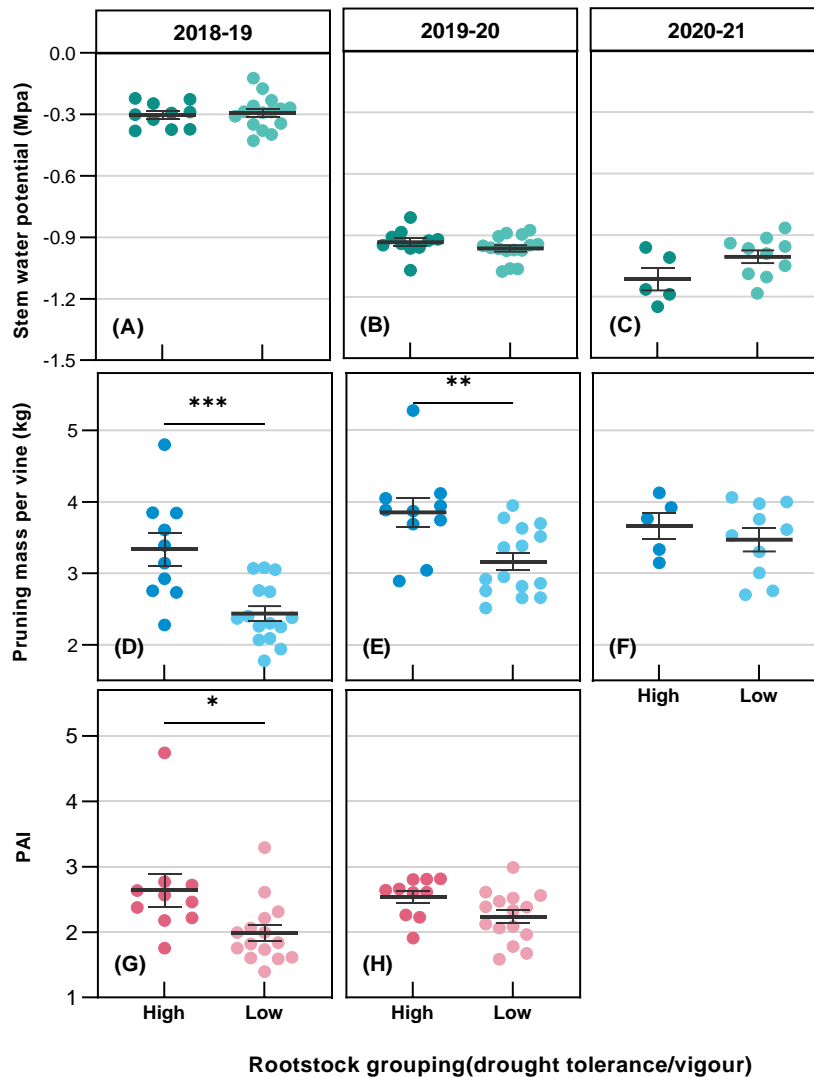
Figure 3 Water potential and canopy development of the two rootstock groupings for the three seasons of study. Shiraz stem water potential (A, B, C), pruning water per vine (D, E, F) and Plant Area Index (PAI) (G, H). Water potentials in 2018-19 were measured at pre-dawn, while midday stem water potentials are shown for season 2019-20 and 2020-21. Point plot with mean ± SEM (n =5 to 15). Unpaired T tests were performed to test the effects of rootstock group on stem water potential, pruning weight per vine and PAI in each season. Rootstock grouping had no significant impacts on stem water potential in all seasons. High drought tolerance/vigour grouping tended to have significant higher pruning mass per vine in 2018-19 and 2019-20 season, and higher PAI in 2018-19 season. * $p < 0.05$, ** $p < 0.01$, *** $p < 0.001$.

3.4. Shiraz berry cell death and temperature

Mesocarp PLT (Figure S7) and berry juice [EtOH] (data not shown) did not differ significantly between Shiraz scions on different rootstocks nor between east and west canopy side on each sampling date by two ANOVA (factors = rootstock, canopy orientation), so the data from all rootstocks and both east and west side of each sampling was combined. Figure 4 shows combined mesocarp PLT of single Shiraz berries and the changes over days after veraison (DAV), indicated with violin plots showing the distribution of data within sample dates. The daily maximum $(T_{canopy\ air\ max\ daily})$ and mean $(T_{canopy\ air\ mean\ daily})$ canopy air temperatures are shown below the plots of PLT for each of the three seasons.

In all three seasons, the mesocarp PLT decreased with DAV and with obvious increased variation with time (DAV) (Figure 4). When there were higher temperature events (normally when $T_{canopy\ air\ max\ daily}$ was above 35 °C as indicated), there was sometimes an apparent step decrease in PLT during or just after these heatwaves. These steps generally occurred with increased PLT variation (dramatic decrease of minimum PLT with slight decrease in maximum PLT). It should be noted that the maximum PLT at each sample date showed only small decreases during the whole of development. Even at the very late stages, the PLT can range from approximately 20% to 95% for season 2019-20 and 2020-21.

To directly quantify the temperature effects on Shiraz mesocarp PLT, regressions were performed between mean Shiraz mesocarp PLT and growing temperature days (GTD_n) base 10 °C with different powers of n from 1 to 4 (Figure S8, Table S1) to reflect non-linearity between PLT response and temperature, the function is:

$$\text{Mean PLT} = a + b*GTD_n, \text{ where } GTD_n = \sum_{DAV=0(veraison)}^{DAV}(ABT - 10)^n \ (n = 1,2,3,4). \quad \text{Eq. 1}$$

This model was developed from data in 2019-20 and 2020-21 season and was fit to all three seasons for predication (Figure S8, Table S1). The results indicate that using higher n (greater non-linearity)

resulted in a better fit compared to using GTD (n=1), and especially better at capturing the step decrease after heatwaves. The model with GTD_4 was the best ($R^2 = .904$, F (2, 11) = 113.7, $p < .0001$) (Table S1). Then predications of average PLT, minimum PLT, and maximum PLT in the three seasons were performed based on the best model (i.e., PLT = a + b*GTD_4) using average bunch temperature (ABT), lowest estimated bunch temperature (LBT) and highest estimated bunch temperature (HBT) respectively as limits. This resulted in the non-linear increased variation of LTP predicted by the model (Figure 4).

During a heatwave on one occasion when daily maximum air temperature was 40 °C at 16:30 (on 28th January 2020, Shiraz berries 19 days after veraison, TSS = ~ 18 °Brix), mesocarp temperatures of five Shiraz berries were measured when the bunches were exposed to the direct solar beam (at approx.16:00), berry surface and internal bunch temperatures over 50 °C were observed (Table S2). Sun exposed berries had internal temperatures between 5 and 10 °C above ambient air temperature so 5 °C above ambient for HBT is a conservative estimate.
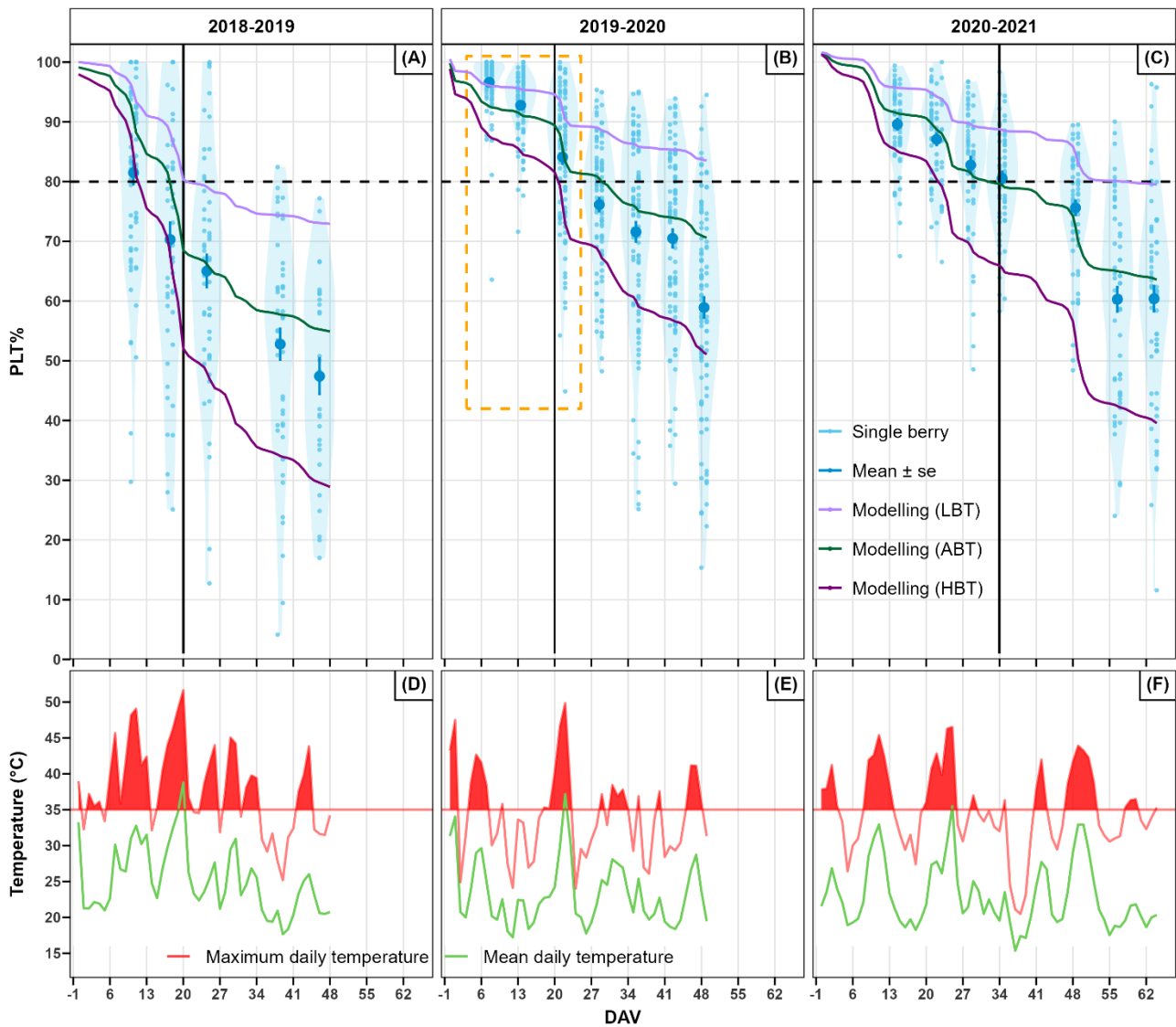
Figure 4 Time course of percentage living tissue (PLT) over three growing seasons for single Shiraz berries and corresponding canopy air temperatures. The PLT is shown plotted against days after veraison (DAV), and the data distribution is shown with violin plots (pale blue) combined with individual data points (light blue dots) of three growing seasons from 2018 to 2021 at Coombe vineyard. (D) (E) and (F) show mean ($T_{canopy\ air\ mean\ daily}$) and maximum ($T_{canopy\ air\ max\ daily}$) daily temperatures. Daily maximum temperatures above 35 °C are indicated by red in-fill. Dark blue dots are PLT data as mean ± SEM (n = ~50 in 2018-19 season, n = ~ 100 in 2019-20 season, n = ~ 60 in 2020-21 season). The regression fit is shown for Mesocarp PLT = a + b*GTD_4, where $GTD_4 = \sum_{DAV = 0(veraison)}^{DAV}(ABT - 10)^4$. Predictions of average PLT (dark green, "Modelling (ABT)"), minimum PLT (light purple, "Modelling (LBT)"), and maximum PLT (dark purple, "Modelling (HBT)") in the three seasons were based on the model using ABT, LBT and HBT. The orange dashed box in (B) indicates the data used for the correlation matrix in Figure 5. The horizon black dashed lines in (A) (B) and (C) indicate the PLT of 80%. The vertical black lines in (A) (B) and (C) indicate 20,20 and 34 DAV when berry mass loss onset in the three consecutive seasons estimated by CMT and SSM (see 3.7, Table 4).

3.5. Shiraz berry cell death, temperature and [EtOH]

The temperature effects on grape berries were further identified from the [EtOH] responses in single Shiraz berries with a correlation matrix (Figure 5, the bottom row of subplots). For the first three samplings from six days in 2019-20 season (on 7, 8, 13, 14, 21, 22 DAV) (orange dashed box in Figure 4), the correlation between TSS, berry mass, [EtOH] and PLT of single Shiraz berries on each sampling date were tested (Figure 5). The temperatures on DAV 7, 8, 13 and 14 were relatively low, and the maximum daily temperature (canopy air) was approximately 30 to 35 °C (Figure 4). On these DAV, the [EtOH] was minimal in all berries (about 0.1 mg/ml or even lower), no significant correlations were observed between all the variables (Figure 5). However, a heatwave occurred during the third sampling (21 and 22 DAV) where the maximum daily temperature (canopy air) was above 45 °C (Figure 4). During and after the heatwave (21 and 22 DAV), the [EtOH] was much higher than that of the first two samplings (DAV 7, 8, 13 and 14), increasing from about 0.1 mg/ml to up to 1.6 mg/ml of berry juice (Figure 5). Also, the [EtOH] showed a significant positive correlation with TSS on both 21 DAV (r (n = 36) = 0.457, $p < 0.01$) and 22 DAV (r (n=56) = 0.707, $p < 0.001$). The [EtOH] were slighted negatively correlated to mesocarp PLT (r (n~60) = -0.319, $p < 0.05$) on 22 DAV.
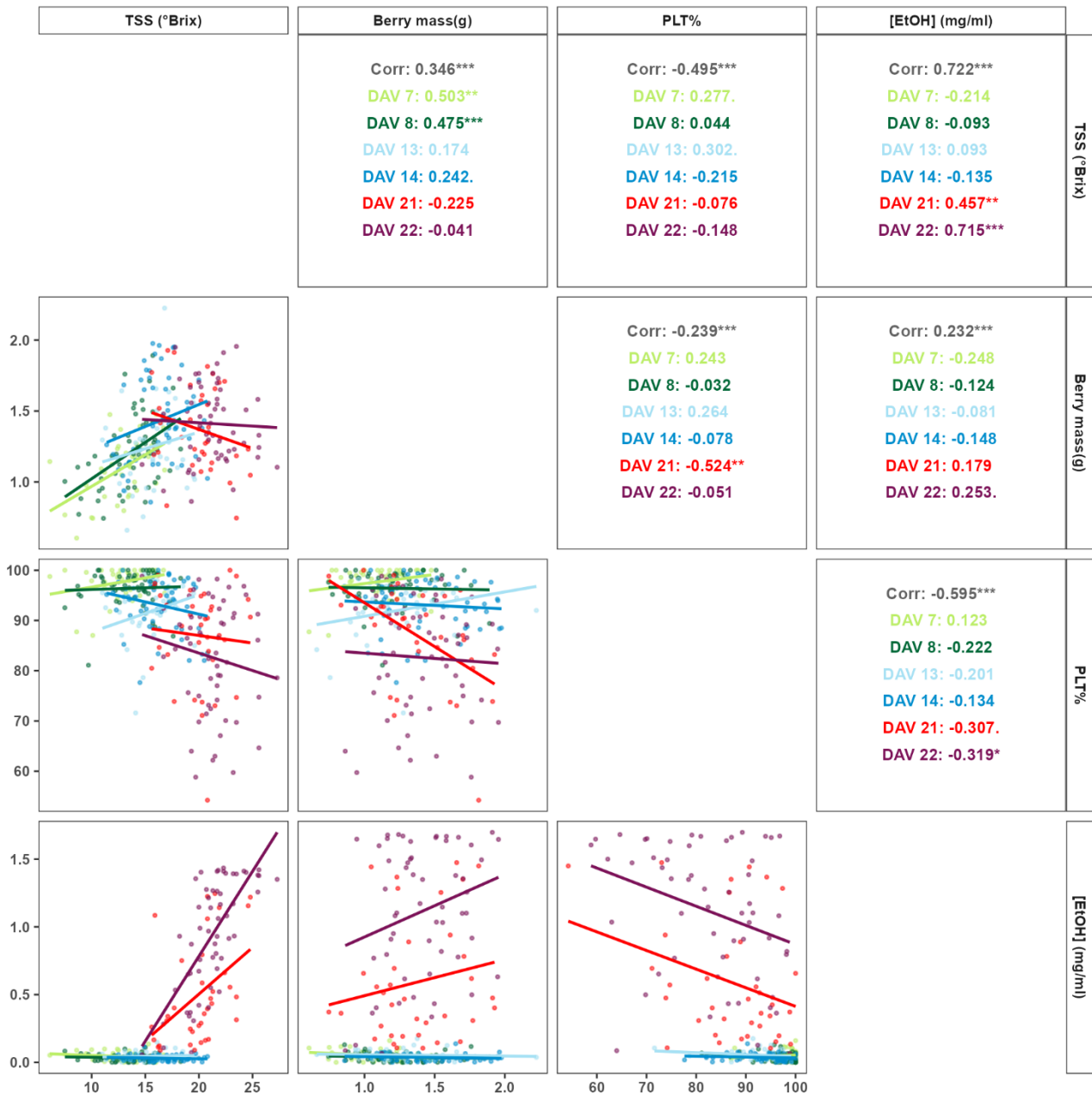
Figure 5 Correlations between Shiraz berry mass, TSS, berry ethanol concentration ([EtOH]) and PLT from a selected period indicating the effects of a heatwave. The correlation matrix (Pearson correlation) of berry mass, TSS, [EtOH] and PLT of single Shiraz berries in 2019-20 season on 7 (n=31), 8 (n=55), 13 (n=38), 14 (n=59), 21 (n=36), 22 (n=56) DAV respectively (see Figure 4, orange box). Correlation coefficients and significance levels are shown, grey colours ("Corr") indicate the overall results. Different colours indicate different DAV. On 7,8,13,14 DAV, there was almost no correlation between each of the variables on these four days. However, [EtOH] was positively correlated with TSS (all $p < 0.01$) on both DAV 21, 22 during a heatwave. [EtOH] was also slightly negatively correlated with PLT but only significantly on 22 DAV ($p < 0.05$). *$p < 0.05$, ** $p < 0.01$, *** $p < 0.001$.

As the TSS and temperature seem to be the most important factors related to berry [EtOH] according to the correlation matrix (Figure 5), a model was fitted using TSS and maximum canopy ambient temperature of the previous day as predicators of [EtOH] (Figure 6). On each sampling date, data from about 10 to 20 berries of similar TSS was summarised to obtain the average [EtOH] ([EtOH]$_{single\ avergage}$) and average TSS (TSS$_{single\ avergage}$). The T$_{canopy\ air\ max\ daily}$ from the previous day was used since it was observed that once EtOH accumulated in berries after a heat event there was a lag (several days) before it dissipated (e.g., Figure 7). This is also linked to the physiological model (see 1. Introduction and Chapter 1) where hypoxia is more likely to occur during a heat event. Based on the shape of the relationships, a 2d sigmoidal model (Figure 6) was fitted using the 'nls' function (package 'Stats') in R, the model equation is specified as

$$[EtOH]_{single\ avergage}) = (\frac{(Asym - mini1)}{(1 + \exp(\ TSS_{single\ avergage}) - xmid1\ )/scal1)))} + mini1) *$$

$$(\frac{Asym - mini2}{(1 + \exp(\ (T_{canopy\ air\ max\ daily} - xmid1\ )/scal2)))} + mini2) \qquad \text{Eq. 2}$$

Where the 'Asym' is the asymptote of the sigmoid function, i.e., the maximum of [EtOH] values. Along the TSS$_{single\ avergage}$ and T$_{canopy\ air\ max\ daily}$ dimensions, 'mini1' and 'mini2' were the minimum of [EtOH] values, 'xmid1' and 'xmid2' denote inflection points at which the growth rate is maximized, 'scal1' and 'scal2' determine the steepness of the curve. These coefficients determine the shape and behaviour of the sigmoid function within the model.

The results show that the relationship between the [EtOH] and the variables TSS$_{single\ avergage}$ and T$_{canopy\ air\ max\ daily}$ roughly followed a two dimensional sigmoid pattern when TSS was between 10 to 32 °Brix and T$_{canopy\ air\ max\ daily}$ was between 32 °C and 50 °C (Figure 6, Table 3). This model indicated that [EtOH] was positively correlated to TSS and ambient temperature, and the influence of TSS and ambient temperature on [EtOH] was highly dependent. When the TSS was lower than 15 °Brix, the [EtOH] was minimal (about 0.1 mg/ml or even lower) even though the T$_{canopy\ air\ maximum\ daily}$ could be above 45 °C. When the TSS was above 15 °Brix, there seemed to

be a $T_{canopy\ air\ maximum\ daily}$ threshold below which [EtOH] was very low (up to about 0.1 mg/ml) and above which the [EtOH] increased dramatically to a maximum of 1.6 mg/ml. This threshold in $T_{canopy\ air\ maximum\ daily}$ decreased with increasing TSS, from about 50 °C at 15 °Brix to about 35 °C when TSS was above about 25 °Brix.
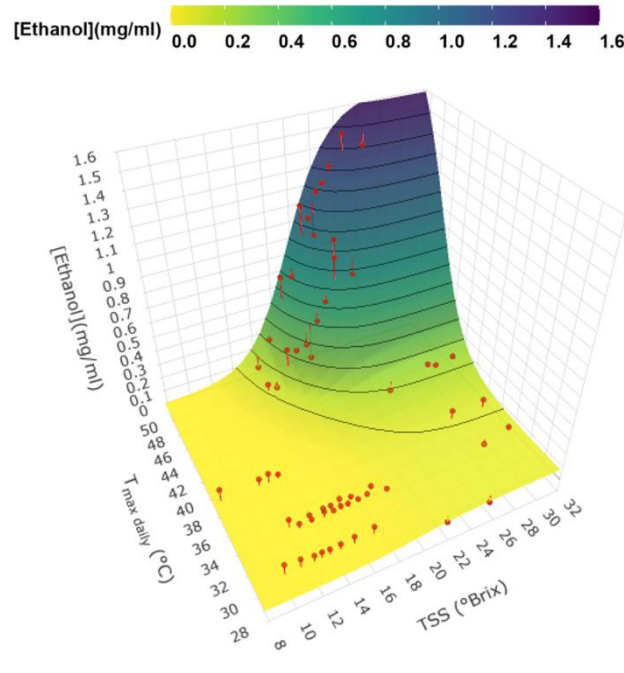
Figure 6 Effect of TSS and temperature on Shiraz berry ethanol concentration. Data is shown for the 2019-20 season. The model fit to the data (details in Table 3) is: $[EtOH]_{single\ avergage} =$

$$\left(\frac{(Asym - mini1)}{(1 + \exp(\ TSS_{single\ avergage}) - xmid1\ )/scal1)))} + mini1\right) * \left(\frac{Asym - mini2}{(1 + \exp((T_{air\ max\ daily} - xmid1\ )/scal2)))} + mini2\right) \qquad .$$

Red dots are original data, and the black lines are contour lines at 0.1 mg/ml [EtOH] intervals.

Table 3 Statistics summary of model to predict [EtOH] with TSS and daily maximum temperature (Figure 6). The equation is: $[EtOH]_{single\ avergage} = (\frac{(Asym-mini1)}{(1+\exp\ (\ TSS_{single\ avergage})\ -xmid1\ )/scal1)))} + mini1) * (\frac{Asym-mini2}{(1+\exp\ (\ (T_{air\ max\ daily}-xmid1\ )/scal2)))} + mini2)$. 'mini1' is not shown as it is not significant; ***, * indicate significant difference ($p < 0.001$, $p < 0.05$).

Parameters	Estimated	Std.Error	t-ratio	*p*-value
Asym (mg/ml)	1.38991	0.09034	15.386	<0.0001***
mini2(mg/ml)	0.05980	0.02630	2.274	<0.05*
xmid1(mg/ml)	19.54446	0.31122	62.800	<0.0001***
xmid2(mg/ml)	46.87128	0.82053	57.123	<0.0001***
scal1 (mg/ml/°Bx)	-1.88926	0.23581	-8.012	<0.0001***
scal2(mg/ml/°C)	-2.41988	0.51415	-4.707	<0.0001***
$R^2 =$		0.9633793		
Residual standard error		0.08279		
Degrees of freedom		58		
Achieved convergence tolerance		4.991e-06		

3.6. Variety differences – [EtOH], cell death and berry mass loss

Ethanol accumulation in berries from different varieties (Shiraz, Cabernet Sauvignon, Chardonnay and Grenache) ([EtOH]*variety group)* was examined in 2020-21 and 2021-22 seasons with respect to temperature during the seasons (Figure 7). The mesocarp PLT (Figure 8), berry mass and TSS (Figure 9) of Cabernet Sauvignon, Chardonnay and Grenache during 2020-21 season were also measured. The mean berry [EtOH] for all varieties is likely to be positively correlated with temperature (Figure 7). In terms of variety differences, Shiraz and Cabernet Sauvignon had similar berry [EtOH] responses during the growing season (Figure 7). The change in mesocarp PLT and berry mass of Cabernet Sauvignon (Figure 8, 9) during development also had similar patterns to that of Shiraz (Figure 4, 10), i.e., berry mass decreased with time after reaching a maximum, and mesocarp PLT decreased with time with obvious increased variation corresponding to extreme heat events. In contrast, the berry [EtOH] in Grenache was much lower than that for Shiraz and Cabernet Sauvignon, especially when the temperatures were above 35 °C (Figure 7). Meanwhile, there was almost no loss

of berry mass nor cell death observed in Grenache during development (Figure 8, 9). Even at very late ripening stages, the PLT of Grenache ranged from approximately 90% to 100%. The [EtOH] of Chardonnay berries was higher than that for Grenache and lower than that for Shiraz and Cabernet Sauvignon (Figure 7). Chardonnay showed lower PLT than Grenache and larger variation, but no obvious trend over time was observed (Figure 8). There was also almost no loss of berry mass in Chardonnay (Figure 9).
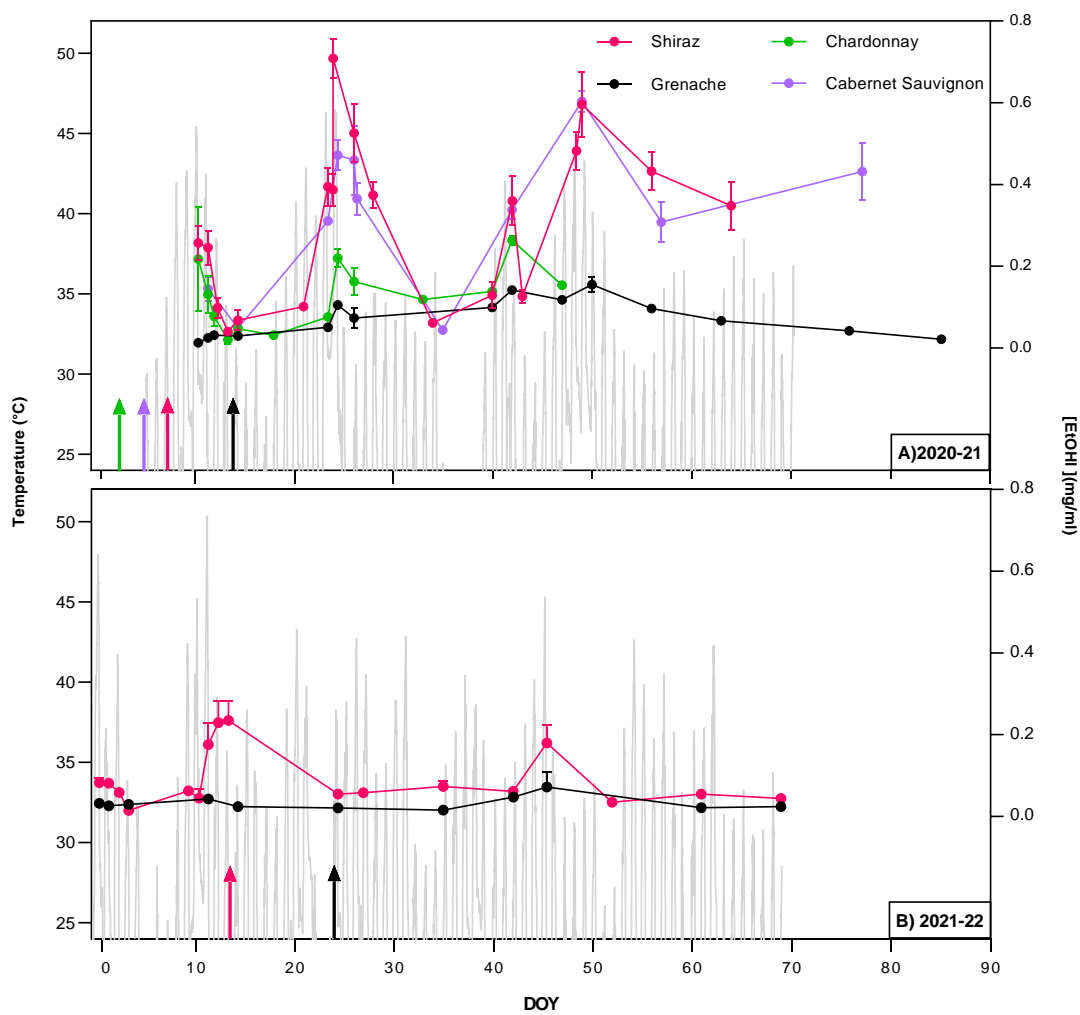
Figure 7 Correlation between high temperature events and berry [EtOH] for Shiraz, Cabernet Sauvignon, Grenache and Chardonnay. The data is shown plotted against days of the year (DOY) during growing seasons 2020-21 (A) and season 2021-22 (B) with canopy temperature recordings every 15 minutes (light grey). Values of [EtOH] are mean ± SEM (n=5), each replicate is from 24 berries. Coloured arrows indicate time when 10 °Brix was reached for each variety.
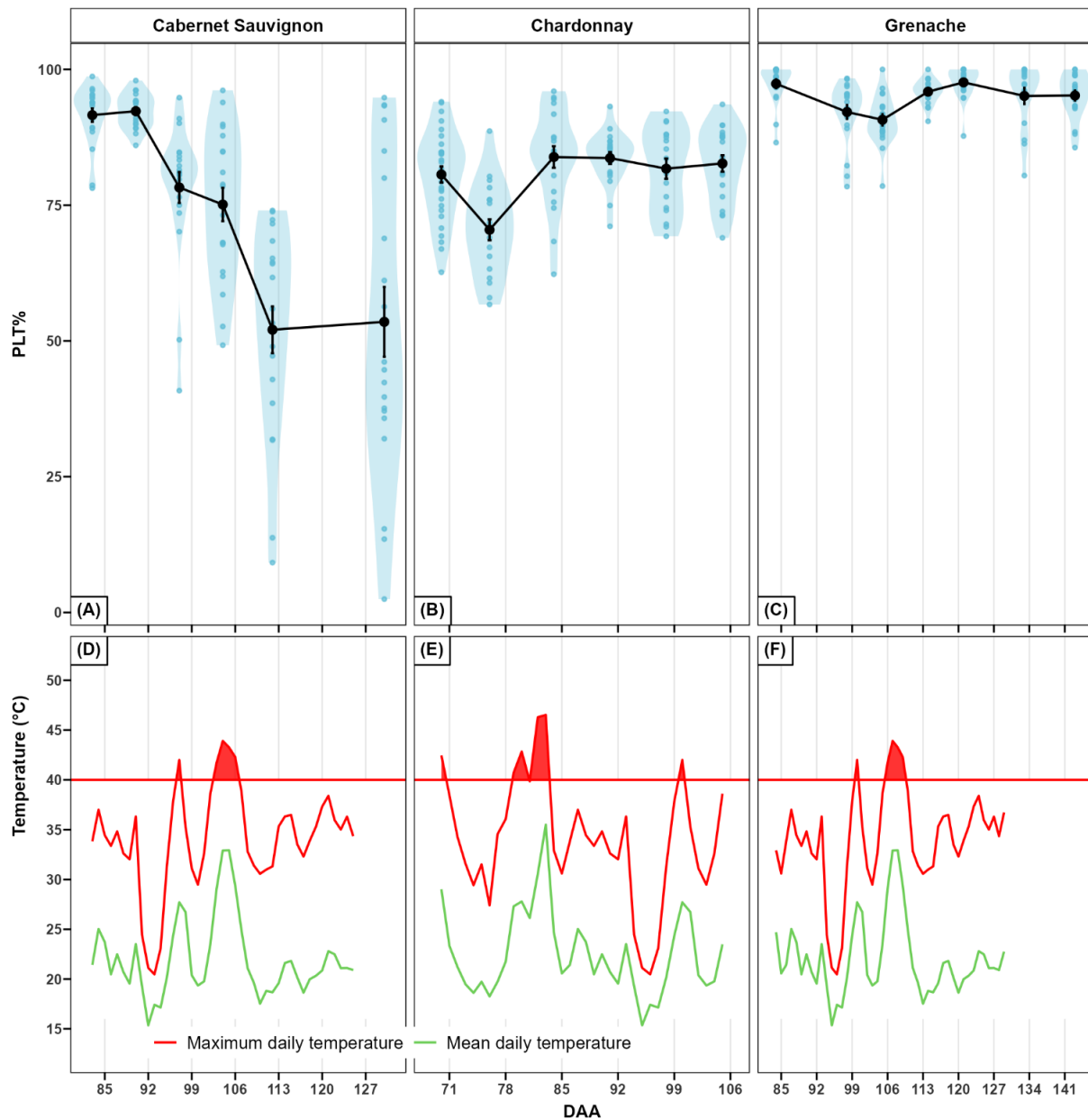
Figure 8 Time course of percentage living tissue (PLT) for single berries of Cabernet Sauvignon (A), Chardonnay (B), and Grenache (C) and corresponding canopy air temperatures. The mesocarp PLT of single berries (blue dots) and data distribution shown with violin plots (pale blue) combined with individual data for season 2020-21. Black dots are PLT data as mean ±SEM (n = 20). Bottom panels show daily mean canopy air temperature $(T_{canopy\ air\ mean\ daily})$ and maximum temperatures $(T_{canopy\ air\ max\ daily})$.
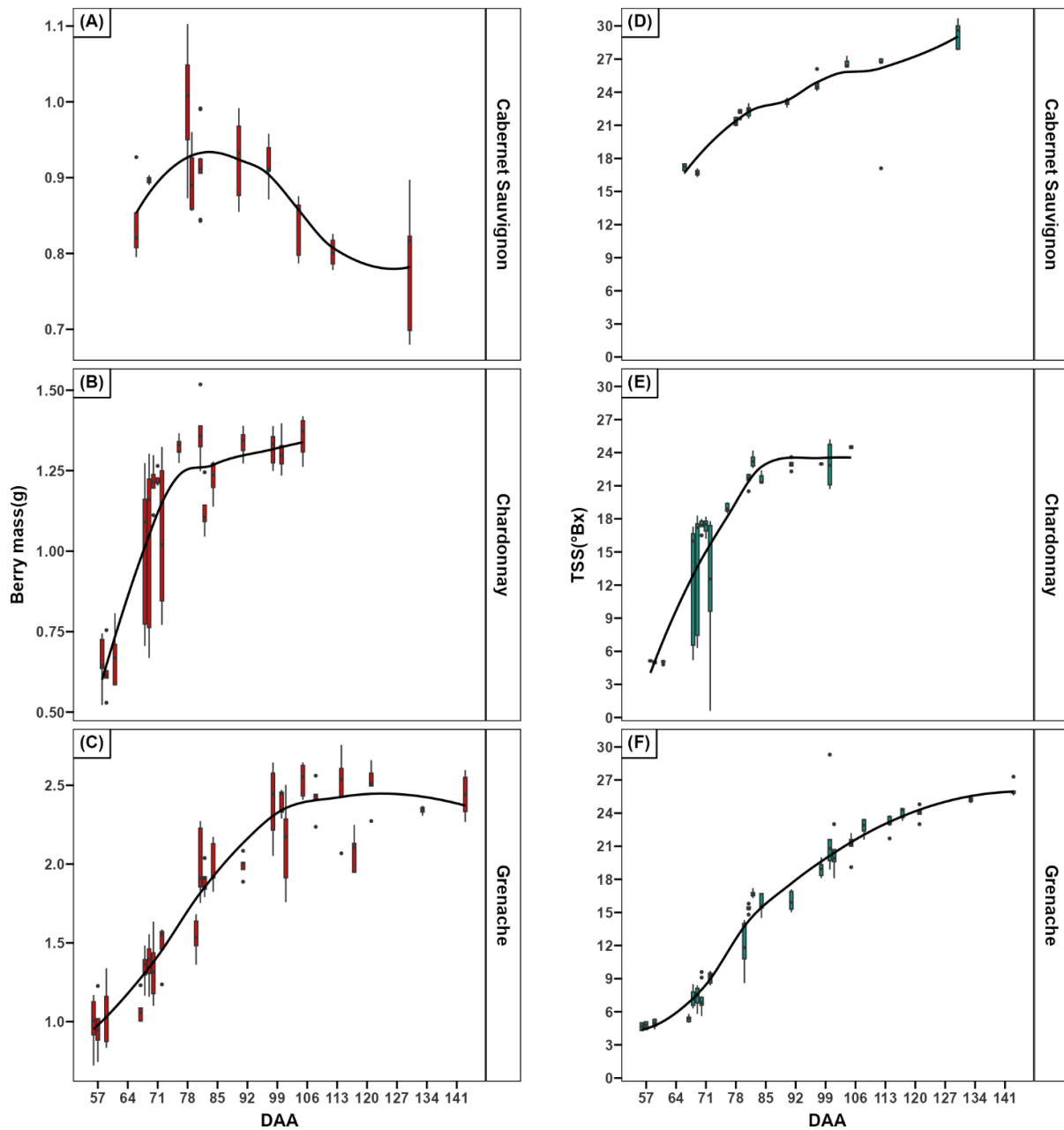
Figure 9 Development of berry mass and TSS for Cabernet Sauvignon (A, D), Chardonnay (B, E) and Grenache (C, F) in season 2020-21. Boxplots are shown for berry mass (A, B, C) and TSS (D, E, F). n= 5 and each replicate contains about 20 berries. Middle line in box represents median value; lower and upper edges of box represent 25th and 75th percentile of data set; and whiskers represent range of data values. Black dots indicate outlier. Loess localised regressions (black lines) were fit to demonstrate the trend (span α= 0.75).

3.7. Allometric analysis of Shiraz berry fresh mass and berry sugar during berry development at different Phases

In all three seasons from 2018 to 2021, changes in Shiraz berry mass (Berry mass$_{average\ Shiraz}$), TSS(TSS$_{average\ Shiraz}$) and sugar per berry (Sugar content$_{average\ Shiraz}$) over time (DAV) were analysed (all the replicates combined) (Figure 10). Although there were differences in TSS and berry mass between rootstock groupings and canopy orientation in different phases (Figure 1, 2, S4, S5), these differences were relatively small, especially on each sampling date.

To test the allomeric models to indicate the transitions between phases, especially the berry net water loss, the slope of the regression between amount of sugar per berry and berry mass on a log-scale (SSM) (Sadras & McCarthy, 2007) and the correlations (by 'Pearson correlation') between average berry mass and TSS (CMT) across cohorts of samples were estimated (Figure 11). The two methods (SSM and CMT) yielded similar results. Both showed distinct characters in different Phases. Besides, by cross-validation, a random resampling of a smaller number of samples (n= ~ 10) on each sampling date was employed with a 100 times simulation. This showed that the correlation between average berry mass and TSS across the samples is likely to have the same trend compared with the original datasets (Figure 11, S9).

According to Figure 10 and Figure 11, in *Phase* 1 before veraison (DAV <=0), that is the first two week's samplings in 2018-19 and 2019-20 season, berry mass on average increased, while there was almost no increase in TSS nor sugar content at this time, the TSSs were minimal (about 5 °Brix) (Figure 10). The correlations between berry mass and TSS (CMT) were negative (r (n~26-50) = ~-0.5-0, all $p < 0.001$) and the slope of the regression between amount of sugar per berry and berry mass in a log-scale (SSM) were less than 1 (all $p < 0.001$) (Figure 11). In *Phase* 2, after veraison during berry ripening (DAV > 0), berry mass, sugar content and TSS increase with time (DAV) rapidly, the CMT were positive (r (n=26-50) = 0 ~ 0.5, all $p < 0.05$) and the SSM were greater than 1 (all $p < 0.001$). Subsequentially, berry mass achieved peak mass, and it tended to plateau for about a

week and loss of berry mass started at about 34 DAV (around 23.8 °Brix), 30 DAV (around 21.8 °Brix) and 28 DAV (21.5 °Brix) respectively at similar TSS (Figure 10) (Table 4). The peak mass was similar in the first 2 seasons (about 1.3 g) and was less than that in season 2020-21 (about 1.5 g) (Figure 10). TSS continued to increase when berry mass loss occurred (Figure 10). However, from the LOESS fit in Figure 11 (the embedded Figures, R vs DAV and Slope vs DAV), the point where mass loss began indicated by when CMT changed from positive to negative and SSM changed from greater than 1 to less than 1, were 20, 20 and 33 DAV respectively in the three consecutive seasons. These transitions were around 2 weeks earlier than the change in slope (to negative) of berry mass as a function of time in 2018-19 (34 DAV) and 2019-20 (30 DAV) seasons (Figure 10-ABC). There was a better match in the 2020-21season (28 DAV) (Figure 10,11, Table 4).

The onset and degree of cell death in Shiraz berries in different seasons were different. Cell death occurred earlier in season 2018-19 and was more extensive than the other two seasons. The 80% average PLT (estimated by Eq. 1) occurred at about 18, 29 and 34 DAV (Figure 4), when the TSSs were 17, 21, and 22.8 °Brix in the three seasons respectively (estimated by Figure 10-GHI) (Table 4). At berry peak mass (estimated by Figure 10-ABC), the PLT in 2020-21 was 82.5 to 90.6% (22-28 DAV) and much higher than that in 2018-19 (58.5 to 64.3%) (27-34 DAV) and 2019-20 (79.4 to 81.6 %) (23-30 DAV) seasons. At 48 DAV (approx. 27 °Brix in all seasons), the average PLTs were about 55%, 70% and 70% respectively for the 2018-19, 2019-20 and 2020-21 seasons respectively (Figure 4). On the date when loss of berry mass indicated by the CMT changed from positive to negative and SSM changed from greater than 1 to less than 1, i.e., 20, 20 and 33 DAV respectively in the three consecutive seasons, PLTs were 74.2%, 89.4% and 79.6% on these days. It is important to note that in 2018-19 and 2019-20 season, there were obvious heatwaves and large decreases of PLT around these dates (Figure 4, Table 4).
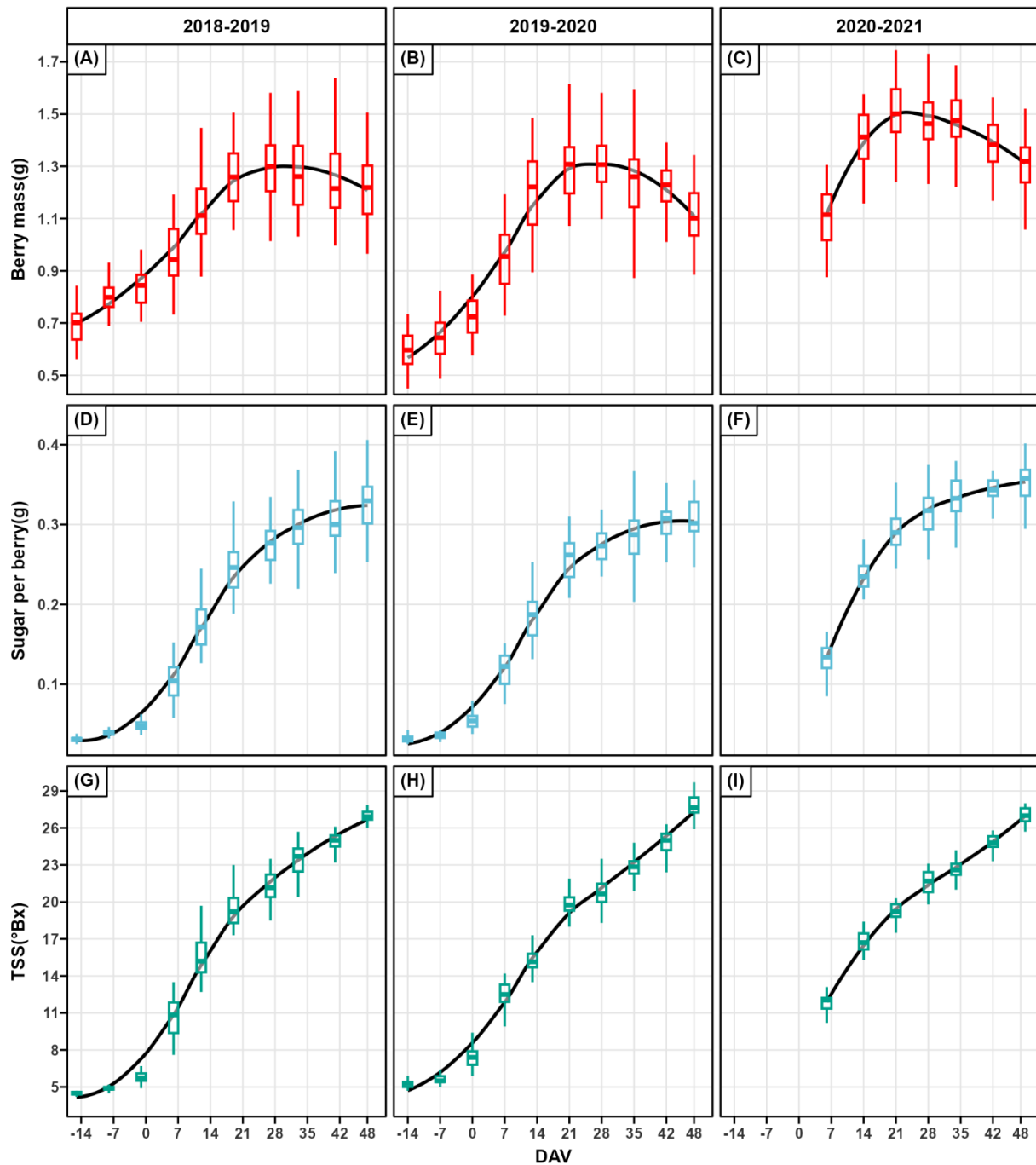
Figure 10 Development of berry mass, sugar per berry and TSS for Shiraz berries (combined all rootstocks) versus days after veraison (DAV) for each of the three seasons of study. Boxplots are shown of berry mass (ABC), sugar per berry (DEF) and TSS (GHI) (n = 46 in 2018-2019, n = 50 2019-20, n = 26). Middle line in box represents median value; lower and upper edges of box represent 25th and 75th percentile of data set; and whiskers represent range of data values. LOESS localised regressions (span α= 0.75) were applied to demonstrate the trend and to identify the onset of *Phase* 3 in berry mass in (A)(B)(C) (berry shrinkage, see Table 4).
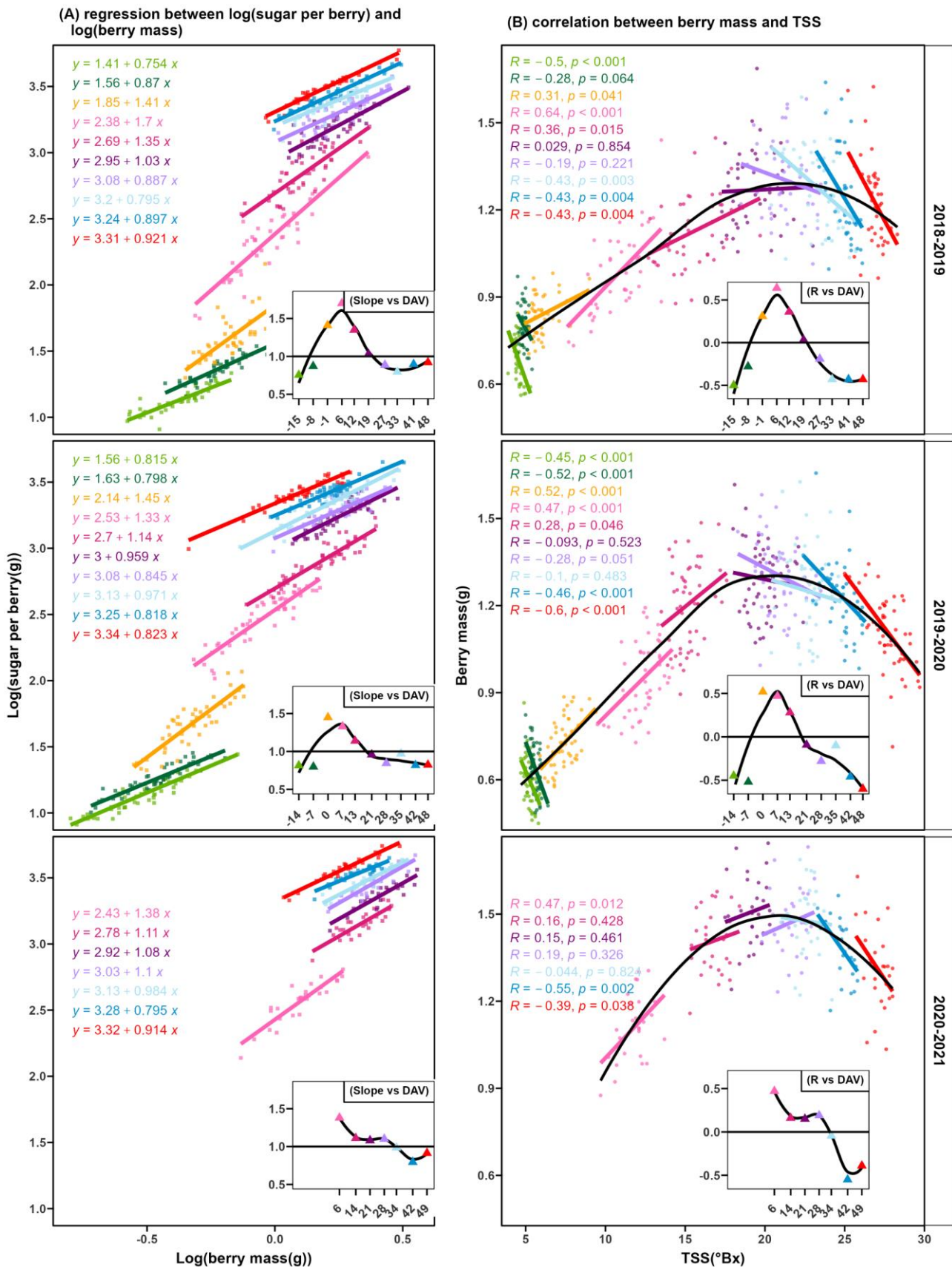
Figure 11 Comparison of two approaches to identify changes in development phases of Shiraz berries (rootstocks combined) from sample cohorts taken at different days during the three growing seasons from 2018-2021. (A) slope of the linear regression between log10 of sugar per berry and log10 berry mass (SSM method, see txt), and (B) correlation (Pearson correlation) between berry mass and TSS (CMT method) on

data from each sampling date (DAV) (n = 46 in 2018-19, n =50 in 2019-20 season, n = 26 in 2020-21 season). The determined slopes (Slope vs DAV) (in A) and correlation coefficients (R vs DAV) (in B) are shown plotted against DAV in the sub panels for each season. LOESS smooths (span α= 0.75) were applied on these plots to show the trend over DAV and where the slope changed from greater to less than 1 in A, and where the correlation coefficient became negative in B. Different colours indicate sampling dates (DAV). All *p* values for the linear regression in (A) were smaller than 0.001.

Table 4 Summary of Shiraz berry properties at the onset of berry shrinkage for the three seasons of study. a) Determination of the onset of berry shrinkage from LOESS fit of berry mass over DAV. b) Onset of berry shrinkage determined by change in slope of $\log_{10}$ of sugar per berry versus $\log_{10}$ berry mass (SSM) and change in slope of the correlation between berry mass and TSS (CMT). Related berry mass, TSS and PLT are given at these determined onsets. For a) peak mass values and the corresponding DAVs were first determined by LOESS fit from Figure 10-ABC. For these DAVS, TSS and PLT were estimated. In b), DAV of onset of berry mass loss determined by Loess fit in Figure 11 (embedded subplots), then on these DAVs, the berry mass, TSS and PLT were determined.

Methods	2018-19	2019-20	2020-21
a) Loess fit (berry mass/DAV) - peak mass duration			
DAV (Estimated by Loess fit in Figure 10-ABC)	27-34	23-30	22-28
Berry mass (g) (Estimated by Loess fit in Figure 10-ABC)	1.30	1.31	1.51
TSS (°Brix) (Estimated by Loess fit in Figure 10-GFI)	21.7-23.8	20.0-21.8	20-21.5
PLT (%) (Estimated by Equ.1 in Figure 4)	64.3 - 58.5	81.6-79.4	90.6-82.7
b) SSM (slope changed from greater to less than 1) and CMT (correlation coefficient became negative)			
DAV (Estimated by Loess fit in Figure 11)	20	20	34
Berry mass (g) (Estimated by Loess fit in Figure 10-ABC)	1.25	1.28	1.45
TSS (°Brix) (Estimated by Loess fit in Figure 10-GHI)	18.8	18.9	22.8
PLT (%) (Estimated by Equ.1 in Figure 4)	74.2	89.4	79.6

4. Discussion

4.1. Berry cell death in Shiraz

Cell death has been clearly demonstrated in several varieties, most often in Shiraz, where decreased membrane integrity is observed in the large mesocarp cells using vital dyes (Krasnow et al., 2008; Tilbrook & Tyerman, 2009; Tyerman et al., 2008) and electrolyte leakage across the berry observed using electrical impedance (Caravia et al., 2015). Ion/electrolyte leakage due to disrupted membrane function is often used as a measure of heat stress and other stresses in crop plants (Wahid et al., 2007).

The impacts of heat stress on grape vines and berries have been widely investigated, especially in the context of global warming, but most of them focus on grapevine physiology, berry composition and wine quality (Rogiers et al., 2022; Venios et al., 2020; Xu et al., 2014), rarely on berry physiology (Bonada et al., 2013; Martínez-Lüscher et al., 2020). Both high temperature and water deficit were observed to induce and/or increase cell death and shrinkage in Shiraz and Chardonnay berries (Bonada et al., 2013; Xiao, Liao, et al., 2018). This present study further explored the effects of high temperature on berry cell death. The possible role of ethanol accumulation in response to heat stress and/or hypoxia was also investigated across different varieties.

4.1.1. Modelling to predict cell death and its variation in response to temperature

The impacts of temperature on berry cell death are non-linear and with an increasing effect above threshold temperatures (see below), a feature that has not been incorporated in previous models to account for cell death in grape berries (Bonada et al., 2013).

During the three growing seasons, the mesocarp PLT decreased with DAV, the step-like decreases in PLT were sometimes observed and these appeared to correspond to high temperature events (above a temperature ($T_{canopy\ air\ max\ daily}$) threshold of approximately 35 °C) (Figure 4). A model was developed to simulate the non-linear and increasing rate of damage to cells when temperature increased, the mean mesocarp PLT of Shiraz was well correlated with accumulated temperature base

10 °C in three different growing seasons of different climate conditions, with non-linearity introduced with the quartic power (Eq. 2, PLT = a + b*GTD_4 , where $GTD_4 = \sum_{DAV=0(veraison)}^{DAV}(ABT-10)^4$ (Figure 4, S8, Table S1). Bonada et al. (2013) also showed that elevated temperature (on average) by 1.5 °C significantly increased cell death in Shiraz and Chardonnay berries, but the linear correlation between mesocarp PLT and GDD after anthesis (°C Day) in their study may have overlooked extreme temperature effects of heatwaves as observed here, as there were almost no maximum daily temperatures above 40 °C in their trial. Also, linear correlation can hardly explain the increasing PLT variation with time (see below).

A feature of the PLT data was the increasing variation between berries as the mean PLT decreased during development (Figure 4). Since high temperature may cause a non-linear increase in PLT and with a nonlinear interaction with berry maturity (Figure 4, 6, Eq.1 and Eq.2), variation in development between berries and variations in berry temperature under the same ambient conditions could account for the increased variation in PLT between berries with time. The increasing variation in PLT with time from temperature effects was also simulated by the model with assumed minimum and maximum berry temperatures, under the assumption that the maximum and minimum daily mean berry temperature was +/- 5 °C (Figure 4).

Individual berries in different locations of the canopy may have different temperature as well as different light intensity exposure due to different degrees of sun exposure or nearness to the vineyard floor (reflected infra-red radiation) (J. M. Gambetta et al., 2021; Hulands et al., 2014). There may be a large (e.g., 15°C) thermal gradients across grape berries in a bunch from the exposed to the shaded ones, as the temperature of shaded berries may be close to the ambient air temperature, while temperatures of berries directly exposed to sunlight could reach over 15 °C above ambient air temperature (Ponce de León & Bailey, 2021; Smart & Sinclair, 1976; Spayd et al., 2002; Stoll & Jones, 2007). Besides, higher light intensity from the more exposed berries may also contribute to more extensive cell damage, as the effect of temperature on sunburn was reported to be exacerbated

by light intensity and *vice versa* (J. M. Gambetta et al., 2021; Hulands et al., 2014). Overhead shading has been reported to significantly alleviate berry cell death and shrinkage in Shiraz by decreasing heat stress (Caravia et al., 2016). A shading study has shown that more exposed berries have lower acidity, higher pH, and more anthocyanins and flavanols. There was lower fresh berry mass, and during a heatwave, more exposed berries tended to be more prone to damage (visible berry shrinkage) regardless of irrigation amount (Martínez-Lüscher et al., 2020). Therefore, more exposed berries are likely to be more heat stressed and show more cell death. Careful canopy manipulation may play an important role in mitigation of berry cell death and shrinkage.

4.1.2. Heat stress effects on cell death indicated by [EtOH]

These non-linear effects from temperature on Shiraz cell death were also revealed by berry [EtOH] (Figure 5, 6). Ethanol accumulation was used as an indicator of berry stress due to hypoxia and/or heat stress (< 50 °C) in this study. During or just after a heatwave (maximum canopy air daily temperature above 45 °C) on 21 and 22 DAV, the [EtOH] increased from approximately 0.1 mg/ml from up to up to 1.6 mg/ml depending on TSS. While during relatively cool days (maximum canopy air daily temperature about 30 to 35 °C) on 7,8,13 and 14 DAV, all berries showed minimal [EtOH] (up to 0.1 mg/ml) with no differences between different TSSs (Figure 5).

These interaction effects between temperature and TSS were further modelled by a 2d sigmoid model (Figure 6, Eq. 2). The [EtOH] in Shiraz berries showed a general increasing and non-linear trend with both increasing canopy air temperature and TSS, indicating increasing stress from higher temperature and more so for mature berries. Moreover, there was an obvious temperature threshold below which the berry [EtOH] was minimal and above which ethanol accumulation started to increase dramatically (Figure 6). The interaction between canopy air temperature and berry maturity resulted in the temperature threshold decreasing as TSS increased. For example, the threshold was about 50 °C at 15 °Brix decreasing to about 35 °C when TSS was above 25 °Brix. Thus, riper berries are more susceptible to heatwaves than younger berries. Similarly, Semillon berries are more susceptible to

sunburn at later stages of development (Hulands et al., 2014). Apples also become more sensitive to heat stress with more advanced ripening, and concurrently more ethanol is produced (Fan et al., 2011).

Therefore, uneven ripening could also contribute the PLT variation as more mature berries may be more vulnerable to heat stress. Uneven ripening in *Vitis vinifera* often manifests among berries within a cluster, among clusters within a vine, among vines within a vineyard, and among vineyards (Amerine & Roessler, 1958; Armstrong et al., 2023; Previtali et al., 2021; Shahood et al., 2020). Within a bunch, the heterogeneity of berry development increases from green growth stage to ripening (Daviet et al., 2023; Deloire et al., 2019). In my study, the differences of TSS can be over 10 °Brix from the same sampling date. Given this large variation in PLT between berries due to berry variation in temperature and ripeness, it is not surprising that no significant differences between rootstocks or canopy orientation were observed in Shiraz berry PLT and [EtOH].

4.1.3. Possible mechanism related to temperature effects on cell death

Temperature exerts an impact on a broad spectrum of cellular components and metabolism (Bita & Gerats, 2013). The optimal temperatures for grape berry growth are generally considered to be 20 °C to 30 °C during the day and 10 °C to 20 °C during the night (Ewart & Kliewer, 1977; Kobayashi et al., 1965). Extreme temperature can impose stresses of variable severity when the ambient temperature rises above a threshold (Greer & Weedon, 2014; Sung et al., 2003; Venios et al., 2020). Heat stress may lead to cell injury and death through loss of membrane integrity, protein denaturation, accumulation of reactive Oxygen Species (ROS), and an oxygen supply crisis (Kelsey & Westlind, 2017; Nievola et al., 2017).

The severity of cell injury and death from heat is determined by the rate of temperature change, intensity and duration (Nievola et al., 2017). During severe heat stress, cell injury and cell death may occur within a few minutes due to rapid protein denaturation, while under mild to moderate heat stress, injury or cell death will only be observed after a longer period of exposure (e.g., hours or days) due to the disruption of metabolic processes (Nievola et al., 2017). For different plant species and different

tissue and cell types, the onset of heat stress injury varies, with different temperature thresholds and durations (Nievola et al., 2017).

Thermal (high temperature) induced death has been investigated in various plant species and organs. One minute at 60 °C is widely recognized as a lethal temperature for most plant tissues (Agee, 1996; Michaletz & Johnson, 2007), and 63 °C is reported to be the lethal temperature for grape berries (Huber, 1935). For the Riesling berry, surface temperatures of approximately 50 °C led to a 10% probability for damage after 15 minutes, 50% probability after 30 minutes and close to 90% probability after 90 minutes of heat exposure (Müller et al., 2023). Therefore, it seems that when berry temperatures are above 50 °C, mesocarp cell death could occur within minutes. It is likely that such temperatures may occur in black berries exposed to the direct solar beam during heatwave events, where surface temperatures can be over 15 °C above ambient temperature due to direct solar radiation as mentioned above (Ponce de León & Bailey, 2021; Smart & Sinclair, 1976; Spayd et al., 2002; Stoll & Jones, 2007). Temperatures of 53 °C were reported in compact Reisling bunch surfaces perpendicular to the sun zenith (Müller et al., 2023). Only on a few occasions were berry temperatures measured in the field in my study and these were deliberately measured during high temperature days (Table S2). Under these conditions berry surface and internal bunch temperatures over 50 °C were observed. Further detailed measures of berry temperatures under such conditions are required. Recovery during the night when temperatures are lower is also a factor that needs to be considered in the cumulative effect of heat stress on the grape berry.

It seems that between 40 to 45 °C a critical threshold occurs where cellular damage is often reported (Grigorova et al., 2012; Kelsey & Westlind, 2017; Paull & Chen, 2000). In broccoli, heat stress measured as the rate of electrolyte leakage is not linearly correlated to temperature but occurs with a threshold (about 42 to 45 °C) where leakage increased exponentially and when cellular damage became more evident (Duarte-Sierra et al., 2016). Electrolyte leakage in grape berries (Riesling) showed a dramatic increase in leakage rate after the berry surface temperature reached about 45 °C

(Heilemann et al., 2023). Electrolyte leakage begins at about 40 to 45°C in leaves and shoots of three-year-old olive (*Olea europaea* L.) and at 45 to 50°C in roots of two holly species (Mancuso & Azzarello, 2002). Grapevine leaves of are also susceptible to a threshold temperature (45 to 55 °C) where irreversible damage to photosynthesis can occur (Martínez-Lüscher et al., 2020; Niinemets, 2018; Venios et al., 2020; Xu et al., 2014). Singh (2010) demonstrated that cell death could be triggered at temperatures between 40-45 °C in Thompson Seedless berries.

Kurtural and Gambetta and (2021) suggested that two famous wine regions have experienced significant warming over the last six decades, and this temperature rise has been a contributing factor to the overall improvement in wine quality until now. However, they also demonstrated that a tipping point may be approaching where there is an uncoupling of the relationship between anthocyanin and sugar accumulation. Temperatures between 40 to 45 °C are likely to be a physiological tipping point where grape berries of susceptible varieties suffer irreversible damage for just a few degrees increase above a threshold. This is either related to the temperature itself (direct effects on membranes and proteins) or a combination with induced hypoxia and resulting high [EtOH]. Even with 80% shading, the bunch temperature may exceed the ambient temperature by 5 °C (Martínez-Lüscher et al., 2020). Here we propose that 35 °C may be considered a tipping point for ambient temperature in the field for susceptible varieties such as Shiraz and Cabernet Sauvignon. Water stress is likely to be an additional factor in determining the tipping point for berry damage (Xiao, Liao, et al., 2018).

4.1.4. Effects of hypoxia and temperature on cell death

Grape berries, especially Shiraz berries, appear to have hypoxic regions in the berry under normal conditions without heat stress (Xiao, Rogiers, et al., 2018) (Chapter 2). The hypoxic regions in the berry became more extensive as ripening advances (Xiao, Rogiers, et al., 2018). This very likely depends on anatomical features of the berry, e.g., lenticel density on the pedicel and diffusion pathways from the pedicel to the berry interior (Xiao et al., 2021; Xiao, Rogiers, et al., 2018) (Chapter 2). The correlation between Shiraz berry cell death and hypoxia has been previously reported, where

the mesocarp areas in the mid-section between the central axis of the berry and the berry skin had the lowest $[O_2]$ and the highest level of cell death (Xiao, Rogiers, et al., 2018). Also, varieties with less cell death are likely to have less hypoxia (Xiao, Rogiers, et al., 2018) as also shown here (Chapter 2) for the first time for Grenache berries (details see 4.4). In trees stems, hypoxia would occur from high oxygen consumption when temperatures go above 30 °C (Kelsey & Westlind, 2017), since respiration rate approximately doubles for every 10 °C increase in temperature (Atkin, 2003). When temperature increases, berries may be more susceptible to hypoxia stress, especially at later stages. Additive effects of the direct effect of elevated temperature with hypoxia indirectly induced by elevated temperature could be the main cause of cell death within the mesocarp.

In addition to increasing hypoxia with berry development, there are other reasons why more mature berries may be more vulnerable to heat stress. Firstly, the ability of berries to cool via transpiration decreases with ripening, especially before and after veraison (Rogiers, Hatfield, Jaudzems, et al., 2004). Under similar ambient temperatures, berries in the late stages (114 DAF) tended to exhibit larger differences with air temperature compared to those in the pre-veraison stage (67 DAV) (Martínez-Lüscher et al., 2020). Secondly, increasing berry size may also contribute to increased PLT due to reduced surface area to volume ratio. This would affect both heat dissipation and the diffusion of oxygen within the berry relative to the respiratory demand for oxygen. When Thompson Seedless berries were treated with gibberellin, which increased berry size, they were reported to be more prone to cell death (Singh, 2010). A contributing factor besides the hormone treatment itself could be the increased size and reduced surface area to volume ratio. However, an early study showed that berry size and transpiration were less important factors affecting berry temperature compared to solar radiation and wind velocity (Smart & Sinclair, 1976). More research should be undertaken to quantify the effects of solar exposure and air temperature on berry temperature as related to berry transpiration and berry size during ripening.

4.1.5. Onset of berry cell death in different seasons with different climate conditions

It has been reported that both berry loss of mass and cell death begin at similar times during berry development, approximately 90 to 100 DAF (days after flowering), and at about 20 °Brix (Fuentes et al., 2010; Tilbrook & Tyerman, 2008). However, this study illustrated that the onset and degree of cell death were more related to temperature conditions during berry development (heat waves and when they occurred), and not necessarily restricted to between 90 to 100 DAF. The 2018-19 season was the hottest and driest season with MJT of 24.5 °C and only 0.2 mm rainfall in January, while the subsequent seasons 2019-20 and 2020-21 were relatively cooler with MJT of approximately 22 °C and about 25 mm total rainfall in January. Cell death in Shiraz tended to start later and with lower levels in season 2020-21 compared to the other two seasons. At peak berry mass, the PLT in 2020-21 (about 90%) was much higher than the other two seasons (about 60% and 80% respectively), especially so for the hot 2018-19 season (Table 4a). These differences may also play an important role in the net water loss from berries contributing to berry shrinkage in different seasons (see below 4.3).

4.2. Dynamics of Shiraz berry growth, shrinkage and sugar accumulation

In the three seasons of this study, after veraison, Shiraz berry development generally followed the patterns reported previously (Coombe, 1976; McCarthy, 1999; Sadras & McCarthy, 2007), that is, with two obvious phases consisting of berry mass increase (*Phase* 2) and berry shrinkage (*Phase* 3).

The transitions between berry development phases were also indicated by the allomeric models (SSM and CMT) from sample cohorts. Sample cohorts taken at particular dates can indicate the phases of berry development, basically because berries are not all exactly at the same ripening stage across a sampling cohort even though the means from two cohorts may be the same. The results from the two allomeric models (SSM and CMT) corresponded in terms of the date for transition between *Phase* 2 and 3. Although this study used 50 samples to develop the model, a smaller sample size of approximately 10 was also tested with similar results. This analysis and sampling strategy could

provide a time efficient and relatively accurate method to monitor the transitions between phases of berry development and particularly the time of onset of berry shrinkage. This may be important for management decisions regarding irrigation and final harvest.

Grape berry size is initially determined by cell division (*Phase* 1) and cell expansion (mostly in *Phase* 2) (Ollat et al., 2002) , and later by loss of mass (mostly net loss of water) (*Phase* 3) in some varieties such as Shiraz (McCarthy, 1997; Rogiers et al., 2000; Sadras & McCarthy, 2007). In the present study, during the lag phase to *Phase* 1 transition just before veraison, berry mass on average increased at this time, while there was almost no increase in TSS (about 5 °Brix), as previously reported (Coombe & McCarthy, 2000). Besides, the SSM were smaller than 1 and the CMT were negative at this time, where the larger berries had lower TSS (Figure 11). This may indicate that the rate of water accumulation exceeded the rate of sugar accumulation during this phase, perhaps due to cell wall loosening and rapid water uptake from xylem (Coombe & McCarthy, 2000; Ollat et al., 2002). This is consistent with a previous study that compared the accumulation of berry fresh mass and berry dry weight (Rogiers et al., 2000). Most of the resources for dry weight accumulation by the berry are provided by phloem, phloem sap contains a higher solute content than xylem sap (15 to 25% w/v, compared to <0.4% w/v) (Pate, 1975). Water inflow is dominated by the xylem before veraison, perhaps was account for the lower sugar accumulation rate than water. Despite the low sugar inflow at this stage, reduction in berry malate concentration may also commence (Sweetman et al., 2009), and sugars may be utilised as an energy source for berry growth and metabolism (Coombe & McCarthy, 2000; Tilbrook & Tyerman, 2006). Larger berries may consume more sugar per unit mass for cell division and cell enlargement compared to smaller berries. These factors could contribute to the lower accumulation rate of TSS compared to water during this time.

During the lag phase, the SSM tended to approach 1, while the CMT was almost 0. The reason could be that, during this time, the lag in fresh weight gain was not accompanied by any lag in dry weight accumulation, as indicated by a continuous increase (Rogiers et al., 2000). Both sugar accumulation

and berry enlargement mainly occur in *Phase* 2 (berry maturation) (Coombe & McCarthy, 2000; Ollat et al., 2002), where increase in TSS indicates sugar accumulation (mostly) per unit water mass. It has been reported that during *Phase* 2, sugar and water increments are linked and depend on the same source (the phloem sap), which predominates solute inflow at this time, but dramatically decreased in late ripening (Coombe & McCarthy, 2000; Keller, 2006; Rogiers et al., 2006). During *Phase* 3 (berry shrinkage) the increase in TSS reflects the concentrating effect of berry net water loss, where sugar accumulation has either stopped or slowed substantially relative to water loss at this time (Coombe & McCarthy, 2000; Keller, 2006; Rogiers et al., 2006; Tilbrook & Tyerman, 2006). In this present study, the relationship between average berry mass and TSS in sample cohorts (CMT) became positive after veraison (Figure 11), i.e., the larger berries also had higher sugar concentration. The slopes of the regression between amount of sugar per berry and berry mass in a log-scale (SSM) were greater than 1, indicating that the rate of sugar accumulation exceeded the rate of water accumulation. Subsequently the CMT became zero and then negative till late harvest and the SSM also changed from greater than 1 to less than 1 (Figure 11), indicating the concentrating effect of net water loss on TSS. The onset of net water loss indicated by CMT and SMM (Figure 11) was around 2 weeks earlier than the change in mean berry mass loss with time (Figure 10-ABC, Table 4) in the 2018-19 and 2019-20 season but was close to the onset of mean berry mass loss in the 2020-21season.

4.3. Heat stress effects and berry water loss

In *phase* 3, water loss could be from continued berry transpiration and backflow (water movement from the berry back to the parent vine) via the xylem vessels, which was observed by several studies in both pre-veraison and post veraison berries (Keller, 2006; Keller et al., 2015; Tilbrook & Tyerman, 2009; Tyerman et al., 2008). However, there is one study demonstrating that in post veraison Shiraz berries, the plant/berry water communication seems to cease progressively and the authors propose that after veraison xylem backflow is unlikely (Carlomagno et al., 2018). Nevertheless, both transpiration and backflow seem to be related to temperature (see below).

In this present study, during the three seasons, during or just after heatwaves, tiny wrinkles on the berry skin and increasing softness of some Shiraz berries were observed in the field. This may indicate extensive transpiration under heatwave conditions that may contribute to shrinkage. This effects of Pinolene treatment reported in Chapter 4 also suggested a possible contribution of transpiration to the reduction in berry size. The factors that determine transpiration rate are berry size and cuticular conductance, but predominantly vapour pressure deficit (VPD), which is determined by ambient temperature and relative humidity (Zhang & Keller, 2015). Even though transpiration rate of post-veraison berries was only 16% of that of pre-veraison berries, studies have demonstrated that transpiration could result in loss of 0.2 to 6% (3 to 100 mg H_2O/day) of fresh berry mass daily (Zhang & Keller, 2015), and 15 mg loss in mass per berry per day (25 °C) in another study (Rogiers, Hatfield, Jaudzems, et al., 2004). Berry transpiration under extreme heat and its contribution to berry water loss require further investigation, especially in terms of variety differences.

In terms of backflow, Tilbrook and Tyerman (2009) suggested that 30% of the weight loss of an average sized Shiraz berry could be achieved after one week with a weight loss of 43 mg (approximately 7% of berry volume) per day. This could be associated with the mesocarp cell death in the berry, loss of berry cell vitality and membrane integrity may reduce or nullify the osmotic potential driving force so that berries are not able to balance xylem and apoplast tensions generated in the vine by leaf transpiration (Krasnow et al., 2008; Tilbrook & Tyerman, 2008). Berry cell death in the mesocarp late in ripening was reported to be correlated with loss of mass (shrivel) in Shiraz and Cabinet Sauvignon, berries with more dead cells tended to have more loss of mass (Fuentes et al., 2010; Krasnow et al., 2008; Tilbrook & Tyerman, 2008, 2009).

The hypothesis outlined above linking cell death with berry shrinkage caused by backflow would indicate a strong link between the onset of cell death and berry shrinkage. This study revealed that significant mesocarp cell death could start relatively early in berry ripening during a hot season (e.g., 10 to 20 DAV) (Figure 4), and backflow in the early stages and its effects on berry mass might have

been overlooked previously. On the other hand, phloem inflow during Phase 2 may not be so affected by cell death in the mesocarp allowing berries to continue water and sugar accumulation (Figure 10-DEF). In this context the vascular tissues in the berry usually remain vital even when significant mesocarp cell death is evident (Chapter 2-Figure 4).

As discussed above, both the transpiration and the cell death (perhaps leading to backflow) are likely to related to temperature. Possibly, during hotter seasons (2018-219 and 2019-20), before about 20 °Brix, when there was extensive cell death in the mesocarp (Table 4) the inflow from phloem may still be high enough to exceed the water loss from backflow via xylem, and transpiration. Water loss from backflow and transpiration exceeded water uptake via phloem at 20 DAV respectively in both the 2018-19 and 2019-20 seasons as indicated by the SSM changing to negative and CMT changing to less than one. However, during a cooler season (2020-21), there was less cell death and the PLT at peak mass was about 90.6% at 22 DAV at about 20 °Brix (Table 4). In this case there may have been less water loss from xylem backflow and from berry transportation before phloem inflow declined. This corresponded to a higher peak mass in the 2020-21 season than the other two seasons. How cell death and transpiration affect peak berry mass requires further investigation. Nevertheless, it is clear that the connection between the onset and the degree of cell death, and the onset and degree of berry shrinkage in Shiraz may not be as directly linked as previously thought.

4.4. Cell death, berry shrinkage and variety differences

The correlation between cell death and berry shrinkage was also supported by varietal differences. Varieties that can retain cell vitality during berry development (e.g., Thompson Seedless), or are hydraulically disconnected to the vine when cell death occurs (e.g., Chardonnay), tend to maintain berry mass late in ripening (Fuentes et al., 2010; Tilbrook & Tyerman, 2008, 2009). In the field, berry cell death and shrivelling are commonly observed in Shiraz and Cabernet Sauvignon berries (Krasnow et al., 2008; Pagay, 2018) but rarely occurs in Grenache berries (Fuentes et al., 2010; Tilbrook & Tyerman, 2008). In the present study, both Shiraz and Cabernet Sauvignon berries

displayed more cell death (Figure 4, 8), and also tended to have higher [EtOH] than Chardonnay and Grenache (Figure 7). As discussed above, heat stress is likely to be a major factor causing cell death in Shiraz berries. Under the same ambient temperature conditions (even above 40 °C), Grenache berries tended to have much less ethanol accumulation (about 0.1 mg/ml) (Figure 7), which was close to the [EtOH] in Shiraz berries on a cool day (below 30 or 35 °C). This may suggest that the better heat tolerance of Grenache berries, which could be related to less hypoxic stress, perhaps due to a higher porosity for oxygen diffusion in the berry (Chapter 2).

During very hot seasons, cell death and related berry shrivel (collapse) can occur in table grapes (Singh, 2010). The widespread and severe berry collapse in Thompson Seedless was observed in the Australian state of Victoria in only 3 of 11 seasons during 1997 to 2008, where these three seasons had much higher temperatures (Singh, 2010). So called berry collapse in Thompson Seedless, most probably similar to shrivel in Shiraz, was reported to correlate with cell death, and from both field and glasshouse trails it was suggested that cell death was triggered by heat stress (40-45 °C) (Singh, 2010). Although there has been no report of hypoxia in Thompson Seedless berries, it was reported that the table grape variety Ruby seedless, also normally without cell death and berry shrivel, tended to show less hypoxia inside berries (Xiao, Rogiers, et al., 2018).

In addition to berry microstructure (porosity) and hypoxia differences between varieties, other physiological and biochemical characteristics of different varieties may affect the degree of berry cell death, especially characteristics related to drought and heat tolerance. For example, Grenache is widely considered a drought tolerant variety, having been selected for wine making in hot and dry regions (Dayer et al., 2020) and was vigorous and productive in the study site (Coombe vineyard) despite not receiving irrigation. In contrast Shiraz and Cabernet Sauvignon berries shown here to be less heat tolerant (Dayer et al., 2020; G. A. Gambetta et al., 2020), were selected in the cooler climates of France.

4.5. Rootstock and canopy orientation effects on berry development

Using rootstocks and scion varieties with better heat and drought tolerance is one of the recommended techniques to ameliorate heat stress (Dry, 2009). The effects of rootstocks of different drought tolerance/vigour and bunch orientation on berry mass and TSS were identified in this study, the results vary in different growing seasons, the different climate conditions from different seasons could one important reason.

As mentioned above, the 2018-19 season was the hottest and driest season while the subsequent seasons 2019-20 and 2020-21 were relatively cooler. In the warmest season (2018-19), berries from drought tolerant rootstocks and from east side of the canopy tended to confer higher berry mass as well as higher TSS in the Shiraz scion till late harvest (Figure 1). In the 2019-20 season, there was no significant effect from rootstock groups, but berries on the east side had higher TSS as well as higher berry mass compared to the west side in *Phase* 1 and *Phase* 3, these differences in *Phase* 3 were only evident in the low drought tolerance and vigour group. For the 2020-21 season, no significant differences in berry mass and TSS were evident between rootstocks nor between bunch orientations (east versus west).

During the hotter and drier season, the differences between rootstocks could be related to a combination of better water uptake and larger canopy size in the drought tolerant/vigour rootstocks, leading to higher leaf density shading the bunch zone and protecting bunches from becoming very hot under heatwave conditions (Bonilla et al., 2015; De la Fuente et al., 2007; Dry & Coombe, 2005). In this present study, high drought tolerant/vigour rootstocks tended to have larger canopies (Figure 3-GH). Besides, rootstocks of both higher drought tolerance and vigour may decrease water stress in hot conditions, due in part to deeper rooting distributions (Fort et al., 2017; Serra et al., 2014). On the other hand, exposed bunches on the west side of north-south oriented rows can have higher maximum temperatures than exposed bunches on the east side during after noon (Figure S3), especially for VSP canopy system (Martínez-Lüscher et al., 2020; Peña Quiñones et al., 2020; Ponce

de León & Bailey, 2021). In this present study, no differences in water potential were observed between rootstocks, and all vines were barely under water stress indicated by the water potential results (larger than -1.5 MPa) (Figure 3-ABC), maybe all vines were well irrigated in the vineyard. Therefore, in hooter seasons (e.g., 2018-19 season), berries on east side and drought tolerance/vigour rootstocks are likely to have bigger berries resulted from more cell division in *Phase* 1 and less berry shrinkage due to less mesocarp cell death and less transpiration with decreased heat stress. In warm and cooler seasons (e.g., 2020-21 season), Shiraz berries may be less influenced by rootstock and bunch orientation. Further research is required to validate these observations, as notable distinctions between rootstock effects and bunch orientation were evident only in the warmest season, perhaps indicating that the effects were small but may become more pronounced under warmer conditions. Canopy management may therefore be critical in hot seasons, for example, allowing the VSP canopies to lay over on the west side to shade west facing bunches. The potential benefits of delaying fruit ripening to mitigate heat-related issues during the early summer season require further investigation.

One survey related to the 2009 heatwave in South-Eastern Australia indicated that, the vineyards with drought tolerant and vigorous rootstocks such as Ramsey and 140 Ruggeri, were least heat damaged (Webb et al., 2009). Those with less drought tolerant and lower vigour rootstocks such as Schwarzmann and 101-14, and those on own roots, had the most heat damage (Webb et al., 2009). Shiraz scion on the drought-tolerant rootstock Ramsey was reported to have a delayed shrinkage compared to rootstock 101-14 Mgt (Rogiers, Hatfield, & Keller, 2004). Also, Singh (2010) compared Thompson Seedless berries on Ramsey rootstock with those on Schwarzman. Berries on Schwarzman were more prone to cell death (and collapse) and sunburn damage, and leaf water potential was more negative.

5. Conclusion

Additive effects of the direct effect of elevated temperature with hypoxia indirectly induced by elevated temperature could be the main cause of cell death within the mesocarp. The effects of temperature on cell death are clearly non-linear with larger effects as temperatures rise. More mature berries would be more valuable with increased temperatures perhaps because of more hypoxic (lower berry porosity) and lower transpiration for cooling under high temperature conditions. A model is presented that can be used to predict cell death in Shiraz berries based on likely berry temperatures that can explain both the time course of increased cell death during ripening and the increase in variance. A separate model was developed to describe the accumulation of ethanol, which is also very non-linear with temperature, but also interacted with sugar accumulation. In both models the non-linear effects of temperature indicate a clear threshold in temperature, above which both ethanol and cell death increase sharply. Ambient temperature of 35 °C is proposed as a tipping point.

Varieties with lower hypoxia like Grenache or table grape varieties may have higher heat tolerance (lower [EtOH] under heatwaves), which could reduce cell death and shrivel during normal growing conditions in the field. Cabernet Sauvignon berries behaved very similarly to Shiraz and the Shiraz models may be also applied to this variety. Shiraz berries on drought tolerant/high vigour rootstocks and on the east side of the canopy (for north-south oriented rows) exhibited a tendency for larger berries, especially during hotter seasons, possibly due to a decreased heat stress through combination of better water uptake and more bunch shading. Heat mitigation in Shiraz and Cabernet vineyards through shading, canopy management, irrigation or sprinkler cooling is highly recommended during heatwaves, especially when ambient temperatures are predicted to rise to the tipping point, above 35 °C.

With a minimum of 10 samples, correlations between TSS and berry mass of sampled cohorts at particular dates revealed trends that could be used to better delineate between different berry development phases, particularly where there is a reversal in slope of the relationship, e.g., onset of

loss of mass later in ripening. A one-time sampling method at a predicted time based on climatic conditions from veraison and previous history for the vineyard may be a more time efficient method to monitor the onset of berry shrinkage and to make decisions regarding irrigation and final harvest. The onset of berry shrinkage is not necessarily strictly dependent on the degree of cell death since shrinkage also depends on transportation and the timing of cell death with respect to when sugar inflow via the phloem likely ceases.

Shiraz berries on drought tolerant/high vigour rootstocks and on the east side of the canopy (for north-south oriented rows) exhibited a tendency for larger berries, especially during hotter seasons, possibly due to a decreased heat stress through combination of better water uptake and more bunch shading.

6. References

Agee, J. (1996). Fire ecology of Pacific northwest forests. *The Bark Beetles, Fuels, and Fire Bibliography*.

Amerine, M. A., & Roessler, E. B. (1958). Methods of determining field maturity of grapes. *American Journal of Enology and Viticulture*, *9*(1), 37–40. https://doi.org/10.5344/ajev.1958.9.1.37

Armstrong, C. E. J., Previtali, P., Boss, P. K., Pagay, V., Bramley, R. G. V., & Jeffery, D. W. (2023). Grape heterogeneity index: Assessment of overall grape heterogeneity using an aggregation of multiple indicators. *Plants*, *12*(7), Article 7. https://doi.org/10.3390/plants12071442

Atkin, O. (2003). Thermal acclimation and the dynamic response of plant respiration to temperature. *Trends in Plant Science*, *8*(7), 343–351. https://doi.org/10.1016/S1360-1385(03)00136-5

Barbato, G., Barini, E. M., Genta, G., & Levi, R. (2011). Features and performance of some outlier detection methods. *Journal of Applied Statistics*, *38*(10), 2133–2149. https://doi.org/10.1080/02664763.2010.545119

Bashir, K., Todaka, D., Rasheed, S., Matsui, A., Ahmad, Z., Sako, K., Utsumi, Y., Vu, A. T., Tanaka, M., Takahashi, S., Ishida, J., Tsuboi, Y., Watanabe, S., Kanno, Y., Ando, E., Shin, K.-C., Seito, M., Motegi, H., Sato, M., … Seki, M. (2022). Ethanol-mediated novel survival strategy against drought stress in plants. *Plant and Cell Physiology*, *63*(9), 1181–1192. https://doi.org/10.1093/pcp/pcac114

Berrar, D. (2019). Cross-Validation. In S. Ranganathan, M. Gribskov, K. Nakai, & C. Schönbach (Eds.), *Encyclopedia of Bioinformatics and Computational Biology* (pp. 542–545). Academic Press. https://doi.org/10.1016/B978-0-12-809633-8.20349-X

Bita, C., & Gerats, T. (2013). Plant tolerance to high temperature in a changing environment: Scientific fundamentals and production of heat stress-tolerant crops. *Frontiers in Plant Science*, *4*, 273. https://doi.org/10.3389/fpls.2013.00273

Bonada, M., Sadras, V. O., & Fuentes, S. (2013). Effect of elevated temperature on the onset and rate of mesocarp cell death in berries of Shiraz and Chardonnay and its relationship with berry shrivel: Thermal shift on mesocarp cell death and shrivel. *Australian Journal of Grape and Wine Research*, *19*(1), 87–94. https://doi.org/10.1111/ajgw.12010

Bondada, B. R., & Keller, M. (2012). Not all shrivels are created equal—Morpho-anatomical and compositional characteristics differ among different shrivel types that develop during ripening of grape (*Vitis vinifera* L.) berries. *American Journal of Plant Sciences*, *03*(07), 879–898. https://doi.org/10.4236/ajps.2012.37105

Bonilla, I., Toda, F. M. de, & Martínez-Casasnovas, J. A. (2015). Unexpected relationships between vine vigor and grape composition in warm climate conditions. *OENO One*, *49*(2), Article 2. https://doi.org/10.20870/oeno-one.2015.49.2.87

Breda, N. J. J. (2003). Ground-based measurements of leaf area index: A review of methods, instruments and current controversies. *Journal of Experimental Botany*, *54*(392), 2403–2417. https://doi.org/10.1093/jxb/erg263

Caravia, L., Collins, C., & Tyerman, S. D. (2015). Electrical impedance of Shiraz berries correlates with decreasing cell vitality during ripening: Impedance of Shiraz berries and cell vitality. *Australian Journal of Grape and Wine Research*, *21*(3), 430–438. https://doi.org/10.1111/ajgw.12157

Carlomagno, A., Novello, V., Ferrandino, A., Genre, A., Lovisolo, C., & Hunter, J. J. (2018). Pre-harvest berry shrinkage in cv 'Shiraz' (*Vitis vinifera* L.): Understanding sap flow by means of tracing. *Scientia Horticulturae*, *233*, 394–406. https://doi.org/10.1016/j.scienta.2018.02.014

Chou, H.-C., Šuklje, K., Antalick, G., Schmidtke, L. M., & Blackman, J. W. (2018). Late-season Shiraz berry dehydration that alters composition and sensory traits of wine. *Journal of Agricultural and Food Chemistry*, *66*(29), 7750–7757. https://doi.org/10.1021/acs.jafc.8b01646

Coombe, B. G. (1976). The development of fleshy fruits. *Annual Review of Plant Physiology*, *27*(1), 207–228. https://doi.org/10.1146/annurev.pp.27.060176.001231

Coombe, B. G. (1992). Research on development and ripening of the grape berry. *American Journal of Enology and Viticulture*, *43*(1), 101–110. https://doi.org/10.5344/ajev.1992.43.1.101

Coombe, B. G., & McCarthy, M. G. (2000). Dynamics of grape berry growth and physiology of ripening. *Australian Journal of Grape and Wine Research*, *6*(2), 131–135. https://doi.org/10.1111/j.1755-0238.2000.tb00171.x

Daviet, B., Fournier, C., Cabrera-Bosquet, L., Simonneau, T., Cafier, M., & Romieu, C. (2023). Ripening dynamics revisited: An automated method to track the development of asynchronous berries on time-lapse images. *Plant Methods*, *19*(1), 146. https://doi.org/10.1186/s13007-023-01125-8

Dayer, S., Herrera, J. C., Dai, Z., Burlett, R., Lamarque, L. J., Delzon, S., Bortolami, G., Cochard, H., & Gambetta, G. A. (2020). The sequence and thresholds of leaf hydraulic traits underlying grapevine varietal differences in drought tolerance. *Journal of Experimental Botany*, *71*(14), 4333–4344. https://doi.org/10.1093/jxb/eraa186

De Bei, R., Fuentes, S., Gilliham, M., Tyerman, S., Edwards, E., Bianchini, N., Smith, J., & Collins, C. (2016). VitiCanopy: A free computer App to estimate canopy vigor and porosity for grapevine. *Sensors (Basel, Switzerland)*, *16*(4), 585. https://doi.org/10.3390/s16040585

De la Fuente, M., Linares, R., Baeza, P., & Lissarrague, J. R. (2007). Efecto del sistema de conducción en climas semiáridos sobre la maduración, composición de la baya y la exposición de los racimos en *Vitis vinifera* L. cv. Syrah. *Revista Enología*, *4*(4), 1–9.

Deloire, A. (2011). The concept of berry sugar loading. *Wineland*, *257*, 93–95.

Deloire, A., Pellegrino, A., & Ristic, R. (2019). Grape sampling: Spatial distribution of berry fresh mass, seed number and sugar concentration on grapevine clusters of Shiraz: Discussion of potential consequences for sampling to monitor vineyard ripening. *Wine & Viticulture Journal*, *34*(2). https://doi.org/10.3316/informit.389267107371643

Dry, P. R. (2009). Bunch exposure management. In *Technical booklet*. Grape and Wine Research and Development Corporation.

Dry, P. R., & Coombe, B. G. (2005). *Viticulture. Volume 1, Resources* (2nd ed., repr. with alterations). Winetitles.

Duarte-Sierra, A., Corcuff, R., & Arul, J. (2016). Methodology for the determination of hormetic heat treatment of broccoli florets using hot humidified air: Temperature–time relationships. *Postharvest Biology and Technology*, *117*, 118–124. https://doi.org/10.1016/j.postharvbio.2016.01.010

Ewart, A., & Kliewer, W. M. (1977). Effects of controlled day and night temperatures and nitrogen on fruit-set, ovule fertility, and fruit composition of several wine grape cultivars. *American Journal of Enology and Viticulture*, *28*(2), 88–95. https://doi.org/10.5344/ajev.1977.28.2.88

Fan, L., Song, J., Forney, C. F., & Jordan, M. A. (2011). Fruit maturity affects the response of apples to heat stress. *Postharvest Biology and Technology*, *62*(1), 35–42. https://doi.org/10.1016/j.postharvbio.2011.04.007

Fan, L., Song, J., Forney, C., & Jordan, M. (2005). Ethanol production and chlorophyll fluorescence predict breakdown of heat-stressed apple fruit during cold storage. *Journal of the American Society for Horticultural Science. American Society for Horticultural Science*, *130*. https://doi.org/10.21273/JASHS.130.2.237

Fort, K., Fraga, J., Grossi, D., & Walker, M. A. (2017). Early measures of drought tolerance in four grape rootstocks. *Journal of the American Society for Horticultural Science*, *142*(1), 36–46. https://doi.org/10.21273/JASHS03919-16

Fuentes, S., Sullivan, W., Tilbrook, J., & Tyerman, S. (2010). A novel analysis of grapevine berry tissue demonstrates a variety-dependent correlation between tissue vitality and berry shrivel: Variety-dependent berry vitality and shrivel. *Australian Journal of Grape and Wine Research*, *16*(2), 327–336. https://doi.org/10.1111/j.1755-0238.2010.00095.x

Gambetta, G. A., Herrera, J. C., Dayer, S., Feng, Q., Hochberg, U., & Castellarin, S. D. (2020). The physiology of drought stress in grapevine: Towards an integrative definition of drought tolerance. *Journal of Experimental Botany*, *71*(16), 4658–4676. https://doi.org/10.1093/jxb/eraa245

Gambetta, J. M., Holzapfel, B. P., Stoll, M., & Friedel, M. (2021). Sunburn in grapes: A review. *Frontiers in Plant Science*, *11*. https://www.frontiersin.org/articles/10.3389/fpls.2020.604691

Greer, D., & Weedon, M. (2014). Temperature-dependent responses of the berry developmental processes of three grapevine (*Vitis vinifera*) cultivars. *New Zealand Journal of Crop and Horticultural Science*, *42*(4), 233–246. https://doi.org/10.1080/01140671.2014.894921

Grigorova, B., Vassileva, V., Klimchuk, D., Vaseva, I., Demirevska, K., & Feller, U. (2012). Drought, high temperature, and their combination affect ultrastructure of chloroplasts and mitochondria in wheat (Triticum aestivum L.) leaves. *Journal of Plant Interactions*, *7*(3), 204–213. https://doi.org/10.1080/17429145.2011.654134

Heilemann, K. K., Stoll, M., Hofmann, M., & Friedel, M. (2023). A mobile device to investigate the response of grapevine berries to heat stress. *OENO One*, *57*(3), Article 3. https://doi.org/10.20870/oeno-one.2023.57.3.7216

Huber, B. (1935). *Die physiologische Bedeutung der Ring-und Zerstreutporigkeit*.

Hulands, S., Greer, D. H., & Harper, J. I. (2014). The interactive effects of temperature and light intensity on *Vitis vinifera* cv. 'Semillon' grapevines. II. Berry ripening and susceptibility to sunburn at harvest. *European Journal of Horticultural Science*, *79*(1), 1–7.

Iland, I., P., Dry, P., Proffitt, T., & Tyerman, S. (2011). *The grapevine: From the science to the practice of growing vines for wine*. Patrick Iland Wine Promotions.

Jackson, M. B., Herman, B., & Goodenough, A. (1982). An examination of the importance of ethanol in causing injury to flooded plants. *Plant, Cell & Environment*, *5*(2), 163–172. https://doi.org/10.1111/1365-3040.ep11571590

Keller, M. (2006). Ripening grape berries remain hydraulically connected to the shoot. *Journal of Experimental Botany*, *57*(11), 2577–2587. https://doi.org/10.1093/jxb/erl020

Keller, M., Zhang, Y., Shrestha, P. M., Biondi, M., & Bondada, B. R. (2015). Sugar demand of ripening grape berries leads to recycling of surplus phloem water via the xylem. *Plant, Cell & Environment*, *38*(6), 1048–1059. https://doi.org/10.1111/pce.12465

Kelsey, R. G., & Westlind, D. J. (2017). Physiological stress and ethanol accumulation in tree stems and woody tissues at sublethal temperatures from fire. *BioScience*, *67*(5), 443–451. https://doi.org/10.1093/biosci/bix037

Kobayashi, A., Fukushima, T., Nii, N., & Harada, K. (1965). Studies on the thermal conditions of grapes. V. Effects of day and night temperatures on yield and quality of Delaware grapes. *Journal of the Japanese Society for Horticultural Science*, *36*(4), 373–379.

Krasnow, M., Matthews, M., & Shackel, K. (2008). Evidence for substantial maintenance of membrane integrity and cell viability in normally developing grape (*Vitis vinifera* L.) berries throughout development. *Journal of Experimental Botany*, *59*(4), 849–859. https://doi.org/10.1093/jxb/erm372

Kurtural, S. K., & Gambetta, G. A. (2021). Global warming and wine quality: Are we close to the tipping point? *OENO One*, *55*(3), Article 3. https://doi.org/10.20870/oeno-one.2021.55.3.4774

Litchfield, W. H. (1951). Soil survey of the Waite Agricultural Research Institute. *CSIRO, Division of Soils, Divisional Report*, *2*, 51. https://doi.org/10.4225/08/58712dac56dd4

Mancuso, S., & Azzarello, E. (2002). Heat tolerance in olive. *Advances in Horticultural Science*, *16*.

Martínez-Lüscher, J., Chen, C. C. L., Brillante, L., & Kurtural, S. K. (2020). Mitigating heat wave and exposure damage to "Cabernet Sauvignon" wine grape with partial shading under two irrigation amounts. *Frontiers in Plant Science*, *11*. https://www.frontiersin.org/articles/10.3389/fpls.2020.579192

Matsui, A., Todaka, D., Tanaka, M., Mizunashi, K., Takahashi, S., Sunaoshi, Y., Tsuboi, Y., Ishida, J., Bashir, K., Kikuchi, J., Kusano, M., Kobayashi, M., Kawaura, K., & Seki, M. (2022). Ethanol induces heat tolerance in plants by stimulating unfolded protein response. *Plant Molecular Biology*, *110*(1), 131–145. https://doi.org/10.1007/s11103-022-01291-8

McCarthy, M. G. (1997). The effect of transient water deficit on berry development of cv. Shiraz (*Vitis vinifera* L.). *Australian Journal of Grape and Wine Research*, *3*(3), 2–8. https://doi.org/10.1111/j.1755-0238.1997.tb00128.x

McCarthy, M. G. (1999). Weight loss from ripening berries of Shiraz grapevines (*Vitis vinifera* L. cv. Shiraz). *Australian Journal of Grape and Wine Research*, *5*(1), 10–16. https://doi.org/10.1111/j.1755-0238.1999.tb00145.x

McCarthy, M. G., & Coombe, B. G. (1999). Is weight loss in ripening grape berries cv. Shiraz caused by impeded phloem transport? *Australian Journal of Grape and Wine Research*, *5*(1), 17–21. https://doi.org/10.1111/j.1755-0238.1999.tb00146.x

McConnaughay, K. D. M., & Coleman, J. S. (1999). Biomass allocation in plants: Ontogeny or optimality? A test along three resource gradients. *Ecology*, *80*(8), 2581–2593. https://www.jstor.org/stable/177242

Michaletz, S., & Johnson, E. (2007). How forest fires kill trees: A review of the fundamental biophysical processes. *Scandinavian Journal of Forest Research*, *22*. https://doi.org/10.1080/02827580701803544

Müller, K., Keller, M., Stoll, M., & Friedel, M. (2023). Wind speed, sun exposure and water status alter sunburn susceptibility of grape berries. *Frontiers in Plant Science*, *14*. https://www.frontiersin.org/articles/10.3389/fpls.2023.1145274

Nievola, C. C., Carvalho, C. P., Carvalho, V., & Rodrigues, E. (2017). Rapid responses of plants to temperature changes. *Temperature*, *4*(4), 371–405. https://doi.org/10.1080/23328940.2017.1377812

Niinemets, Ü. (2018). When leaves go over the thermal edge. *Plant, Cell & Environment*, *41*(6), 1247–1250. https://doi.org/10.1111/pce.13184

Ollat, N., Carde, J.-P., Gaudillère, J.-P., Barrieu, F., Diakou-Verdin, P., & Moing, A. (2002). Grape berry development: A review. *OENO One*, *36*(3), Article 3. https://doi.org/10.20870/oeno-one.2002.36.3.970

Pagay, V. (2018). *Is berry shrivel in Cabernet Sauvignon influenced by climate and does this potentially affect characteristics of the resulting wine?* (UA 1702). the University of Adelaide. https://limestonecoastwine.com.au/library/64-is-berry-shrivel-in-cabernet-sauvignon-influenced-by-climate-and-does-this-potentially-affect-characteristics-of-the-resulting-wine/

Pate, J. S. (1975). Exchange of solutes between phloem and xylem and circulation in the whole plant. In M. H. Zimmermann & J. A. Milburn (Eds.), *Transport in Plants I* (pp. 451–473). Springer Berlin Heidelberg. https://doi.org/10.1007/978-3-642-66161-7_19

Paull, R. E., & Chen, N. J. (2000). Heat treatment and fruit ripening. *Postharvest Biology and Technology*, *21*(1), 21–37. https://doi.org/10.1016/S0925-5214(00)00162-9

Peña Quiñones, A. J., Hoogenboom, G., Gutiérrez, M. R. S., Stöckle, C., & Keller, M. (2020). Comparison of air temperature measured in a vineyard canopy and at a standard weather station. *Plos One*, *15*(6), Article 6. https://doi.org/10.1371/journal.pone.0234436

Perkins, S. E., Alexander, L. V., & Nairn, J. R. (2012). Increasing frequency, intensity and duration of observed global heatwaves and warm spells. *Geophysical Research Letters*, *39*(20), 2012GL053361. https://doi.org/10.1029/2012GL053361

Ponce de León, M. A., & Bailey, B. (2021). A 3D model for simulating spatial and temporal fluctuations in grape berry temperature. *Agricultural and Forest Meteorology*, *306*, 108431. https://doi.org/10.1016/j.agrformet.2021.108431

Previtali, P., Dokoozlian, N., Capone, D., Wilkinson, K., & Ford, C. (2021). Exploratory study of sugar and C_6 compounds in single berries of grapevine (*Vitis vinifera* L.) cv. Cabernet Sauvignon throughout ripening. *Australian Journal of Grape and Wine Research*. https://doi.org/10.1111/ajgw.12472

Rogiers, S. Y., Greer, D. H., Hatfield, J. M., Orchard, B. A., & Keller, M. (2006). Solute transport into Shiraz berries during development and late-ripening shrinkage. *American Journal of Enology and Viticulture*, *57*(1), 73–80. https://doi.org/10.5344/ajev.2006.57.1.73

Rogiers, S. Y., Greer, D. H., Liu, Y., Baby, T., & Xiao, Z. (2022). Impact of climate change on grape berry ripening: An assessment of adaptation strategies for the Australian vineyard. *Frontiers in Plant Science*, *13*. https://www.frontiersin.org/articles/10.3389/fpls.2022.1094633

Rogiers, S. Y., Hatfield, J. M., Jaudzems, V. G., White, R. G., & Keller, M. (2004). Grape berry cv. Shiraz epicuticular wax and transpiration during ripening and preharvest weight loss. *American Journal of Enology and Viticulture*, *55*(2), 121–127. https://doi.org/10.5344/ajev.2004.55.2.121

Rogiers, S. Y., Hatfield, J. M., & Keller, M. (2004). Irrigation, nitrogen, and rootstock effects on volume loss of berries from potted Shiraz vines. *Vitis*, *43*(1), 1–6. https://doi.org/10.5073/vitis.2004.43.1-6

Rogiers, S. Y., Keller, M., Holzapfel, B. P., & Virgona, J. M. (2000). Accumulation of potassium and calcium by ripening berries on field vines of *Vitis vinifera* (L) cv. Shiraz. *Australian Journal of Grape and Wine Research*, *6*(3), 240–243. https://doi.org/10.1111/j.1755-0238.2000.tb00184.x

Sadras, V. O., & McCarthy, M. G. (2007). Quantifying the dynamics of sugar concentration in berries of *Vitis vinifera* cv. Shiraz: A novel approach based on allometric analysis. *Australian Journal of Grape and Wine Research*, *13*(2), 66–71. https://doi.org/10.1111/j.1755-0238.2007.tb00236.x

Saltveit, M. E., & Ballinger, W. E. (1983). Effects of anaerobic nitrogen and carbon dioxide atmospheres on ethanol production and postharvest quality of 'Carlos' grapes. *Journal of the American Society for Horticultural Science*, *108*(3), 462–465. https://doi.org/10.21273/JASHS.108.3.462

Seidel, K. W. (1986). Tolerance of seedlings of ponderosa pine. Douglas-fir, grand fir, and engelmann spruce for high temperatures. *Northwest Science.*, *60*(1).

Serra, I., Strever, A., Myburgh, P. a., & Deloire, A. (2014). Review: The interaction between rootstocks and cultivars (*Vitis vinifera* L.) to enhance drought tolerance in grapevine. *Australian Journal of Grape and Wine Research*, *20*(1), 1–14. https://doi.org/10.1111/ajgw.12054

Shahood, R., Torregrosa, L., Savoi, S., & Romieu, C. (2020). First quantitative assessment of growth, sugar accumulation and malate breakdown in a single ripening berry. *OENO One*, *54*(4), Article 4. https://doi.org/10.20870/oeno-one.2020.54.4.3787

Shivashankara, K. S., Laxman, R. H., Geetha, G. A., Roy, T. K., Srinivasa Rao, N. K., & Patil, V. S. (2013). Volatile aroma and antioxidant quality of 'Shiraz' grapes at different stages of ripening. *International Journal of Fruit Science*, *13*(4), 389–399. https://doi.org/10.1080/15538362.2013.789235

Singh, D. (2010). *Causes and prevention of table grape berry collapse*. Horticulture Australia Ltd.

Smart, R. E., & Dry, P. R. (1980). A climatic classification for Australian viticultural regions. *Annual Technical Issue*.

Smart, R. E., & Sinclair, T. R. (1976). Solar heating of grape berries and other spherical fruits. *Agricultural Meteorology (Netherlands)*, *17*(4), 241–259. https://doi.org/doi:10.1016/0002-1571(76)90029-7

Spayd, S., Tarara, J., Mee, D. L., & Ferguson, J. C. (2002). Separation of sunlight and temperature effects on the composition of *Vitis vinifera* cv. Merlot berries. *American Journal of Enology and Viticulture*, *53*(5), 171–182. https://doi.org/10.5344/ajev.2002.53.3.171

Stoll, M., & Jones, H. G. (2007). Thermal imaging as a viable tool for monitoring plant stress. *OENO One*, *41*(2), Article 2. https://doi.org/10.20870/oeno-one.2007.41.2.851

Šuklje, K., Zhang, X., Antalick, G., Clark, A. C., Deloire, A., & Schmidtke, L. M. (2016). Berry shriveling significantly alters Shiraz (*Vitis vinifera* L.) grape and wine chemical composition. *Journal of Agricultural and Food Chemistry*, *64*(4), 870–880. https://doi.org/10.1021/acs.jafc.5b05158

Sung, D.-Y., Kaplan, F., Lee, K.-J., & Guy, C. L. (2003). Acquired tolerance to temperature extremes. *Trends in Plant Science*, *8*(4), 179–187. https://doi.org/10.1016/S1360-1385(03)00047-5

Sweetman, C., Deluc, L. G., Cramer, G. R., Ford, C. M., & Soole, K. L. (2009). Regulation of malate metabolism in grape berry and other developing fruits. *Phytochemistry*, *70*(11), 1329–1344. https://doi.org/10.1016/j.phytochem.2009.08.006

Tesnière, C., Romieu, C., Dugelay, I., Nicol, M. Z., Flanzy, C., & Robin, J. P. (1994). Partial recovery of grape energy metabolism upon aeration following anaerobic stress. *Journal of Experimental Botany*, *45*(1), 145–151. https://doi.org/10.1093/jxb/45.1.145

Tilbrook, J., & Tyerman, S. (2006). *Water, sugar and acid: How and where they come and go during berry ripening*. Australian Society of Viticulture and Oenology Seminar (2006 : Mildura, Vic.). https://www.semanticscholar.org/paper/Water%2C-sugar-and-acid%3A-how-and-where-they-come-and-Tilbrook-Tyerman/16c552dc41efba382364ac16876a1467499ddc78

Tilbrook, J., & Tyerman, S. D. (2008). Cell death in grape berries: Varietal differences linked to xylem pressure and berry weight loss. *Functional Plant Biology*, *35*(3), 173. https://doi.org/10.1071/FP07278

Tilbrook, J., & Tyerman, S. D. (2009). Hydraulic connection of grape berries to the vine: Varietal differences in water conductance into and out of berries, and potential for backflow. *Functional Plant Biology*, *36*(6), 541. https://doi.org/10.1071/FP09019

Tyerman, S. D., Tilbrook, J., Pardo, C., Kotula, L., Sullivan, W., & Steudle, E. (2008). Direct measurement of hydraulic properties in developing berries of *Vitis vinifera* L. cv Shiraz and Chardonnay. *Australian Journal of Grape and Wine Research*, *10*(3), 170–181. https://doi.org/10.1111/j.1755-0238.2004.tb00020.x

Venios, X., Korkas, E., Nisiotou, A., & Banilas, G. (2020). Grapevine responses to heat stress and global warming. *Plants*, *9*(12), Article 12. https://doi.org/10.3390/plants9121754

Wahid, A., Gelani, S., Ashraf, M., & Foolad, M. (2007). Heat tolerance in plants: An overview. *Environmental and Experimental Botany*, *61*(3), 199–223. https://doi.org/10.1016/j.envexpbot.2007.05.011

Webb, Watt, A., Hill, T., Whiting, J., Wigg, F., Dunn, G., Needs, S., & Barlow, S. (2009). Extreme heat: Managing grapevine response based on vineyard observations from the 2009 heatwave across south-eastern Australia. *Australian Viticulture*, *13*(5), 39–50.

Xiao, Rogiers, S. Y., Sadras, V. O., & Tyerman, S. D. (2018). Hypoxia in grape berries: The role of seed respiration and lenticels on the berry pedicel and the possible link to cell death. *Journal of Experimental Botany*, *69*(8), 2071–2083. https://doi.org/10.1093/jxb/ery039

Xiao, Stait-Gardner, T., Willis, S. a., Price, W. S., Moroni, F. J., Pagay, V., Tyerman, S. D., Schmidtke, L. M., & Rogiers, S. Y. (2021). 3D visualisation of voids in grapevine flowers and berries using X-ray micro computed tomography. *Australian Journal of Grape and Wine Research*, *27*(2), 141–148. https://doi.org/10.1111/ajgw.12480

Xiao, Z., Liao, S., Rogiers, S. Y., Sadras, V. O., & Tyerman, S. D. (2018). Effect of water stress and elevated temperature on hypoxia and cell death in the mesocarp of Shiraz berries: Berry hypoxia and death under water/heat stress. *Australian Journal of Grape and Wine Research*, *24*(4), 487–497. https://doi.org/10.1111/ajgw.12363

Xu, H., Liu, G., Liu, G., Yan, B., Duan, W., Wang, L., & Li, S. (2014). Comparison of investigation methods of heat injury in grapevine (*Vitis*) and assessment to heat tolerance in different cultivars and species. *BMC Plant Biology*, *14*(1), 156. https://doi.org/10.1186/1471-2229-14-156

Zhang, Y., & Keller, M. (2015). Grape berry transpiration is determined by vapor pressure deficit, cuticular conductance, and berry size. *American Journal of Enology and Viticulture*, *66*(4), 454–462. https://doi.org/10.5344/ajev.2015.15038

7. Appendix

Figure S1 Illustration of the temperature sensor in the field located in the bunch zone, temperature sensor was protected by two shells made of white Stevenson-type plastic funnels.
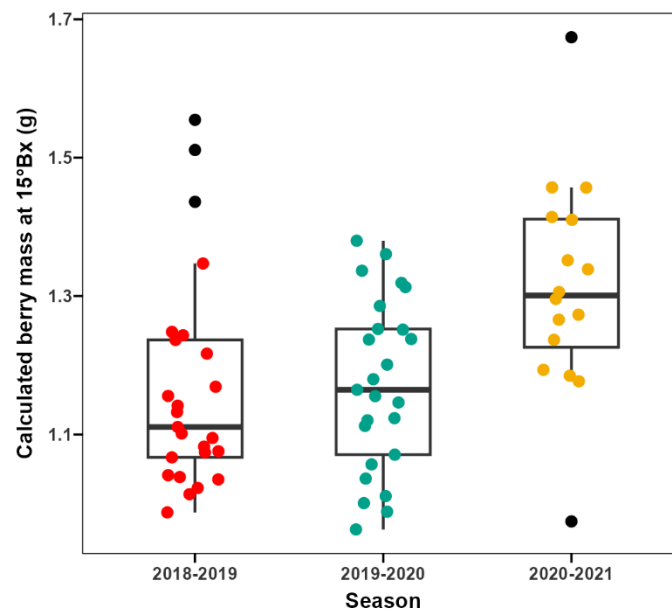

Figure S2 Calculated berry mass at 15 °Brix of each rootstock replicate of Shiraz vines in three growing seasons from 2018 to 2021 at Coombe vineyard. Boxplots with individual values are shown, outliers (black dots) were identified by IQR method (range=1). Middle line in box represents median value; lower and upper edges of box represent 25th and 75th percentile of data set; and whiskers represent range of data values.
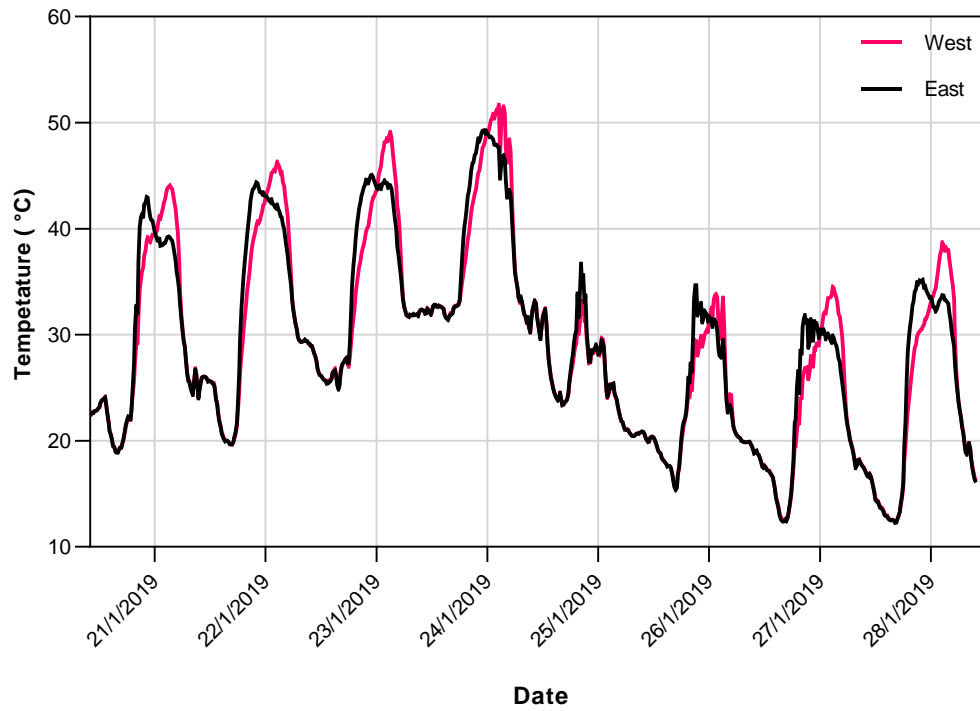
Figure S3 Comparing canopy air temperature every 15 minutes during a heatwave from 21/1/2019 to 28/1/2019. Different colours indicate temperatures at different sides of the canopy (east versus west), dates on the x axis occur at 14:00.
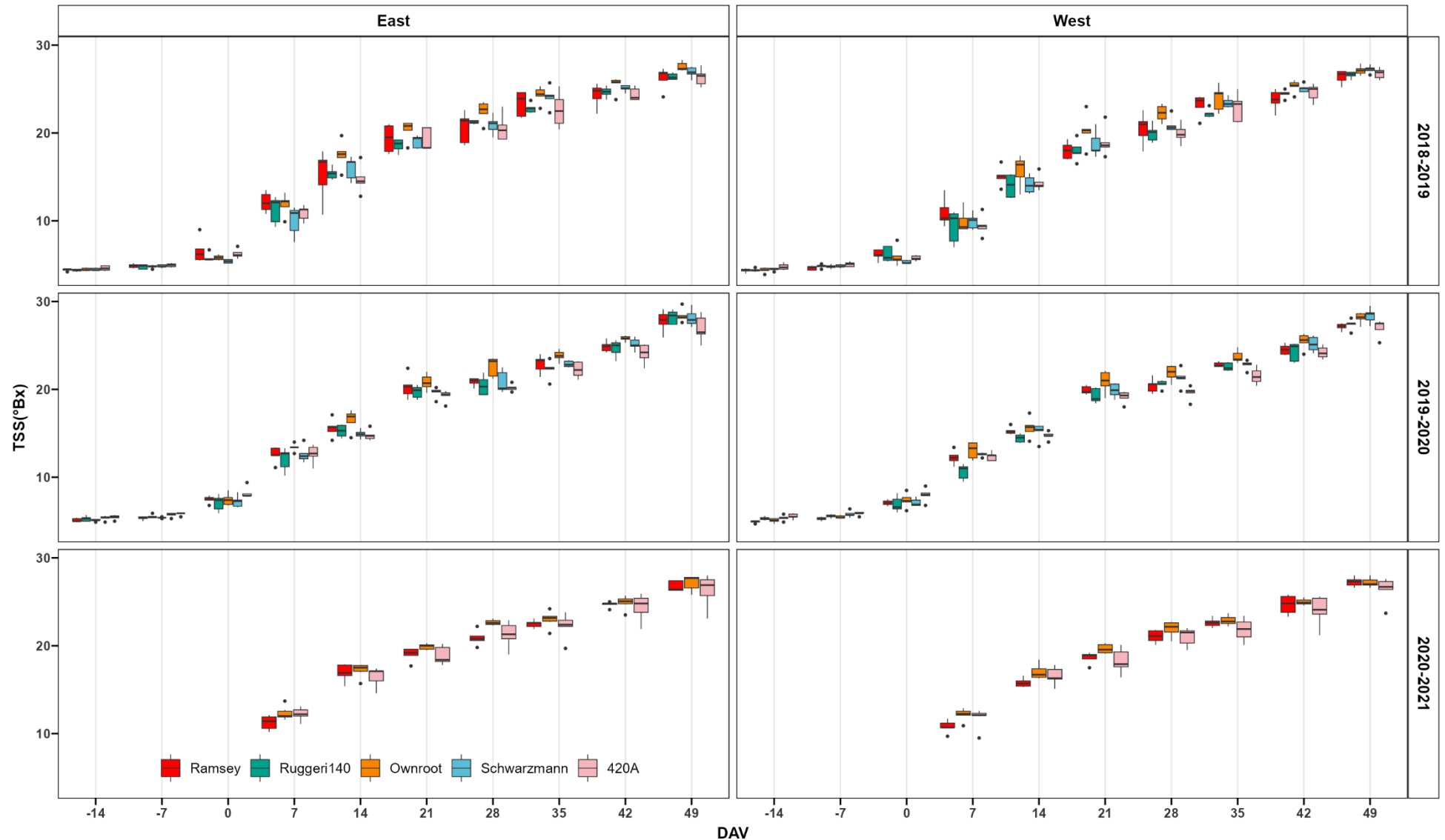
Figure S4 Shiraz overall berry TSS from different rootstocks on east and west side of the canopy in three growing seasons from 2018 to 2021 at Coombe vineyard. Boxplots with are shown. n = 5 and each replicate contains about 24 berries. Middle line in box represents median value; lower and upper edges of box represent 25th and 75th percentile of data set; and whiskers represent range of data values. Black dots indicate outlier. No significant differences were observed between different rootstock on each sampling date in each high and low drought tolerances/ vigour group (one-way ANOVA and T test).
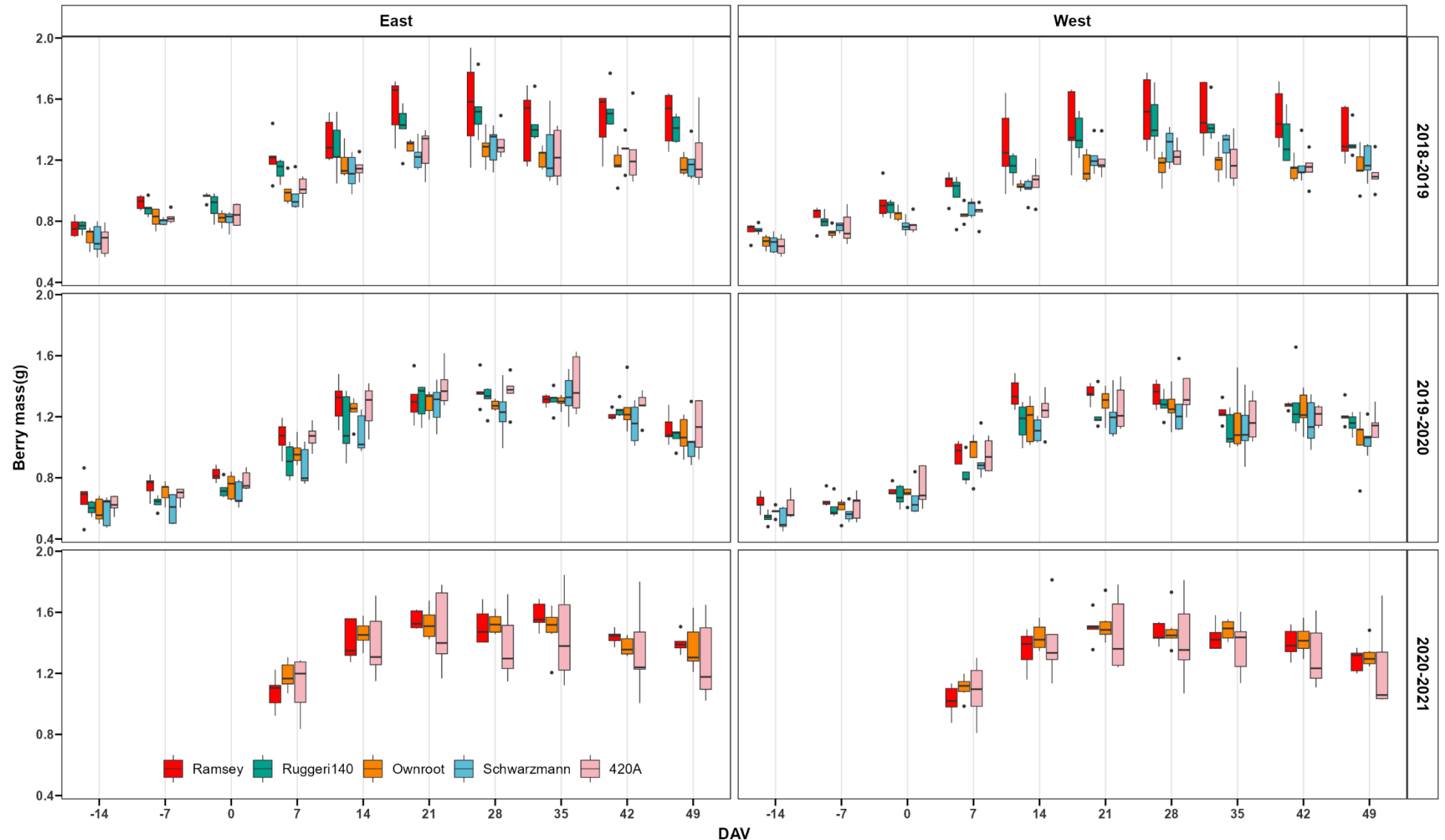
Figure S5 Shiraz overall berry mass from different rootstocks on east and west sides of the canopy in three growing seasons from 2018 to 2021 at Coombe vineyard. Boxplots with are shown. n = 5 and each replicate contains about 24 berries. Middle line in box represents median value; lower and upper edges of box represent 25th and 75th percentile of data set; and whiskers represent range of data values. Black dots indicate outlier. No significant differences were observed between different rootstock on each sampling date in each high and low drought tolerances/ vigour group (one-way ANOVA and T test).
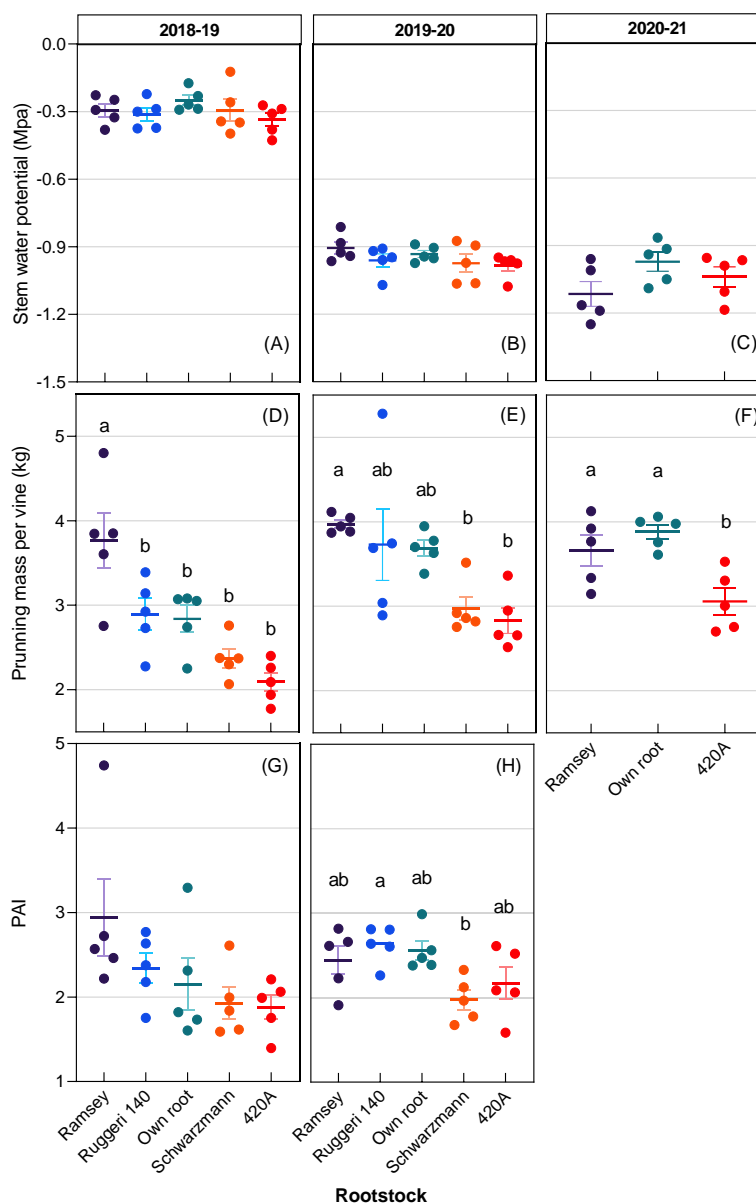
Figure S6 Water potential and canopy development of the different rootstocks for the three seasons of study. Shiraz stem water potential (A, B, C), pruning water per vine (D, E, F) and Plant Area Index (PAI) (G, H). Water potentials in 2018-19 were measured at pre-dawn, while midday stem water potentials are shown for season 2019-20 and 2020-21. Point plot with mean ± SEM (n =5). One-way ANOVA was performed to test the effects of rootstocks on stem water potential, pruning weight per vine and PAI in each season. High drought tolerance/ vigour rootstocks (Ramsey and Ruggeri 140) tended to have significant higher pruning mass per vine as well as PAI than that low drought tolerance/ vigour rootstocks (Own root, Schwarzmann and 420A), but the differences were only significant between Ramsey and some of other rootstocks. Different letters indicate statistically significant differences ($p < 0.05$) in each subplot. No letters indicate no significant differences.
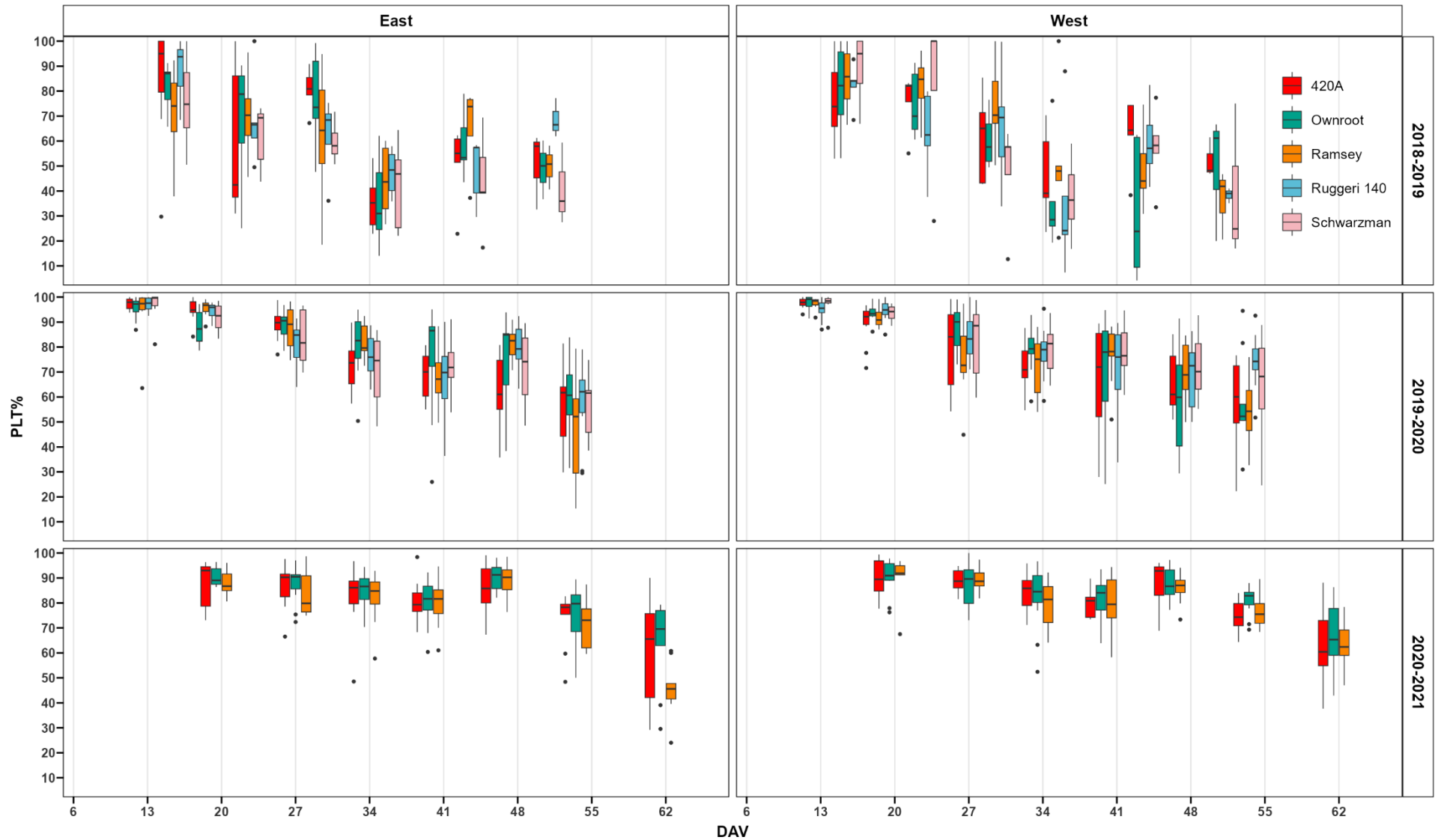
Figure S7 Shiraz mesocarp percentage living tissue (PLT) from different rootstocks from east and west sides of the canopy in three growing seasons from 2018 to 2021 at Coombe vineyard. DAV, days after veraison. Boxplots with are shown (n = 10). Middle line in box represents median value; lower and upper edges of box represent 25th and 75th percentile of data set; and whiskers represent range of data values. No significant differences were observed between different rootstock nor canopy orientations on each sampling date (two-way ANOVA).
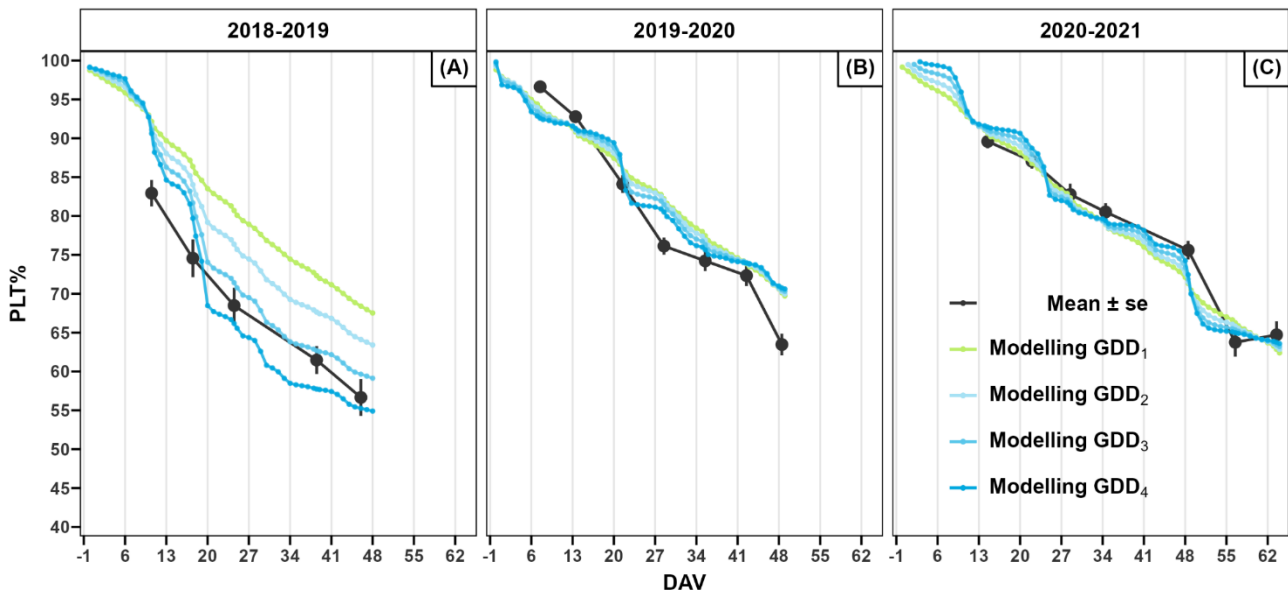
Figure S8 Mean percentage living tissue (PLT) versus days after veraison (DAV) in three growing seasons from 2018-2021 with mean ± SEM (n = ~ 100) and modelling with GTD_n (n = 1,2,3,4). A regression model was developed between Shiraz mesocarp PLT mean values and growing temperature days of (GTD_n) base 10 °C from data in 2019-20 and 2020-21 season, the function is: Mesocarp PLT = a + b*GTD_n, where GTD_n = $\sum_{DAV=0(veraison)}^{DAV}(ABT-10)^n$ ($n = 1,2,3,4$), predications of the all the three seasons were based on the model comparing different power of GTD.

Table S1 Statistics summary of regression model fit with GTD_n to predict Shiraz mesocarp PLT from 2019-2020 and 2020-2021 season (**** indicate significant difference (p <0.0001).

Models	Independent variables	Intercept (%)	Slope	F-ratio (1,11)	Adjusted R^2
1	GTD$_1$	99.79	-0.040799****	83.62 ****	0.8732
2	GTD$_2$	100.7	-0.002859****	89.8 ****	0.881
3	GTD$_3$	101.4	-1.795e-04****	99.47 ****	0.8914
4	GTD$_4$	102	-1.020e-05****	113.7****	0.9038

Table S2 Berry temperature (inside) of Shiraz in Coombe vineyard on 28/1/2020 at about 16:00.

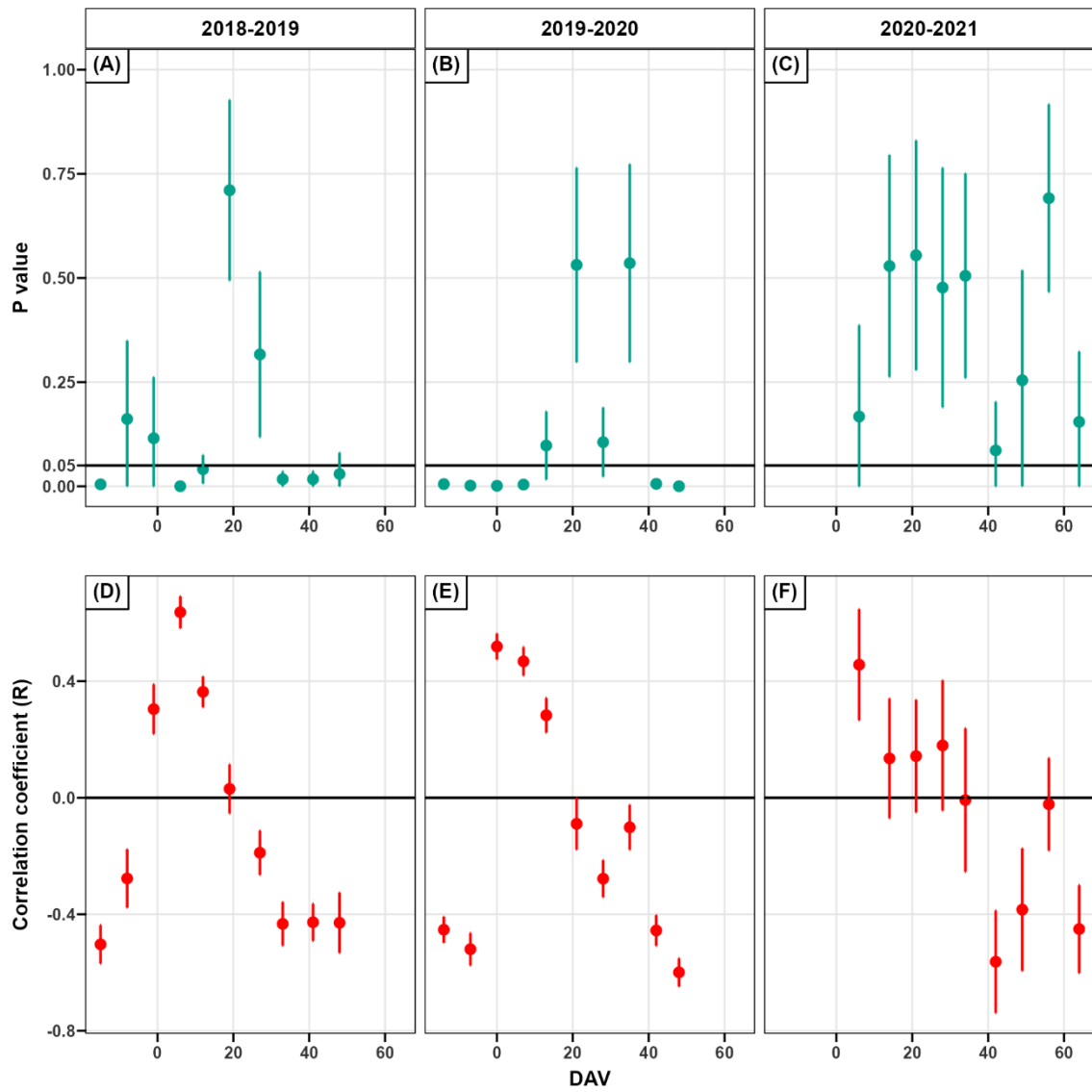| Berry 1	Berry 2	Berry 3	Berry 4	Berry 5
49.1 °C	45 °C	49.7 °C	50.2 °C	50.2 °C
Air temperature: approx. 40 °C				

Figure S9 *P* values (ABC) and correlation coefficient (DEF) by "Pearson correlation" between berry mass and TSS in different sampling dates in three seasons, 2018-19, 2019-20 and 2020-21. Values are mean ± SD (n = 500 for season 2018-19 and 2019-20, n = 200 for season 2020-21).

Chapter 4

Effect of application of Kaolin and Pinolene on Shiraz and Grenache berry cell death, mass loss and ethanol accumulation
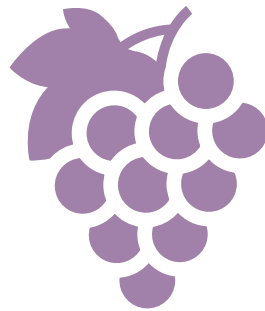
Table of Contents

Effect of application of Kaolin and Pinolene on Shiraz and Grenache berry cell death, mass loss and ethanol accumulation

1. Introduction

Berry cell death and shrinkage of *Vitis vinifera* L. during late ripening have been significant problems in Australia and overseas. These issues are linked to decreased yield and deterioration of grape and wine quality, such as excess sugar accumulation, poor colour and flavour development in grapes, and more dead/stewed fruit characters in resulting wines (Chou et al., 2018; Shivashankara et al., 2013; Šuklje et al., 2016). Cell death in the mesocarp of Shiraz berries becomes evident earlier than desirable winemaking flavour ripeness and phenolic maturity are achieved (Fuentes et al., 2010; McCarthy, 1999; Rogiers & Holzapfel, 2015; Tilbrook & Tyerman, 2008). Furthermore, these issues are anticipated to worsen due to 'global warming', with predictions indicating an increase in the frequency and severity of heatwaves and drought events (Perkins et al., 2012). However, vineyard interventions to mitigate berry cell death and shrinkage are few so far and are related to reducing the effect of heat events via over-head shading (Caravia et al., 2016) or in-canopy micro sprinklers (Caravia et al., 2017).

Late ripening berry shrivel is variety dependent and is caused by a net water loss from the berry through either water flow back to the parent vine (backflow), or as a result of continued transpiration when phloem transport to the berry ceases (Keller, 2006; Rogiers et al., 2004; Tilbrook & Tyerman, 2009; Tyerman et al., 2008; Zhang & Keller, 2015). There is a strong correlation between the degree of shrivel and cell death (Fuentes et al., 2010; Krasnow et al., 2008; Tilbrook & Tyerman, 2008, 2009). Backflow has been hypothesised to be an important cause of shrivel in Shiraz since the berries are hydraulically connected to the vine (via the xylem) when cell death occurs and continues through the shrinkage phase, while Chardonnay, which generally shows a similar degree of cell death, does not shrivel and has low hydraulic connectivity to the vine (Fuentes et al., 2010; Krasnow et al., 2008; Tilbrook & Tyerman, 2008, 2009). Varieties that can maintain high cell vitality during late berry development like Grenache and some table grape varieties, and/or that are hydraulically disconnected

to the vine late in ripening when cell death occurs (e.g., Chardonnay), could be exempt from berry shrivel (Fuentes et al., 2010; Tilbrook & Tyerman, 2008, 2009).

The reason behind berry mesocarp cell death is not fully understood, and various factors are known to play a role, such as heat stress, water stress and hypoxia within the berries (Bonada et al., 2013; Caravia et al., 2015; Xiao, Liao, et al., 2018). Elevated temperature and water stress were found to induce and/or increase cell death and shrinkage in grape berries (Bonada et al., 2013; Caravia et al., 2015; Xiao, Liao, et al., 2018). Both grape berry oxygen concentration ($[O_2]$) and cell vitality declined with ripeness, also, in the mesocarp interior between the skin and the centre axis, low $[O_2]$ corresponded to the highest cell death (Xiao, Rogiers, et al., 2018). Treatments like water stress or blocking the berry pedicle to reduce O_2 diffusion via lenticels also decreased average berry $[O_2]$, inducing increased ethanol synthesis and increased cell death (Xiao, Liao, et al., 2018).

Two types of film-forming antitranspirants, Kaolin ($A_{l4}Si_4O_{10}(OH)_8$) and Di-1-p-menthene ($C_{20}H_{34}$) (also known as Pinolene), are used in viticulture and other horticultural crops to reduce transpiration and hence improve water use efficiency, water potential and metabolism (Brillante et al., 2016; Cantore et al., 2009; Mphande et al., 2023). Kaolin, a non-abrasive and non-toxic white clay comprised of layered aluminium silicate, is well regarded as the most important reflective antitranspirants both in research and in commercial fruit and nut horticultural production (Cantore et al., 2009; Mphande et al., 2023). Kaolin can be used to reduce damage from high-irradiance effects (sunburn) and high temperatures by reflecting radiation especially UV wavelengths reaching the surface of leaves and fruits (Brillante et al., 2016; Cantore et al., 2009), but its effects on berry oxygen and cell death are unknown. Pinolene, an emulsifiable terpenic polymer obtained through the distillation of pine resins, creates a flexible, glossy, and transparent film upon application (Palliotti et al., 2010). This film-forming antitranspirant may effectively restricting plant transpiration and minimizing water loss (Palliotti et al., 2010). It has been demonstrated that Pinolene can reduce Shiraz leaf transpiration and water loss from Merlot bunches but causing increased temperature in both

presumably via loss of evaporative cooling (Fahey, 2018; Fahey & Rogiers, 2019). The effect of direct treatment on grape bunches has not been reported and it is not known how antitranspirants may affect berry oxygen concentrations and cell death. Possible increase in berry temperature due to reduced evaporation or blockade of oxygen ingress through skin or lenticels could be counterproductive and result in more cell death and berry shrivel.

The goal of this study was to identify the effects of two film-forming antitranspirants coatings Kaolin $(Al_4Si_4O_{10}(OH)_8)$ and Pinolene (Di-1-p-menthene), on berry cell death and mass loss on Shiraz and Grenache, by testing their impacts on $[O_2]$, ethanol concentration [EtOH] and bunch temperature. It was hypothesised that both treatments may block oxygen uptake into berries by virtue of their impermeable barrier nature, as well as water loss resulting in a more complicated response in berry cell death and berry shrivel.

2. Materials and Methods

2.1. Experimental site, vines, and treatments

The experiments were conducted in the Coombe Vineyard at Waite Campus of the University of Adelaide (34°58'03.12" S and 138°38'00.21" E) during growing season 2019-20. Adelaide's climate falls into the category of a hot Mediterranean climate, characterized by wet winters and hot, dry summers. It is considered a warm to hot region, with the mean January temperature (MJT) ranging from 21 °C to 25 °C (Smart & Dry, 1980). Seasonal temperature (station 23034), rainfall (station 23005) during the growing season were sourced from the Australian Bureau of Meteorology website (Bureau of Meteorology, www.bom.gov.au) (Table 1). Growing Season Temperature (GST) is the mean of monthly average temperatures for September to April, calculated from mean monthly maximum and minimum temperatures. Data from these stations were similar comparing to the local weather station in the vineyard.

Experimental vines were *Vitis vinifera* L. Shiraz (Clone BVRC12) grafted to Schwarzman, 420A, planted in 1990 and Grenache (Clone 137) on own roots, planted in 2000. According to Wine

Australia Rootstock Selector Tool (https://www.grapevinerootstock.com/), both Schwartzmann and 420 A are classified as having low to moderate drought tolerance and low to moderate vigour. Rows (3 m spacing) are oriented north south. Irrigation regimes were approximately 1.1 ML/ha of water per season for Shiraz under drip irrigation, while no irrigation was applied for Grenache vines for the previous 8 seasons. All vines were pruned to two bud spurs and trained in a vertical shoot positioned (VSP) trellis system. There were five replications of Grenache with each replicate consisting of three vines across one panel (between posts). Shiraz had six replications in total with three on rootstock Schwarzman and three on rootstock 420A and where replicates consisted each of four vines in two adjacent panels. The experiments were conducted from veraison to late harvest.

2.2. Treatments and measurements overview

Three treatments were applied to grape bunches: (A) Kaolin dissolved in Milli-Q water, (B) Pinolene dissolved in Milli-Q water and, (c) Milli-Q filtered water as control (Figure 1). Within each replicate, two healthy bunches per treatment were labelled randomly on the west side of the canopy. Based on the manufacturer's recommendation and previous studies (Brillante et al., 2016; Di Vaio et al., 2019; Fahey, 2018). Kaolin and Pinolene treatments were used at 6% (w/w) and 1% (w/w) concentration, respectively. Kaolin (30g) (Surround® WP) was dissolved into and 471 g Milli-Q filtered water, Pinolene (5 g) (AgsureVapor Gard) was dissolved in 495 g Milli-Q filtered water, both were dissolved and sprayed using a 500 ml sprayer respectively. The Kaolin, Pinolene and Milli-Q filtered water were sprayed on the bunches including pedicels until totally wet (Figure 1). All the treatments were applied 4 times on Shiraz bunches and 3 times on Grenache bunches during berry ripening at 7-to-15-day intervals to make sure that bunches were always covered in the compounds.
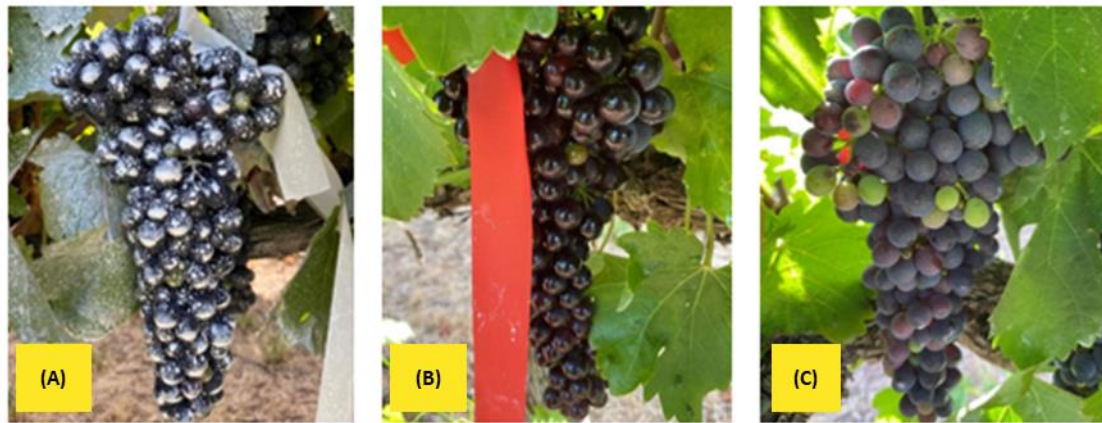
Figure 1 Kaolin (A), Pinolene (B) and water (C) treatments on Shiraz bunches in Coombe Vineyard (2019/20 season).

Berry sampling started approximately one week after the first spray application. Berry sampling for berry mass, juice TSS, mesocarp percentage living tissue (PLT), and juice ethanol concentration ([EtOH]) were conducted on the same berry. For these measurements, Shiraz berries were sampled approximately every week from 80 DAA to late harvest, while three samplings for Grenache were conducted from 90 DAA to late harvest. Berry [O_2] profiles were conducted three times for Shiraz from approximately 80 DAA to late harvest, but only once in Grenache at 113 DAA. All the sampled berries were normally collected from the outward side of the bunch. Sampled berries were stored in groups and placed in a polystyrene box with an ice pack during transportation to the laboratory (approximately 15 minutes). Temperatures of Shiraz bunches were measured once on 28th January 2020. All the bunches were harvested on 12th March 2020 and juice TSS, pH, and total acidity (TA) were measured.

2.3. Berry mass, juice TSS and sugar per berry, percentage living tissue (PLT), and juice [EtOH]

One berry per labelled bunch from the middle part was collected by cutting the pedicel with sharp scissors to avoid possible damage to berries. Once samples were taken to the laboratory, berry mass, TSS, cell vitality and [EtOH] (details see Chapter 3) were estimated for each berry. Sugar per berry was taken as berry mass times TSS (Deloire, 2011).

2.4. Berry internal [O_2] profiles

One berry per bunch from the middle part of the labelled bunch was collected (2 per replicate), but only 1 was randomly selected for [O_2] profiles (details see Chapter 2).

2.5. Bunch temperature

Shiraz bunch surface temperatures were measured on 28th January 2020 during a heatwave (daily maximum air temperature was 40 °C at 16:30) and when the bunches were exposed to the direct solar beam (during 15:30 to 16:30) using an IR thermometer (Fluke 568; Fluke Corporation, Everett, WA, USA) and with a type-K thermocouple bead probe (Fluke 80PK-1). Three measures on each bunch were taken from top, middle, and bottom of the bunch.

2.6. Bunch TSS, pH and TA

All the labelled bunches of Grenache and Shiraz (2 bunches per replicate) were harvested on 12th March 2020. Then all berries from each bunch were sampled and hand-crushed in plastic bags, with the juice then collected in 50 mL tubes and centrifuged (Hettich Universal) at 5000 rpm for 5 minutes. Then juice pH, TA and TSS were measured according to Iland et al. (2011) using an automatic titrator (G20S Compact Titrator, Mettler Toledo) and a digital refractometer (Model PR101, Atago, Tokyo, Japan) respectively.

2.7. Statistical analysis

Significant differences between different treatments over time were examined by multiple linear regressions in each subplot (Figure 2), except for Figure 2-B, in which two-way repeated ANOVA (and Tukey post-test) was applied with DAA (time) and treatment. One-way ANOVAs were applied to test bunch TSS, pH, TA (Figure 3) and bunch temperature (Figure 4) differences. Multiple linear regressions were applied to test significant differences of [O_2] profiles from different treatments, different depths and different DAAs (Figure 5). Two-way repeated ANOVAs (and Tukey) were applied to test the significant differences of [EtOH] between treatments and time (DAA) (Figure 6). All analysis was performed using Prism 9 (GraphPad Software, La Jolla, CA, USA).

3. Results

3.1. Seasonal climate conditions and phenology for Shiraz and Grenache

In 2019-20 seasons, the average temperature during the growing season from September to April was 19.22 °C while the mean January temperature was 21.95 °C with total rainfall of 196.80 mm during the season (Table 1). The flowering and veraison dates were 3rd November 2019 and 9th January 2020 respectively for Shiraz, and 6th November 2019 and 19th January 2020 respectively for Grenache.

Table 1 Growing season monthly mean temperature (°C), growing degree days (°C days), monthly total rainfall (mm) and in Coombe Vineyard in 2019-20 season.

Month	Mean temperature (°C)	GDD (°C days)	Total rainfall (mm)
Sep	13.60	108.00	50.2
Oct	17.60	343.60	23.2
Nov	17.70	574.60	23.0
Dec	22.85	972.95	17.0
Jan	21.95	1,343.40	27.6
Feb	20.90	1,659.50	51.6
Mar	19.95	1,967.95	4.2
Apr	16.90	2,174.95	102.0
Average	19.22		
Total			196.8

3.2. Berry mass, juice TSS, sugar per berry and percentage living tissue

Kaolin treatment did not have any significant effect on berry mass, juice TSS, sugar per berry or percentage living tissue (PLT) compared to the control treatment in both Shiraz and Grenache (Figure 2). Pinolene treatment did not significantly affect mesocarp PLT or sugar per berry in both varieties (Figure 2-CDGH).

Both berry mass and mesocarp PLT decreased in Shiraz after approximately 85 DAA (Figure 2A, 2C). The berry mass loss rate was significantly lower for the Pinolene treatment compared to the control and Kaolin treatment in Shiraz (all $p < 0.01$) (multiple linear regression, factors = DAA, treatment). This contrasted to Grenache where measurement of mass at 103 and 125 DAA were similar and PLT remained high (Figure 2B, 2D). Berry mass of Grenache was higher under Pinolene than that of both Kaolin and control in these dates (all $p < 0.05$, two-way repeated ANOVA and Tukey).

Juice TSS, pH and TA from the harvest bunches of Shiraz and Grenache were also measured (Figure 3). No significant differences between Kaolin and control treatments were observed while Pinolene treatment significantly decreased TSS in both varieties (all $p < 0.001$) but did not affect juice pH or TA significantly.
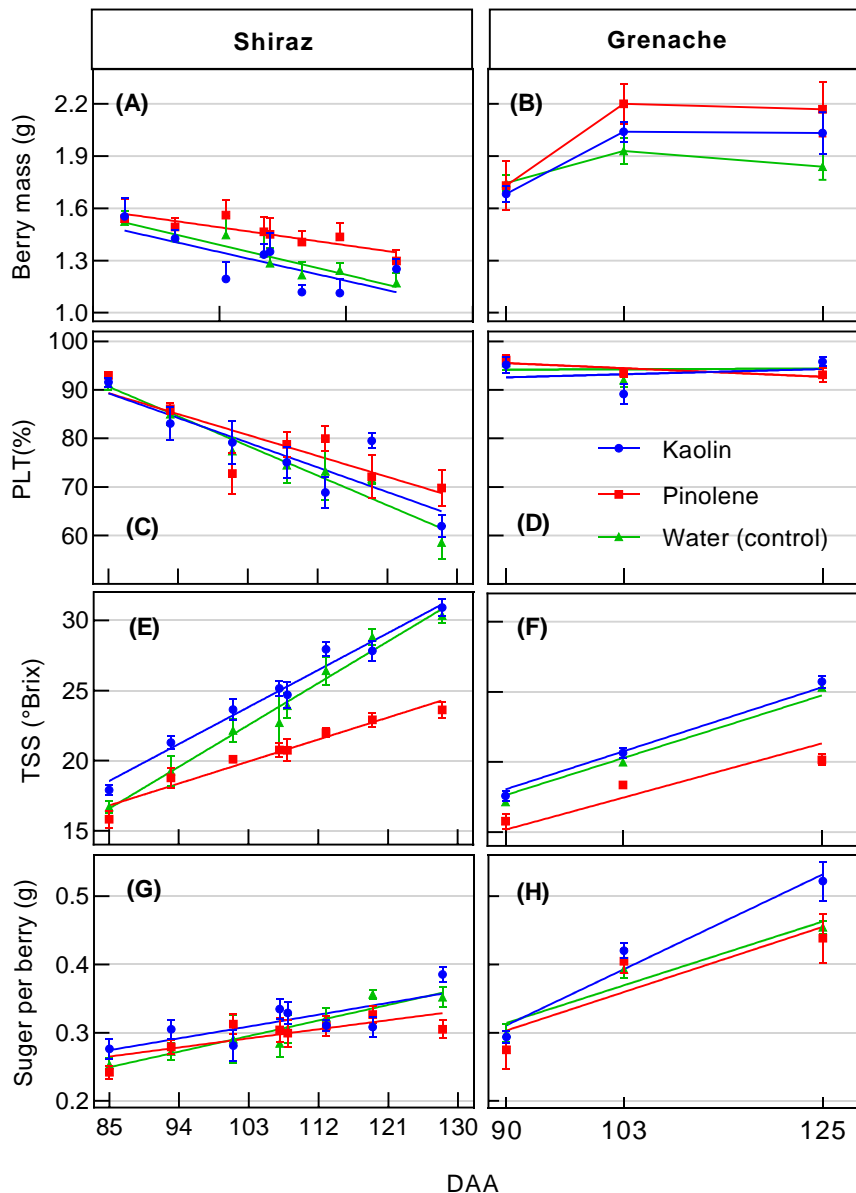
Figure 2 Effect of antitranspirants on development of berry mass (A, B), percentage living tissue (PLT, C, D), TSS (E, F) and sugar per berry (G, H) plotted against days after anthesis (DAA) for Shiraz (A, C, E, G) and Grenache (B, D, F, H) at Coombe Vineyard during season 2019/20. The three treatments applied were Kaolin (blue), Pinolene (red) and water control (green). Each point is mean ± SEM (n=6 for Shiraz and n = 5 for Grenache) with 2 samples for each biological replicate, lines in all subplots are linear regression except for (B), in which just lines connected the points. Multiple linear regressions were applied in all subplots with DAA and different treatments except for (B), in which two-way repeated ANOVA (and Tukey) applied with DAA and treatments. Also, the multiple linear regression showed that the TSS accumulation rate was significantly lower under Pinolene treatment than that of controls and Kaolin treatment in both Shiraz (all $p < 0.0001$) and Grenache (all $p < 0.05$) (2E, 2F).
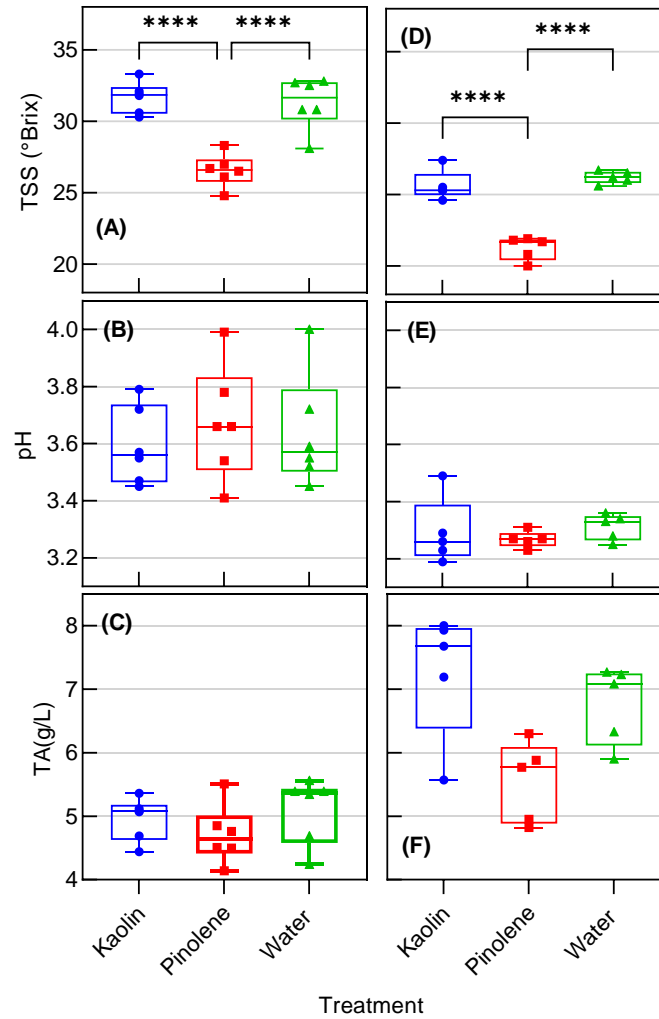
Figure 3 Effect of antitranspirants on harvest properties of juice from Shiraz and Grenache. Boxplots are shown of bunch TSS, pH and TA of Shiraz ((A), (B), (C)) (n = 6) and Grenache ((D), (E), (F)) (n =5) under treatments of Kaolin (blue), Pinolene (red) and water control (green). Middle line in box represents median value; lower and upper edges of box represent 25th and 75th percentile of data set; and whiskers represent range of data values. **** $p < 0.0001$.

3.3. Bunch temperature, internal [O₂] profiles and [EtOH]

Bunch temperatures were compared between treatments when the environmental conditions would potentially exacerbate difference between treatments, i.e., during a heatwave and when the western side of the vine was exposed to the direct solar beam (during 15:30 to 16:30). Although bunch surface temperatures (by IR gun) ranged from 39 to 46 °C and were above ambient air temperature (approximately 37 to 40 °C), no significant differences were observed in bunch temperature (one way ANOVA, $p = 0.19$) (Figure 4).
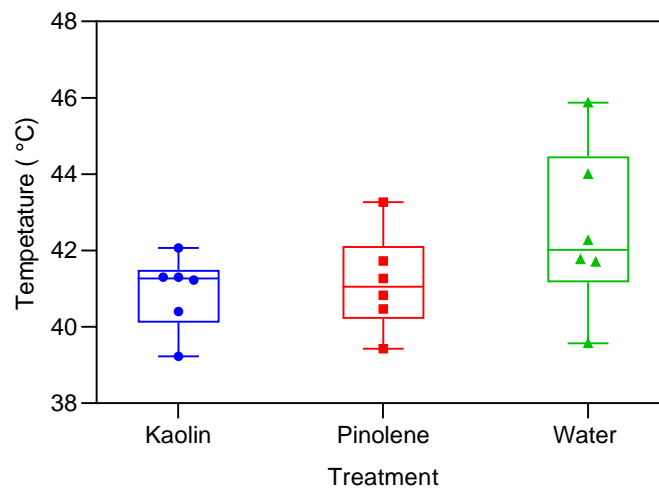
Figure 4 The surface temperature of Shiraz bunches under different antitranspirant treatments measured on 28th January 2020 during a heatwave (daily maximum air temperature was 40 °C at 16:30). Boxplots are shown for each treatment (n= 5). Middle line in box represents median value; lower and upper edges of box represent 25th and 75th percentile of data set; and whiskers represent range of data values. One-way ANOVA showed no significant differences between treatments ($p = 0.19$).

Multiple linear regressions (factors = DAA, depth and treatment) showed that in Shiraz, [O_2] was significantly decreased with increasing DAA ($p < 0.0001$) (from 86, 108 to 123 DAA) and depths ($p < 0.0001$) (from 0.5, 1.0 to 1.5mm), but no differences between treatments ($p > 0.080$) (Figure 5). In Grenache berries measured at 100 DAA, [O_2] was significantly decreased with depth ($p < 0.0001$) (from 0.5, 1, 1.5 to 2 mm), but no differences between treatments ($p > 0.60$) (two-way ANOVA) (Figure 5).
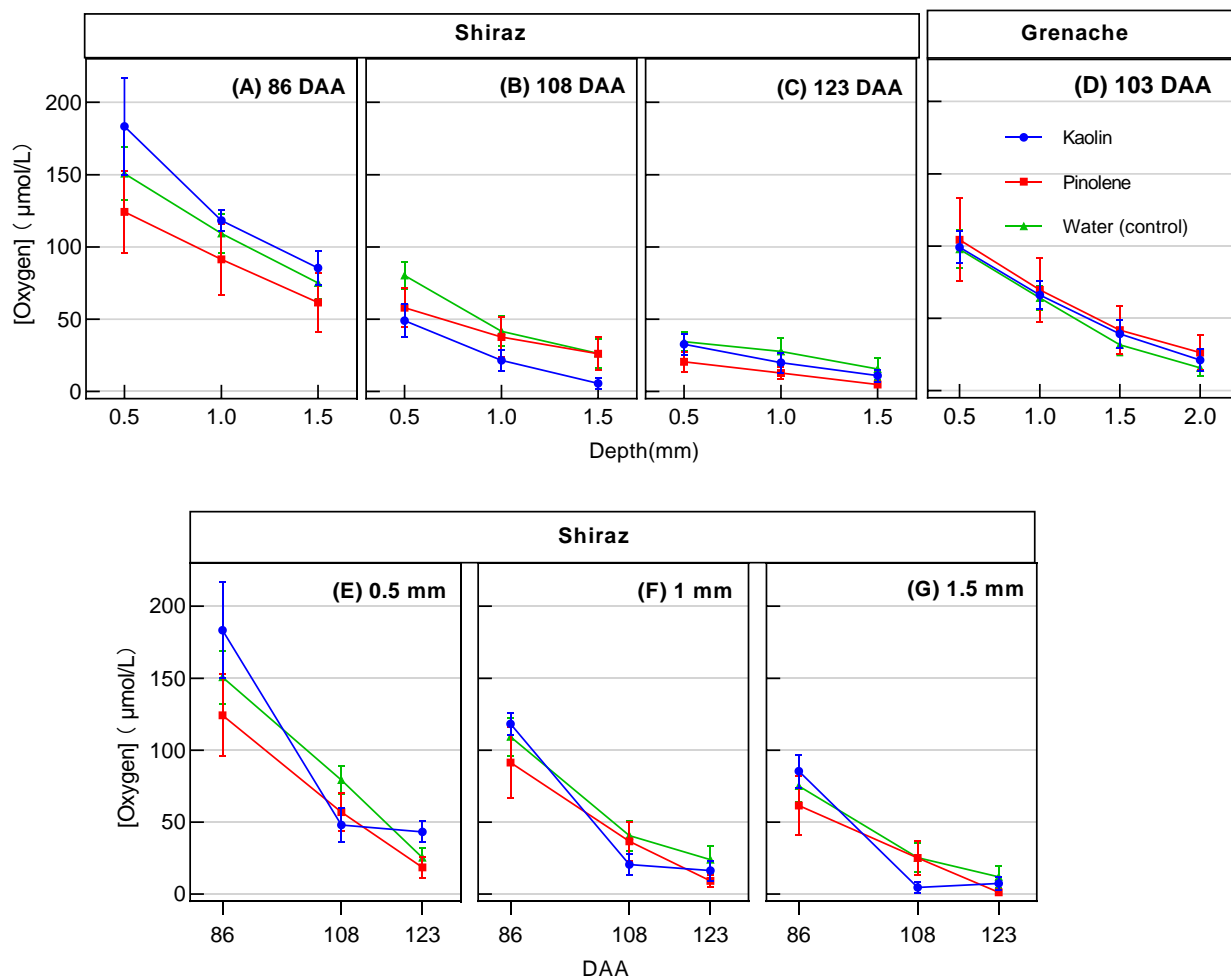
Figure 5 Effect of antitranspirant treatments on oxygen concentration profiles in Shiraz and Grenache berries. Three depths from the berry surface are recorded (0.5 mm, 1 mm and 1.5 mm) at 86 DAA (A), 108 DAA (B),123 DAA(C) and on Grenache berries at 4 different depths (0.5 mm, 1 mm, 1.5 mm, 2 mm) on 103 DAA (D). Each point connected by lines is mean ± SEM (n=6 for Shiraz and n = 5 for Grenache) with 1 sample for each biological replicate.

Juice [EtOH] for each treatment is shown versus DAA in Figure 6. No significant differences were observed between different treatments at each sampling in both varieties ($p = 0.37$, two-way repeated ANOVA). The [EtOH] from Grenache were about 10 times lower than that from Shiraz (note different Y-axis scale in Figure 6). The [EtOH] in Shiraz berries corresponded with the daily maximum temperature of the previous day (Figure 7), with higher [EtOH] after higher temperatures.
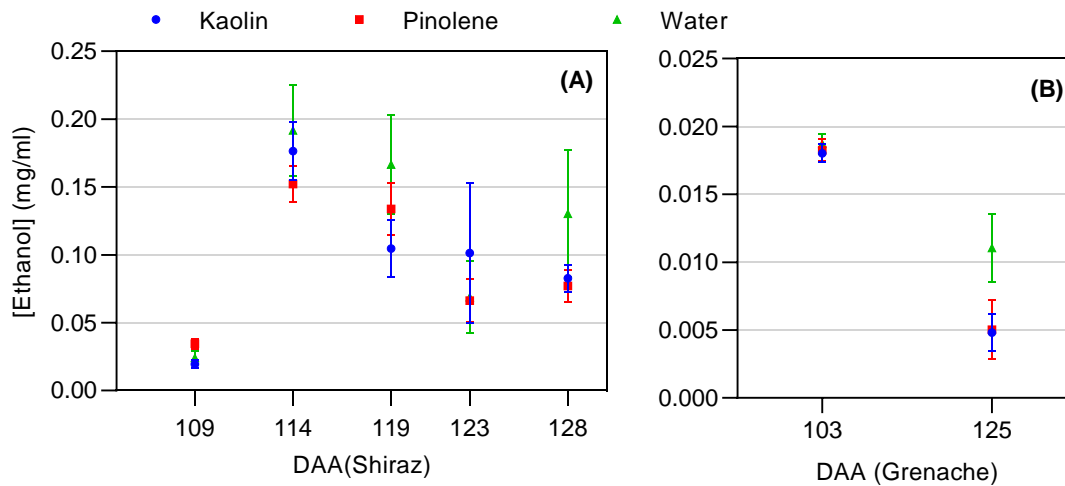
Figure 6 Effect of antitranspirants on juice ethanol concentration with time (DAA) for Shiraz (A) and Grenache (B) berries. Means ± SEM, n = 5, with 2 samples for each biological replicate. Two-way repeated ANOVA showed no differences between treatments in both varieties ($p = 0.3763$).
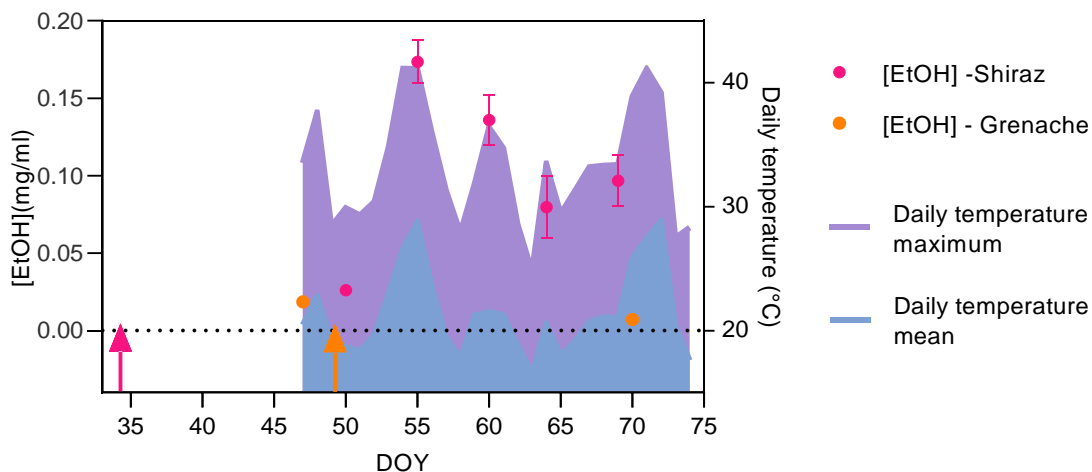
Figure 7 Changes in juice ethanol concentration ([EtOH]) with time (day of the year, DOY) in Grenache and Shiraz berries relative to daily maximum and mean temperatures. Mean ± SEM, n =10. Coloured arrows indicate DOY when 10 °Brix was achieved for each variety (red for Shiraz, orange for Grenache).

4. Discussion

Shiraz typifies berry cell death and berry shrivel, contrasting to Grenache that can maintain high cell vitality with almost no loss of berry mass during ripening (Fuentes et al., 2010; Krasnow et al., 2008; Rogiers et al., 2004; Tilbrook & Tyerman, 2009). The findings of the present study align with prior research where Shiraz berries showed substantial loss of berry cell vitality and loss of berry mass after 85 DAA, while this was not evident in Grenache accounting for the more limited sampling that would have shown these effects in Shiraz.

In this study, Shiraz and Grenache berries were treated with Pinolene and Kaolin spray resulting in a film of these compounds forming on the berry skin and pedicels (Figure 1). Such films should either reduce diffusion of gases into and out of the berry (water vapour and oxygen) and also potentially affect berry albedo, which could be expected to impact on berry temperature. Effects of these films on living tissue percentage, berry mass and TSS were measured. Since oxygen diffusion into the berry may have been compromised by the films, the effect of the treatments on $[O_2]$ profiles and $[EtOH]$ were measured, since $[EtOH]$ would be expected to increase under hypoxia (Benkeblia, 2021; Fan et al., 2005; Xiao, Liao, et al., 2018). Likewise, if there is a functional connection between greater hypoxia and cell death and shrivel, this may also become evident with the treatments.

Surprisingly, among all the measurements (bunch temperature, $[O_2]$, $[EtOH]$, cell vitality, berry mass, TSS), only bunches with Pinolene showed higher berry mass with lower TSS in both Grenache and Shiraz. These two film applications to bunches showed no effect on all other measured parameters taken including berry temperatures during a heatwave in sun exposed conditions.

4.1. Berry mass, TSS and sugar per berry

Pinolene spray clearly results in a film forming on the berry (Figure 1-B) and it also resulted in a significant effect in reducing berry shrivel in Shiraz with a concomitant decrease in TSS. This reduced

TSS effect was also evident in Grenache (Figure 3-D) which normally does not show berry shrivel, however Pinolene treated berries attained an overall higher mass in Grenache at 103 and 125 DAA.

Interestingly, despite no apparent effect on oxygen diffusion, Pinolene did appear to reduce berry transpiration (i.e., block of water vapour diffusion) as inferred by the reduced loss of berry mass in Shiraz and greater berry mass in Grenache compared to controls. Previous studies showed that Pinolene was effective in reducing Merlot berry transpiration at all stages of development (Fahey & Rogiers, 2019). This effect on transpiration but not on oxygen diffusion is interesting and potentially a positive outcome for continuing use of Pinolene as an antitranspirant. How Pinolene is able to block water vapour loss but have no effect on oxygen uptake remains to be determined but could be related to different sites of diffusion of the two gases (i.e., lenticels for oxygen and berry skin for water vapour) or to an (unknown) intrinsic property of Pinolene. It may be the case that lenticels are not able to be coated by this compound perhaps related to the hydrophobic properties of lenticels in general (Schönherr & Bukovac, 1972; Schönherr & Ziegler, 1975). That backflow was considered to be the main cause of loss of berry mass in Shiraz (Tilbrook & Tyerman, 2009; Tyerman et al., 2008) is not supported by the results presented here, if it is assumed that Pinolene only acts as an antitranspirant. Alternatively, there may be other effects internal to the berry, perhaps Pinolene blockage of xylem vessels or membrane located aquaporins that could influence loss of berry mass. The impacts of Pinolene on oxygen transfer and water transport in grape berries may need further investigation.

Pinolene also did not influence sugar inflow in both varieties, as there were no significant differences between Pinolene and control treatments of sugar per berry during berry development (Figure 2). This also indicates that there was no metabolic effect on phloem movement of sugars or sugar unloading from the phloem in the berry.

4.2. Berry internal [O₂] profile, [EtOH] and percentage living tissue

A previous study showed that blocking the lenticels (with silicone grease) on the berry pedicel in Chardonnay berries resulted in greater hypoxia, [EtOH] and cell death (Xiao, Liao, et al., 2018). No differences in cell vitality between treatments were observed for either variety in this study. This would suggest that both film-forming treatments did not significantly impede oxygen uptake by the berries and had no effect on berry hypoxia and resulting [EtOH] due to stimulation of fermentation. Although no significant differences of [O₂] and [EtOH] were observed between treatments in this study, the [O₂] distribution pattern was consistent with previous research (Xiao, Rogiers, et al., 2018), decreasing with both berry development (TSS) and depths towards the berry mesocarp centre. The [EtOH] in the berries showed the expected response to air temperature especially in Shiraz which is more susceptible to air temperature then Grenache (Chapter 3). Large variation of [O₂] between single berries were observed, further research could be conducted to validate the [O₂] differences from these treatments, since only up to 6 berries per replication were used in this study.

4.3. Bunch temperature

Antitranspirants may influence leaf and fruit temperature in different ways, they may increase temperature by decreasing transpiration (e.g., Pinolene), or decrease temperature by reflection of incident radiation (e.g., Kaolin) (Brillante et al., 2016; Cantore et al., 2009). However, in this study, no effects on bunch temperature were observed from treatments. The present study was conducted in the field as opposed to a pot trial (ibid), temperature differences exposure may not be detected due to other factors (wind variation or variation in exposure) (Martínez-Lüscher et al., 2020; Müller et al., 2023).

Conflicting results on the effects of Kaolin on leaf temperatures have been reported; both increasing, decreasing and no effects have all been reported on different species (Cantore et al., 2009; Glenn et al., 2001; Steiman et al., 2007). It was hypothesised that Kaolin reduces leaf temperature by increasing light reflection, but its effect is reduced or even nulled when the light intensity is low, and

counteracting this effect is the possible limitation of transpiration that would increase temperature (Brillante et al., 2016).

Previous research showed that Merlot berries and Shiraz leaves with Pinolene treatment had higher temperature presumed to be caused by reduced transpirational cooling, but this was a small effect by up to just 1 °C on both leaves and bunches (Fahey & Rogiers, 2019). If there was a small and higher berry temperature on average for Pinolene treatment, it did not translate to increased cell death or [EtOH] in either variety, especially considering that the temperature gradient across shaded and exposure berries could potentially be more than 15 °C (Coombe, 1987; Stoll and Jones, 2007; Ponce de León and Bailey, 2021).

5. Conclusion

Kaolin and Pinolene sprays causing films on berries of Grenache and Shiraz did not significantly influence O_2 inflow and bunch and berry temperature, and there was no degrading effect on berry cell death, internal [O_2], or [EtOH]. In Shiraz Pinolene does appear to reduce loss of berry mass, most likely by reducing transpiration, though other possibilities remain to be explored for this compound. It does this effectively without impacts on sugar content per berry.

6. References

Benkeblia, N. (2021). Physiological and biochemical response of tropical fruits to hypoxia/anoxia. *Frontiers in Plant Science*, *12*, 670803. https://doi.org/10.3389/fpls.2021.670803

Bonada, M., Sadras, V. O., & Fuentes, S. (2013). Effect of elevated temperature on the onset and rate of mesocarp cell death in berries of Shiraz and Chardonnay and its relationship with berry shrivel: Thermal shift on mesocarp cell death and shrivel. *Australian Journal of Grape and Wine Research*, *19*(1), 87–94. https://doi.org/10.1111/ajgw.12010

Brillante, L., Belfiore, N., Gaiotti, F., Lovat, L., Sansone, L., Poni, S., & Tomasi, D. (2016). Comparing kaolin and pinolene to improve sustainable grapevine production during drought. *PLOS ONE*, *11*(6), e0156631. https://doi.org/10.1371/journal.pone.0156631

Cantore, V., Pace, B., & Albrizio, R. (2009). Kaolin-based particle film technology affects tomato physiology, yield and quality. *Environmental and Experimental Botany*, *66*(2), 279–288. https://doi.org/10.1016/j.envexpbot.2009.03.008

Caravia, L., Collins, C., Petrie, P. R., & Tyerman, S. D. (2016). Application of shade treatments during Shiraz berry ripening to reduce the impact of high temperature: Shade reduces impact of high temperature on Shiraz. *Australian Journal of Grape and Wine Research*, *22*(3), 422–437. https://doi.org/10.1111/ajgw.12248

Caravia, L., Collins, C., & Tyerman, S. D. (2015). Electrical impedance of Shiraz berries correlates with decreasing cell vitality during ripening: Impedance of Shiraz berries and cell vitality. *Australian Journal of Grape and Wine Research*, *21*(3), 430–438. https://doi.org/10.1111/ajgw.12157

Caravia, L., Pagay, V., Collins, C., & Tyerman, S. d. (2017). Application of sprinkler cooling within the bunch zone during ripening of Cabernet Sauvignon berries to reduce the impact of high temperature. *Australian Journal of Grape and Wine Research*, *23*(1), 48–57. https://doi.org/10.1111/ajgw.12255

Chou, H.-C., Šuklje, K., Antalick, G., Schmidtke, L. M., & Blackman, J. W. (2018). Late-season Shiraz berry dehydration that alters composition and sensory traits of wine. *Journal of Agricultural and Food Chemistry*, *66*(29), 7750–7757. https://doi.org/10.1021/acs.jafc.8b01646

Deloire, A. (2011). The concept of berry sugar loading. *Wineland*, *257*, 93–95.

Di Vaio, C., Marallo, N., Di Lorenzo, R., & Pisciotta, A. (2019). Anti-transpirant effects on vine physiology, berry and wine composition of cv. Aglianico (*Vitis vinifera* L.) grown in south Italy. *Agronomy*, *9*(5), 244. https://doi.org/10.3390/agronomy9050244

Fahey, D. J. (2018). *Manipulating winegrapes with antitranspirants* (DPI 1702; p. 22). NSW Department of Primary Industries | Plant Systems.

Fahey, D. J., & Rogiers, S. Y. (2019). Di-1-*p*-menthene reduces grape leaf and bunch transpiration: Di-1-*p*-menthene reduces transpiration. *Australian Journal of Grape and Wine Research*, *25*(1), 134–141. https://doi.org/10.1111/ajgw.12371

Fan, L., Song, J., Forney, C., & Jordan, M. (2005). Ethanol production and chlorophyll fluorescence predict breakdown of heat-stressed apple fruit during cold storage. *Journal of the American Society for Horticultural Science. American Society for Horticultural Science*, *130*. https://doi.org/10.21273/JASHS.130.2.237

Fuentes, S., Sullivan, W., Tilbrook, J., & Tyerman, S. (2010). A novel analysis of grapevine berry tissue demonstrates a variety-dependent correlation between tissue vitality and berry shrivel: Variety-dependent berry vitality and shrivel. *Australian Journal of Grape and Wine Research*, *16*(2), 327–336. https://doi.org/10.1111/j.1755-0238.2010.00095.x

Glenn, D. M., Puterka, G., Drake, S., Unruh, T., Knight, A., Baherle, P., Prado, E., & Baugher, T. (2001). Particle film application influences apple leaf physiology, fruit yield, and fruit quality. *Journal of the American Society for Horticultural Science*, *126*. https://doi.org/10.21273/JASHS.126.2.175

Iland, I., P., Dry, P., Proffitt, T., & Tyerman, S. (2011). *The grapevine: From the science to the practice of growing vines for wine*. Patrick Iland Wine Promotions.

Keller, M. (2006). Ripening grape berries remain hydraulically connected to the shoot. *Journal of Experimental Botany*, *57*(11), 2577–2587. https://doi.org/10.1093/jxb/erl020

Krasnow, M., Matthews, M., & Shackel, K. (2008). Evidence for substantial maintenance of membrane integrity and cell viability in normally developing grape (*Vitis vinifera* L.) berries throughout development. *Journal of Experimental Botany*, *59*(4), 849–859. https://doi.org/10.1093/jxb/erm372

Martínez-Lüscher, J., Chen, C. C. L., Brillante, L., & Kurtural, S. K. (2020). Mitigating heat wave and exposure damage to "Cabernet Sauvignon" wine grape with partial shading under two irrigation amounts. *Frontiers in Plant Science*, *11*. https://www.frontiersin.org/articles/10.3389/fpls.2020.579192

McCarthy, M. G. (1999). Weight loss from ripening berries of Shiraz grapevines (*Vitis vinifera* L. cv. Shiraz). *Australian Journal of Grape and Wine Research*, *5*(1), 10–16. https://doi.org/10.1111/j.1755-0238.1999.tb00145.x

Mphande, W., Farrell, A. D., & Kettlewell, P. S. (2023). Commercial uses of antitranspirants in crop production: A review. *Outlook on Agriculture*, *52*(1), 3–10. https://doi.org/10.1177/00307270231155257

Müller, K., Keller, M., Stoll, M., & Friedel, M. (2023). Wind speed, sun exposure and water status alter sunburn susceptibility of grape berries. *Frontiers in Plant Science*, *14*. https://www.frontiersin.org/articles/10.3389/fpls.2023.1145274

Palliotti, A., Poni, S., Berrios, J. G., & Bernizzoni, F. (2010). Vine performance and grape composition as affected by early-season source limitation induced with anti-transpirants in two red *Vitis vinifera* L. cultivars. *Australian Journal of Grape and Wine Research*, *16*(3), 426–433. https://doi.org/10.1111/j.1755-0238.2010.00103.x

Rogiers, S. Y., Hatfield, J. M., Jaudzems, V. G., White, R. G., & Keller, M. (2004). Grape berry cv. Shiraz epicuticular wax and transpiration during ripening and preharvest weight loss. *American Journal of Enology and Viticulture*, *55*(2), 121–127. https://doi.org/10.5344/ajev.2004.55.2.121

Rogiers, S. Y., & Holzapfel, B. P. (2015). The plasticity of berry shrivelling in 'Shiraz': A vineyard survey. *Vitis-Journal of Grapevine Research*, *54*(1), 1–8.

Schönherr, J., & Bukovac, M. J. (1972). Penetration of stomata by liquids: Dependence on surface tension, wettability, and stomatal morphology. *Plant Physiology*, *49*(5), 813–819. https://doi.org/10.1104/pp.49.5.813

Schönherr, J., & Ziegler, H. (1975). Hydrophobic cuticular ledges prevent water entering the air pores of liverwort thalli. *Planta*, *124*(1), 51–60. https://www.jstor.org/stable/23371613

Shivashankara, K. S., Laxman, R. H., Geetha, G. A., Roy, T. K., Srinivasa Rao, N. K., & Patil, V. S. (2013). Volatile aroma and antioxidant quality of 'Shiraz' grapes at different stages of ripening. *International Journal of Fruit Science*, *13*(4), 389–399. https://doi.org/10.1080/15538362.2013.789235

Smart, R. E., & Dry, P. R. (1980). A climatic classification for Australian viticultural regions. *Annual Technical Issue*.

Steiman, S. R., Bittenbender, H. C., & Idol, T. W. (2007). Analysis of kaolin particle film use and its application on coffee. *HortScience*, *42*(7), 1605–1608. https://doi.org/10.21273/HORTSCI.42.7.1605

Šuklje, K., Zhang, X., Antalick, G., Clark, A. C., Deloire, A., & Schmidtke, L. M. (2016). Berry shriveling significantly alters Shiraz (*Vitis vinifera* L.) grape and wine chemical composition. *Journal of Agricultural and Food Chemistry*, *64*(4), 870–880. https://doi.org/10.1021/acs.jafc.5b05158

Tilbrook, J., & Tyerman, S. D. (2008). Cell death in grape berries: Varietal differences linked to xylem pressure and berry weight loss. *Functional Plant Biology*, *35*(3), 173. https://doi.org/10.1071/FP07278

Tilbrook, J., & Tyerman, S. D. (2009). Hydraulic connection of grape berries to the vine: Varietal differences in water conductance into and out of berries, and potential for backflow. *Functional Plant Biology*, *36*(6), 541. https://doi.org/10.1071/FP09019

Tyerman, S. D., Tilbrook, J., Pardo, C., Kotula, L., Sullivan, W., & Steudle, E. (2008). Direct measurement of hydraulic properties in developing berries of *Vitis vinifera* L. cv Shiraz and Chardonnay. *Australian Journal of Grape and Wine Research*, *10*(3), 170–181. https://doi.org/10.1111/j.1755-0238.2004.tb00020.x

Xiao, Rogiers, S. Y., Sadras, V. O., & Tyerman, S. D. (2018). Hypoxia in grape berries: The role of seed respiration and lenticels on the berry pedicel and the possible link to cell death. *Journal of Experimental Botany*, *69*(8), 2071–2083. https://doi.org/10.1093/jxb/ery039

Xiao, Z., Liao, S., Rogiers, S. Y., Sadras, V. O., & Tyerman, S. D. (2018). Effect of water stress and elevated temperature on hypoxia and cell death in the mesocarp of Shiraz berries: Berry hypoxia and death under water/heat stress. *Australian Journal of Grape and Wine Research*, *24*(4), 487–497. https://doi.org/10.1111/ajgw.12363

Zhang, Y., & Keller, M. (2015). Grape berry transpiration is determined by vapor pressure deficit, cuticular conductance, and berry size. *American Journal of Enology and Viticulture*, *66*(4), 454–462. https://doi.org/10.5344/ajev.2015.15038

Chapter 5

Concluding remarks and future perspectives

Table of Contents

1. Overview

Variety-dependent late-ripening berry shrinkage (dehydration or shrivel), the third and last phase defined during grape berry development, is marked by loss of water and concentration of sugars (Fuentes et al., 2010; Krasnow et al., 2008; McCarthy, 1997; McCarthy & Coombe, 1999; Sadras & McCarthy, 2007; Tilbrook & Tyerman, 2008). It is usually accompanied by loss of cell vitality within the berry mesocarp *(ibid)*. Cell death is characterized by decreased plasma membrane integrity observed using vital dyes (Krasnow et al., 2008; Tilbrook & Tyerman, 2008, 2008) and electrolyte leakage using electrical impedance (Caravia et al., 2015).

2. Micro-CT and berry microstructure

The high-resolution micro-CT scan study in Chapter 2 has provided new insights into features of berry microstructure, especially the porous gas-filled structures characterised that probably provide a pathway for gas diffusion into the berry. These most likely determine the efficiency of gas exchange, including O_2 transport (Cukrov, 2018; Ho et al., 2008; Rajapakse et al., 1990; van Dongen & Licausi, 2015). From the development of the porous network in grape berries both in the mesocarp and in seeds, it is clear that there is a gas diffusion pathway from the lenticels on the pedicel that extends into the seeds and mesocarp. The porous channels are only present in the berry axis and mesocarp periphery, potentially causing steep oxygen concentration gradients and hypoxic regions towards the mesocarp interior. These hypoxic regions are correlated to the regions of low cell vitality in the berry mesocarp. This study also revealed the possible connection between the porous channels and the vascular system (xylem and phloem), which also branches in three directions from the brush area, dividing into peripheral vasculature, central vascular and ovular vasculature to the seeds as a hook (Xie et al., 2023). The aeration system seems to be located inside this non-void tissue (possible vascular system) as an aeration canal.

Micro-CT has been widely applied in plant studies, however it has rarely been applied to grape berries (Knipfer et al., 2015; H. Xiao et al., 2021), and further application of the technology may provide

novel insights into grape berry physiology; 1) Combined with high resolution Micro-CT and conventional anatomical stains of the vascular system, or the use of contrasting agents in Micro-CT, could provide more information on the developmental link between the vascular system and the aeration system. In this study care was taken to avoid cavitation and embolism in the berry xylem since voids in embolised vessels could be mistaken for gas diffusion channels. Further study on deliberately cavitated and embolised vessels and/or with contrasting agents in Micro CT may help in resolving the effect of xylem embolism in the berry. 2) Micro-CT could provide a non-destructive, more rapid and easier way to determine cell death comparing to FDA staining, as when cell death occurs, the airspace between cells could be filled with fluid because of membrane leakage. A validated and reproducible method has been introduced based on a grayscale-porosity correlation model to accurately map the porosity distribution of entire fruit and vegetable organs (Nugraha et al., 2019).

3. Modelling to predict cell death

Both the decreasing trend and the increased variation with time of cell death in Shiraz berries were simulated by a model based on temperature in three growing seasons with different climatic conditions. This model demonstrated the strong non-linear effect of temperature that has not been accounted for in previous models (Bonada et al., 2013). This strong non-linear effect of temperature was also evident in the model describing ethanol concentration in the berry. From single berry analysis for Shiraz, the ethanol concentration was also dependent on ripeness (TSS), i.e., more mature berries were more vulnerable to accumulation of ethanol when temperature increased. This corresponds to the decreased porosity and increased hypoxia with increasing ripeness. These effects may well relate to the effect of temperature on respiration as the basis of the development of hypoxia due to restricted O_2 diffusion at high respiratory rates. However, as fermentation takes over and as cell death occurs this would alleviate the demand for O_2 in the berry which complicates the way berry porosity relates to the increase in cell death that is observed in Shiraz.

The rapid increasing effect of rising temperature above a threshold on cell death in Shiraz and probably also applicable to Cabernet Sauvignon, is indicative of a tipping point in berry health that will become more evident in the future. A tipping point (Kurtural & Gambetta, 2021), i.e., a point where irreversible effects increase rapidly is indicated from these two models. A temperature of about 35 °C may be considered a tipping point for ambient temperature in the field for susceptible varieties such as Shiraz and Cabernet Sauvignon, above this temperature both ethanol and cell death increase sharply. Applications to mitigate berry cell death due to heat stress like mulching the inter-row or using cover crops to reduce reflected infrared radiation warrant further investigation.

Both temperature and ethanol models have some limitations. The temperature model may only be applicable to Shiraz or Cabernet Sauvignon, and it did not include interaction between temperature and ripeness as was evident with the model describing berry ethanol. Both Chardonnay and Grenache show contrasting behaviour in respect of berry cell death and ethanol accumulation and both these varieties do not normally show berry shrinkage. To indicate the effects of heat stress on berries the ethanol model has limitations particularly for extreme temperatures since over 50 °C, the relevant enzymes may lose functionality. It may be possible to combine features of the two models and incorporate functions related to respiration rate and physical properties of the berries to more accurately predict cell death that can be more generally applicable.

4. Hypoxia, cell death and variety differences

Berry shrinkage and cell death is particularly common in Shiraz and becoming more common in Cabernet Sauvignon (Krasnow et al., 2008; Pagay, 2018), while it rarely occurs in Grenache (Fuentes et al., 2010; Tilbrook & Tyerman, 2008). This study also showed that Grenache tended to show minimal cell death and berry mass loss. The dramatically lower ethanol concentration in Grenache berries under heatwave conditions indicated its higher heat tolerance. This corresponds to the overall higher oxygen concentration and less hypoxia in Grenache berry mesocarp, most probably arising from the retention of the porous structures during development compared to Shiraz as mentioned

above. However, whether other physiological and biochemical characteristics of different varieties affect the degree of berry cell death needs further investigation, especially characteristics related to drought and heat tolerance both in the vine and berry, which could provide valuable information for grape variety selection for warmer climates.

Berry heat tolerance may be related to how hypoxia can cause cell death. Under hypoxia, cytoplasmic acidosis, energy reduction, moisture loss, the accumulation of toxic products of anaerobic metabolism, electron leakage and reactive oxygen species (ROS) production, together significantly contribute to post-anoxic damage and lead to programmed cell death or necrosis (Jethva et al., 2022). Especially ROS production, which occurs as the by-products of aerobic metabolism in plants (Considine et al., 2017). Transitions between hypoxia and normoxia or less hypoxia, as may occur in the grape berry over a diurnal cycle (hot day, to cool night) also can generate ROS (Considine & Foyer, 2021). The activation of programmed cell death in plants has been associated with a reduction in cytosolic potassium induced by ROS (Shabala, 2017). Hypoxia has been implicated in regulating genes involved in cell death as a result of changes in ROS (Jethva et al., 2022), and oxygen sensing and ROS sensing pathways can converge. It would be worthwhile exploring gene expression profiles and comparing varieties such as Grenache and Shiraz for differences in ROS and oxygen-sensing pathway genes.

5. Berry shrinkage and cell death

The connection between the onset and degree of cell death, and the onset and degree of berry shrinkage in Shiraz may not be as directly linked as previously thought. An allometric analysis between berry sugar content and fresh mass accumulation based on a single sampling was developed to track the progression of berry development that can indicate more accurately the initiation of berry shrinkage. Obvious berry mass loss commenced at about 20 °Brix between 90 to 100 DAA in all 3 seasons in this study although with different climate conditions, which is consistent with the literature. However, mesocarp cell death corresponded more to temperature conditions during the growing

season. Cell death could start relatively early in berry ripening during a hot season (e.g., 10 to 20 days after veraison), which may result in backflow occurring much earlier than previously thought. It can be concluded that the onset of berry shrinkage is not necessarily strictly dependent on the degree of cell death since shrinkage also depends on the timing of cell death with respect to when sugar inflow via the phloem likely ceases. The phloem may not be so affected by cell death as vascular tissue remained vital and sugar accumulation continued despite large regions of cell death in the mesocarp. Future research could address the quantitative relationship between the level of mesocarp cell death and water backflow from the berry, and the timing and degree of cell death as it may impact on peak berry mass. Incorporating models developed above that predict cell death from climate data with the onset and level of water loss from backflow could provide valuable information for yield optimization. In this context it has been demonstrated previously that water stress is also a factor in causing Shiraz berry cell death (Bonada et al., 2013; Z. Xiao et al., 2018), and water stress in the parent vine would also potentially increase the degree of backflow from the berry, particularly earlier in development when the hydraulic conductance of the berry xylem is still high (Keller, 2006; Tilbrook & Tyerman, 2009; Tyerman et al., 2008).

6. Antitranspirants effects on berry mass loss and cell death

Application of antitranspirants was reported to be an important technique to mitigate heat stress (Dry, 2009), however, in this study, the application of two film-forming antitranspirants Kaolin ($Al_4Si_4O_{10}(OH)_8$) and Pinolene (Di-1-p-menthene) on Shiraz and Grenache bunches, did not significantly influence bunch temperature, hypoxia in the berry, ethanol concentration or berry cell death. Pinolene treatment on bunches was shown here to reduce berry shrinkage without impacts on sugar content. However, if Pinolene solely functions as an antitranspirant, its strong effect in reducing berry shrinkage calls into question the role of backflow to the vine as the main cause of berry shrinkage (Fuentes et al., 2010; Tilbrook & Tyerman, 2009; Tyerman et al., 2008). Note that in the treatments performed here only the bunches were treated not the entire grapevine canopy, so leaf transpiration was assumed to be unimpeded. It also demonstrates that mesocarp cell death does not

directly lead to berry shrinkage as is also evident for Chardonnay berries where cell death can be significant, but berry shrinkage does not occur. If berry transpiration plays such an important role in berry water loss, it may warrant further investigation that why some varieties show almost no berry shrinkage related to berry transpiration differences. Further research on the effects of Pinolene needs to be undertaken since it is not possible to exclude from the available data whether Pinolene also has other effects besides impeding transpiration, especially since it has been shown that berry transpiration becomes very low later in ripening. It is also hard to reconcile that the bunch application of Kaolin, also an antitranspirant, did not show any impacts on berry mass loss. Further exploration is needed to understand the effects of Pinolene on oxygen transfer and water transport within grape berries.

7. Clone

Clones are a potential source of genetic diversity, traditionally for selection of vines free of virus to improve yield. Different clones of Shiraz may vary in pruning weights, yield components (compactness of bunches, berry size etc.), fruit composition and ripening duration (Nicholas, 2006). Some characters may be helpful in reducing heat stress, like higher pruning weight (more shading) or less compact bunches (better heat dissipation), or late ripening time which could experience less heat stress. Whether these differences between different clones could mitigate cell death and berry shrivel warrant further investigation.

8. References

Bonada, M., Sadras, V. O., & Fuentes, S. (2013). Effect of elevated temperature on the onset and rate of mesocarp cell death in berries of Shiraz and Chardonnay and its relationship with berry shrivel: Thermal shift on mesocarp cell death and shrivel. *Australian Journal of Grape and Wine Research*, *19*(1), 87–94. https://doi.org/10.1111/ajgw.12010

Caravia, L., Collins, C., & Tyerman, S. D. (2015). Electrical impedance of Shiraz berries correlates with decreasing cell vitality during ripening: Impedance of Shiraz berries and cell vitality. *Australian Journal of Grape and Wine Research*, *21*(3), 430–438. https://doi.org/10.1111/ajgw.12157

Cukrov, D. (2018). Progress toward understanding the molecular basis of fruit response to hypoxia. *Plants (Basel, Switzerland)*, *7*(4), E78. https://doi.org/10.3390/plants7040078

Dry, P. R. (2009). Bunch exposure management. In *Technical booklet*. Grape and Wine Research and Development Corporation.

Fuentes, S., Sullivan, W., Tilbrook, J., & Tyerman, S. (2010). A novel analysis of grapevine berry tissue demonstrates a variety-dependent correlation between tissue vitality and berry shrivel: Variety-dependent berry vitality and shrivel. *Australian Journal of Grape and Wine Research*, *16*(2), 327–336. https://doi.org/10.1111/j.1755-0238.2010.00095.x

Ho, Q. T., Verboven, P., Verlinden, B. E., Lammertyn, J., Vandewalle, S., & Nicolaï, B. M. (2008). A continuum model for metabolic gas exchange in pear fruit. *PLOS Computational Biology*, *4*(3), e1000023. https://doi.org/10.1371/journal.pcbi.1000023

Keller, M. (2006). Ripening grape berries remain hydraulically connected to the shoot. *Journal of Experimental Botany*, *57*(11), 2577–2587. https://doi.org/10.1093/jxb/erl020

Knipfer, T., Fei, J., Gambetta, G. A., McElrone, A. J., Shackel, K. A., & Matthews, M. A. (2015). Water transport properties of the grape pedicel during fruit development: Insights into xylem anatomy and function using microtomography. *Plant Physiology*, *168*(4), 1590–1602. https://doi.org/10.1104/pp.15.00031

Krasnow, M., Matthews, M., & Shackel, K. (2008). Evidence for substantial maintenance of membrane integrity and cell viability in normally developing grape (*Vitis vinifera* L.) berries throughout development. *Journal of Experimental Botany*, *59*(4), 849–859. https://doi.org/10.1093/jxb/erm372

Kurtural, S. K., & Gambetta, G. A. (2021). Global warming and wine quality: Are we close to the tipping point? *OENO One*, *55*(3), Article 3. https://doi.org/10.20870/oeno-one.2021.55.3.4774

McCarthy, M. G. (1997). The effect of transient water deficit on berry development of cv. Shiraz (*Vitis vinifera* L.). *Australian Journal of Grape and Wine Research*, *3*(3), 2–8. https://doi.org/10.1111/j.1755-0238.1997.tb00128.x

McCarthy, M. G., & Coombe, B. G. (1999). Is weight loss in ripening grape berries cv. Shiraz caused by impeded phloem transport? *Australian Journal of Grape and Wine Research*, *5*(1), 17–21. https://doi.org/10.1111/j.1755-0238.1999.tb00146.x

Nicholas, P. (2006). *Grapevine clones used in Australia*. South Australia Research and Development institute.

Nugraha, B., Verboven, P., Janssen, S., Wang, Z., & Nicolaï, B. M. (2019). Non-destructive porosity mapping of fruit and vegetables using X-ray CT. *Postharvest Biology and Technology*, *150*, 80–88. https://doi.org/10.1016/j.postharvbio.2018.12.016

Pagay, V. (2018). *Is berry shrivel in Cabernet Sauvignon influenced by climate and does this potentially affect characteristics of the resulting wine?* (UA 1702). the University of Adelaide. https://limestonecoastwine.com.au/library/64-is-berry-shrivel-in-cabernet-sauvignon-influenced-by-climate-and-does-this-potentially-affect-characteristics-of-the-resulting-wine/

Rajapakse, N. C., Banks, N. H., Hewett, E. W., & Cleland, D. J. (1990). Development of oxygen concentration gradients in flesh tissues of bulky plant organs. *Journal of the American Society for Horticultural Science*, *115*(5), 793–797. https://doi.org/10.21273/JASHS.115.5.793

Sadras, V. O., & McCarthy, M. G. (2007). Quantifying the dynamics of sugar concentration in berries of *Vitis vinifera* cv. Shiraz: A novel approach based on allometric analysis. *Australian Journal of Grape and Wine Research*, *13*(2), 66–71. https://doi.org/10.1111/j.1755-0238.2007.tb00236.x

Tilbrook, J., & Tyerman, S. D. (2008). Cell death in grape berries: Varietal differences linked to xylem pressure and berry weight loss. *Functional Plant Biology*, *35*(3), 173. https://doi.org/10.1071/FP07278

Tilbrook, J., & Tyerman, S. D. (2009). Hydraulic connection of grape berries to the vine: Varietal differences in water conductance into and out of berries, and potential for backflow. *Functional Plant Biology*, *36*(6), 541. https://doi.org/10.1071/FP09019

Tyerman, S. D., Tilbrook, J., Pardo, C., Kotula, L., Sullivan, W., & Steudle, E. (2008). Direct measurement of hydraulic properties in developing berries of *Vitis vinifera* L. cv Shiraz and Chardonnay. *Australian Journal of Grape and Wine Research*, *10*(3), 170–181. https://doi.org/10.1111/j.1755-0238.2004.tb00020.x

van Dongen, J. T., & Licausi, F. (2015). Oxygen sensing and signaling. *Annual Review of Plant Biology*, *66*(1), 345–367. https://doi.org/10.1146/annurev-arplant-043014-114813

Xiao, H., Piovesan, A., Pols, S., Verboven, P., & Nicolaï, B. (2021). Microstructural changes enhance oxygen transport in tomato (Solanum lycopersicum) fruit during maturation and ripening. *New Phytologist*, *232*(5), 2043–2056. https://doi.org/10.1111/nph.17712

Xiao, Z., Liao, S., Rogiers, S. Y., Sadras, V. O., & Tyerman, S. D. (2018). Effect of water stress and elevated temperature on hypoxia and cell death in the mesocarp of Shiraz berries: Berry hypoxia and death

under water/heat stress. *Australian Journal of Grape and Wine Research*, *24*(4), 487–497. https://doi.org/10.1111/ajgw.12363

Xie, Z., Fei, T., Forney, C. F., Li, Y., & Li, B. (2023). Improved maceration techniques to study the fruit vascular anatomy of grape. *Horticultural Plant Journal*, *9*(3), 481–495. https://doi.org/10.1016/j.hpj.2022.06.008